[Catégorie]

Polar Monitoring WP2: Assessment and consolidation of mission requirements

Reference:	CLS-ENV-NT-19-0364
Nomenclature:	[Nomenclature]
Issue:	1. 0
Date:	2019,Dec.06

CLS headquarters
11 rue Hermès
Parc technologique du Canal
31520 Ramonville Saint-Agne
FRANCE

Tel. +33 (0)5 61 39 47 00
Fax +33 (0)5 61 75 10 14
Mail: info@cls.fr
www.cls.fr

CLS Brest Le Ponant
Zone du technopôle de Brest Iroise
Avenue La Pérouse
29280 Plouzané
FRANCE

Tel. 33 (0)2.98.05.76.80
Fax 33 (0)2.98.05.76.90

Chronology Issues:

Issue:	Date:	Reason for change:	Author
1.0	02/10/2019	First version	J.Aublanc P.Thibaut M.McMillan E.Rinne H.Sallila
2.0	20/12/2019	Second version	J.Aublanc P.Thibaut M.McMillan E.Rinne H.Sallila ML.Denneulin

People involved in this issue:

Written by (*):	jaublanc	Date + Initials:(visa or ref)
Checked by (*):	pthibaut	Date + Initial:(visa ou ref) [Checker]
Approved by (*):		Date + Initial:(visa ou ref) [Approver]
Application authorized by (*):		Date + Initial:(visa ou ref)

**In the opposite box: Last and First name of the person + company if different from CLS*

[Mots clés]

List of tables and figures

List of tables:

List of figures:

Reference documents

RD1	PEG-1 Report, User Requirements for a Copernicus Polar Mission, Step 1 Report, Polar Expert Group, Issue: 12th June 2017
RD2	PEG-2 Report, Polar Expert Group, Phase 2 Report on Users Requirements, Issue: 31st July 2017
RD3	Copernicus polaR Ice and Snow Topography ALtimeter (CRISTAL) Mission Requirements Document, version 2.0, ESA-EOPSM-CPTM-MRD-3350, Issued 28/02/2019.
RD4	Polar Monitoring Mission, Assessment and Consolidation of Requirements and Analysis of Campaign Data, Technical Note 1: Task 1 Report, version 1, 24/5/2019.
RD5	PolarIce: Mission Performance Simulator Description and Results, PICE-CLS-TN-0004 , Issued 2018 Aug.23

FORM-NT-GB-10-1

List of Contents

1. Introduction

In the first work package (WP1), the objective was to provide ESA with a snapshot of the user requirements and with the context of 2025 Earth Observing System for a potential future polar altimetry mission. The study was performed accounting for the specificities of the cryosphere areas (ice sheets, glaciers & sea-ice) along with the oceanic surface.

The objective of this second work package (WP2) is to examine level 1 and level 2 preliminary product definitions listed in the Mission Requirement Document [RD3]. Afterwards, to describe/discuss the associated algorithms necessary to derive the geophysical parameters present in the products. The choices of level-1 and level-2 processing applied on altimeter measurements are crucial for optimizing the processing of the different measurements acquired over the various surfaces and the optimization of the geophysical retrieval performances.

The observation system will also be reviewed, mainly: the altimeter operating modes and its expected performances, the orbit and its spatial/temporal sampling, the need for a radiometer and finally the synergy with the future constellation. Requirements present in the MRD regarding these aspects will also be discussed. The final objective of this task is to provide expert feedback and new inputs and elements to the Mission Requirements Document.

2. Level-1 products & processing

2.1. Introduction

With the Delay-Doppler operating mode that will be implemented on CRISTAL mission (heritage from Cryosat-2 and Sentinel-3), the interest for exploring different level-1 processing options must be introduced. It was not the case for conventional altimeters, for which waveforms are formed on-board with the consequence that only the retracking algorithm (at level-2) has to be adapted to the observation of a particular surface. For Delay-doppler altimetry, various L1 SAR processing configurations can be foreseen and can be considered depending on the observed surface. A clear consensus is now emerging on the algorithms that should be applied. They will be implemented in the coming months/years for the current missions (Cryosat-2 and Sentinel-3 A&B). We propose in this section to review the different Level-1 algorithms, their potential benefits, applicability and drawbacks. Of course, further analyses will be mandatory to clearly qualify and quantify their respective benefits. It is finally important to note that these Level-1 processing choices do not modify drastically the structure of the level-1 product which is presented hereafter.

2.2. Level-1 products

Based on historical mission products, the table below describes the different categories of parameters that will be present on the level-1 products:

Parameters(s)	Comment
Time tag	Time related variables and corrections (uso)
Location	Location variables (lat, lon, surface type, ...)
Orbit and attitude	Orbit and attitude related variables (altitude, mispointing, velocity)
Navigation bulletin	
Altimeter & tracker configuration	Configuration of the altimeter IRIS (Mode, Instr., …) & tracker
Altitude commands H0 and COR2	Altitude commands
Range related variable	Tracker range and related corrections
Doppler beams related variables	Variable related to the stack doppler beams (doppler angles, numbers of waveforms summed in stack…)
Waveform related variable	Waveforms and all variables related (scale factor, flags, …)

Table 1: Categories of parameters present at level-1

<u>Time tag category</u>

Variables related to the datation of the measurements, relative to UTC.

Location category

Variables related to the location of the measurements, namely: latitude/longitude at nadir regarding a reference ellipsoid such as WGS84.

Orbit and attitude category

Variables related to orbital parameters:
- Altitude and radial velocity
- Platform mispointing from startrackers instruments (roll / pitch / yaw)
- Vector position in a geodetic frame (X/Y/Z)
- Vector velocity in a geodetic frame (X/Y/Z)

Altimeter & tracking configuration category

Variables related to the altimeter & tracking configuration, we can expect flags to indicate:
- Altimeter operation mode for each Ku/Ka band: SAR closed-burst / SAR open-burst / SARIn closed-burst / SARIn open-burst
- Activation/Deactivation of the on-board RMC
- Tracking operation mode: closed-loop / open-loop

Altitude commands category

Variables related to the tracking commands H0 & COR2:
- H0: reference altitude computed from on-board DEM (open-loop) and/or retrieved from closed-loop
- COR2: radial velocity computed from on-board DEM (open-loop) and/or retrieved from closed-loop

Range category

Variables related to the altimeter range:
- Tracker range, computed from H0 & COR2. We can expect different tracker ranges, depending on (P)LRM & SAR/SARIn modes.
- Ultra Stable Oscillator (USO) correction
- Internal path delay correction
- Doppler correction, only in (P)LRM, as it is directly applied to the stack during level-1b processing in SAR mode

Doppler beams category

Variables related to the stack in SAR/SARin modes, including:
- Number of Doppler beams stacked to generate the SAR/SARIn waveform
- Look angles of each Doppler beams
- Potential statistics on the stack Range Integrated Power (RIP): standard deviation, kurtosis, skewness…

Waveforms category

Category including the waveforms themselves, in all possible modes (LRM/SAR/SARIn/FF-SAR) and bands (Ku-Ka), in addition with scale factors. In SARIn mode, coherence and difference phase vectors will also be available in the products

2.3. Level-1 processing

2.3.1. Delay-Doppler processing description

<u>SAR unfocused processing</u>
Different doppler processing can be considered to exploit the measurements obtained by a Delay-doppler altimeter such as CRISTAL, of course with different benefits and expected performances. The "SAR-altimetry" or "delay-Doppler altimetry" is a recent technique to process altimetry data. It was first operationally implemented in the CryoSat-2 mission, launched in 2010. SAR-altimetry is for a large part a question of processing.

Compared to conventional altimetry (or "LRM": Low Resolution Mode) radar waves (or pulses) are emitted at a higher rate (~18 kHz Pulse Rate Frequency (PRF) for Sentinel-3 instead of about 2 KHz in conventional LRM). At such a rate, the phase of the signals remains relatively constant along consecutive pulses. Since the satellite is in motion, ground reflectors backscatter the emitted signals at different frequencies, depending on their along-track locations. This is caused by the Doppler effect on which SAR-altimetry relies. A Fast Fourier Transform applied to a pack (or burst) of consecutive reflected pulses (time dimension) discriminates the surface sampled on different Doppler strips on ground (frequency dimension). In practice, **unfocused SAR altimetry processing** is usually applied to bursts of 64 pulses. The radar wave footprint is thus split in 64 Doppler strips (or cells) **about 300 meters-wide** in the along-track direction. (Sentinel-3A / CryoSat-2 configurations).

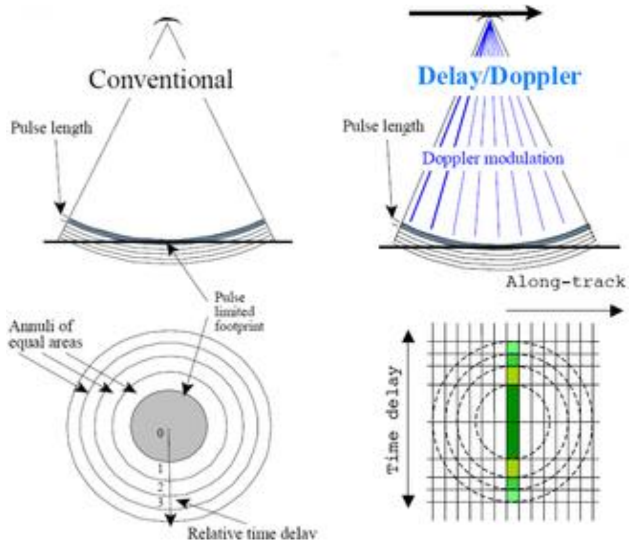

Figure 1: Comparison between conventional radar altimeter (left) and Delay Doppler/SAR (right) altimetry. Credits R.K. Raney, Johns Hopkins University Applied Physics Laboratory.

In the Sentinel-3 / CryoSat-2 configurations, a given Doppler strip is seen in the radar footprint during 2 seconds approximately. Hence, a same Doppler strip on ground can be sampled at different satellite locations. The combination (or "stacking") of different samplings of the same Doppler strip allows speckle noise reduction. This method is called the multi-looking processing. It improves the precision of the estimated geophysical parameters. For instance, the noise level on the Sea Surface Height estimated from Sentinel-3A (SAR altimetry) is 25% lower compared to Jason-3 (conventional altimetry).

Globally the unfocussed processing appears to be valuable over all surfaces, significantly improving the performances on several cases compared to conventional LRM. Over sea-ice & inland waters, the reduction of the along-track footprint can be very beneficial for better discriminating the surface heterogeneities (river, leads). Over ice sheets, it allows to be non-sensitive to the along-track slope-induced errors, and in addition the waveform leading edge is less sensitive to volume scattering.

Unfocused SARIn processing

The SARIn processing relies on the same processing as the unfocused SAR. The exploitation of the phase coherence along a burst of 64 pulses emitted at high frequency allows to reach a fine along-track resolution. In addition, the signal emitted by a single antenna is received by two antennas, and the phase difference between the received signals is used to determinate the location of the scatterer through the across-track direction. Nevertheless, several constraints exist, notably due to surface ambiguities on the received signal [Gray et al., 2013].

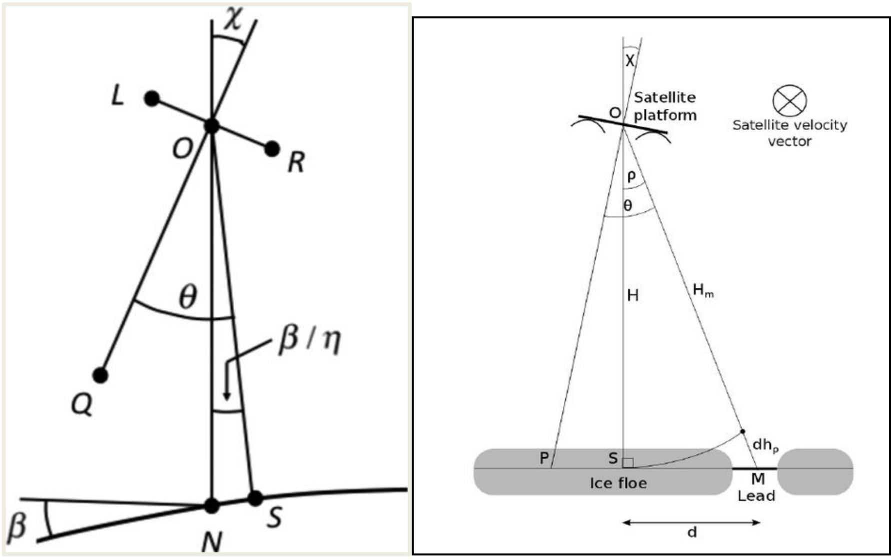

Figure 2: Illustration of SARIn measure over ice sheets (left) & sea-ice (right)

The processing is particularly efficient over steep surfaces of the ice sheet margins, where the Point Of Closest Approach (POCA) can be shifted upslope by dozen kilometres [McMillan et al., 2017]. As illustrated in the above figure, the phase difference is used to determine the across-track look angle β, where the signal originates, at POCA location. Over the ice-covered ocean, SARIn mode is valuable to improve our knowledge of the lead location within the SAR footprint. In fact, in LRM or SAR altimetry, the estimated range associated to a lead is computed considering a nadir reflection. Off-nadir lead creates therefore a positive bias of the altimeter range and consequently tends to underestimate the sea level heights (which also has consequences in the estimation of ice freeboard and thickness). The above figure (right) illustrates the problematic. The same utility is observed over inland waters, being as well an area with high contrast between river and land surfaces.

Finally, a preliminary study performed at CLS showed the capacity of the SARIn mode to capture the relative strong cross-track slopes induced by the Mean Sea Surface. But the cross-track slope noise is currently large as it stands, and probably prevents from reaching signals linked to oceanic dynamics. Dedicated processing strategies and efficient noise filtering are perspectives that might improve the estimation.

FF-SAR processing:

The Fully-Focussed SAR is a very promising level-1 processing introduced by [Egido, 2016], that dramatically reduces the along-track resolution compared to LRM and even SAR unfocused modes. FF-SAR waveforms are obtained by performing a coherent integration of the altimeter echoes along the entire illumination time of a scatterer on the surface. For instance, the altimeter configuration of Sentinel-3 allows to reach an along-track resolution of ~50cm. The relevance of this processing has already been demonstrated particularly when measuring stationary and highly reflective backscattering surfaces (sea ice leads and hydrology surfaces). This algorithm offers great advantages **especially if** the instrument is operating in SAR interleaved mode. The interleaved mode (including SAR and SARin) is already proposed for sea ice regions as specified in the Polar Ice Mission Requirement Document (MR-OBS-200) fulfilling the requirement to detect sea-ice leads with dimensions of 10 to 30 m wide centered on a ground track.

Considering the closed burst operation mode of the current SAR altimeters instrument (Cryoat-2 & Sentinel-3), it imposes a lacunar sampling of the Doppler spectrum. This results in sidelobes in the full along-track point target response, creating replicas of specular targets along the track. Figure 2 shows the along track point target responses obtained with SAR processing. An interleaved mode would provide the along track PTR in red at the center of the figure (sinc function with first zero at doppler frequency equal to $1/T_{illumination}$, zoom on the bottom right figure). In closed burst mode, secondary lobes appear (in blue) equally spaced by 1/Burst_Repetition_Interval. The amplitudes of the side lobes are modulated by the along track unfocused Point Target Response (sinc function with first zero at $1/T_{burst}$). Considering an interleaved mode, BRI would be equal to T_{burst} and the side lobes will move to the zeros of the unfocused PTR.

For Sentinel-3 instrumental features (altitude, closed burst mode, PRF, …), the width of the FFSAR along track PTR is equal to 0.51 m (corresponding to the along track resolution), the side lobes appear at regular intervals of 94.35 m and the zeros of the unfocussed SAR PTR are at 334.6 m.

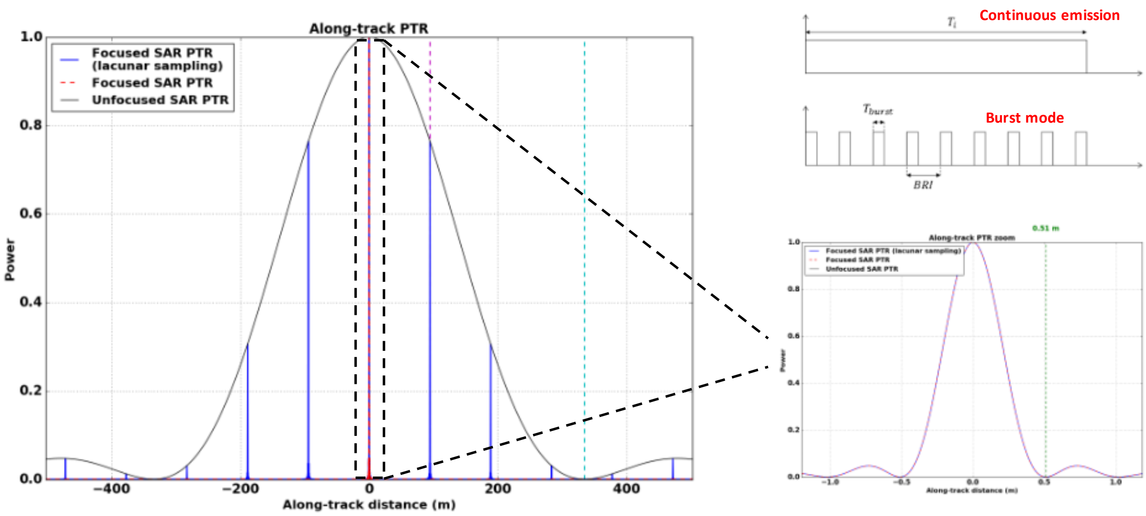

Figure 3: Along Track Point Target Responses with focused and unfocused processing.

For CRISTAL, FF-SAR is supposed to be activated over Sea-Ice areas, where the altimeter will operate in open-burst (or interleaved) mode. Therefore, replicas will be avoided, which will be extremely beneficial to prevent errors when discriminating specular leads on-ground. However, the retained configuration over inland water surfaces, is the Closed burst mode. The impact of such a configuration of the observed echoes can be seen in the following figure obtained with Sentinel-3. This is the Sentinel-3 radargram obtained with a fully focused processing applied over a small pond (70 m width in the along-track direction). The pond is clearly seen on the echoes but “replicas” are also observed spaced by about 100 m as described previously. Such replica can certainly be processed to isolate the main return when coming from an unique reflective surface with well-known position. The problem is more complex over complex hydrological zones, complex sea ice configurations or when the surface is larger than the distance between replicas (> 100m).

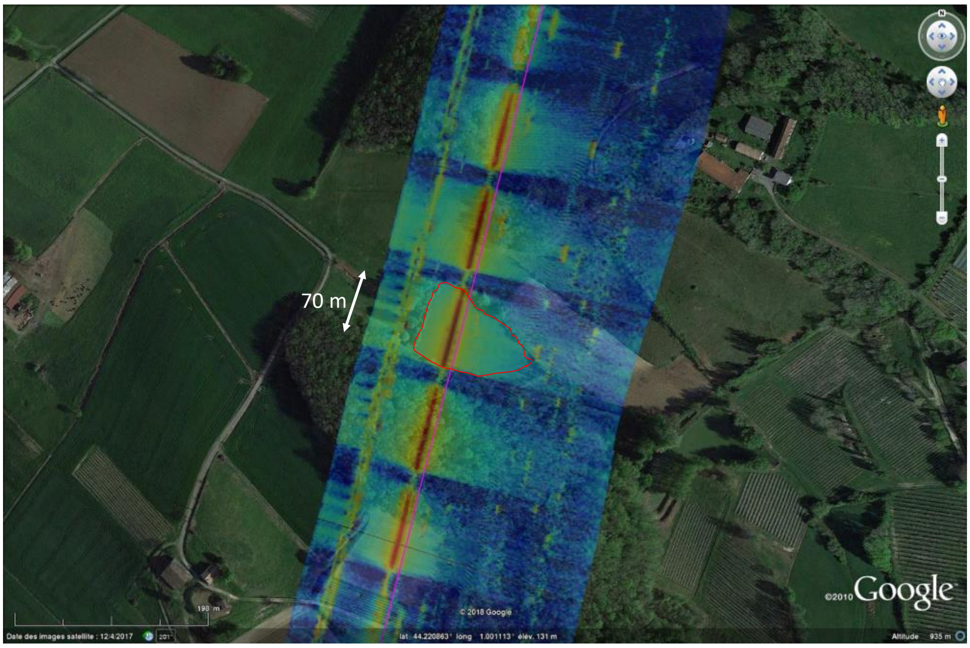

Figure 4: Illustration of the radargram obtained by fully focused processing on Sentinel-3A overflying a very small pond (70 m under the S3A track)

The replicas that are seen in Figure 3 would be removed in the interleaved configuration. It is worth recalling that Cryosat-2 and Sentinel-3 A/B instruments have been designed considering a closed burst approach while the new generation of instrument, Sentinel-6 in particular, will operate in “interleaved mode”. **According to us, in order to fulfil the requirements of the PolarIce mission, it is thus important to consider the interleaved instrumental configuration not only for sea ice regions but also for ocean and inland water surfaces.**

The FF-SAR along-track resolution is given by [Curlander & McDonough, 1991]:

AzRes = (1/DB) * Vsat = L/2

With: L = Antenna diameter
Vsat = satellite velocity
DB = Doppler Bandwidth

Therefore, the finest along-track resolution that can be reached in FF-SAR will be ~70cm, in both Ku & Ka bands. Nonetheless, this resolution is reached if there is no “Doppler ambiguities” occurring, such as the ones that will happen in the future Sentinel-6 measurements. Doppler ambiguities happened when the digitized signal is not sampled at a rate above the Nyquist frequency, concretely when PRF is lower than the Doppler Bandwidth. The high PRF of CRISTAL (18 kHz) will allow to avoid Doppler ambiguities. On the other hand, the longer window analysis will increase the illumination time and therefore, a precise assessment of this configuration should be performed.

In the FF-SAR processing, it is possible to adjust the along-track resolution, which will depend on the number of individual pulses kept for the coherent integration. An increase of the along-track resolution allows in counterparts to cumulate different looks of the same sampled surface, reducing speckle noise by multi-looking (similarly to classical unfocused SAR). Therefore, the optimal along-track resolution of the potential CRISTAL FF-SAR processing will probably be a trade-off between ~70cm and a hundred of meters. Future studies will be required to determine this optimal along-track resolution for sea-ice needs. The processing should also be considered for hydrological surfaces.

It is also important to consider how such an algorithm can be implement or not in an operational ground processing with limited CPU availability. In the case of FF-Sar processing, the more the along-track resolution is reduced, the more the processing will be time consuming. In this respect, it is important to note that Guccione et al. [2018] developed an innovative method to perform delay-Doppler processing, solving the high computational effort required. The processing is named Omega-kappa and is an “efficient focusing algorithm for high PRF radar altimeters that is performed in a two-dimensional wavenumber domain”. <u>It is important to note that such a processing could also be used for the SAR unfocused</u>. First tests are ongoing at CLS and results are very promising, showing a CPU time reduction of a factor 500, in line with metrics given by Guccione et al. [2018], without any performance degradation on level-2 geophysical estimations. Such an innovative processing should be considered for the future CRISTAL ground segment.

<u>LR-RMC processing:</u>

The Low Resolution Range Migration Correction (LR-RMC) is a processing initially developed by Thales during the on-ground tests. The concept was recently taken over by CLS/CNES, and new developments were made to improve it, along with the calibration/validation of a long time series of Sentinel-3A data. The figure below is a diagram describing the processing which is basically much more simple than other UF-SAR or FF-SAR processing:

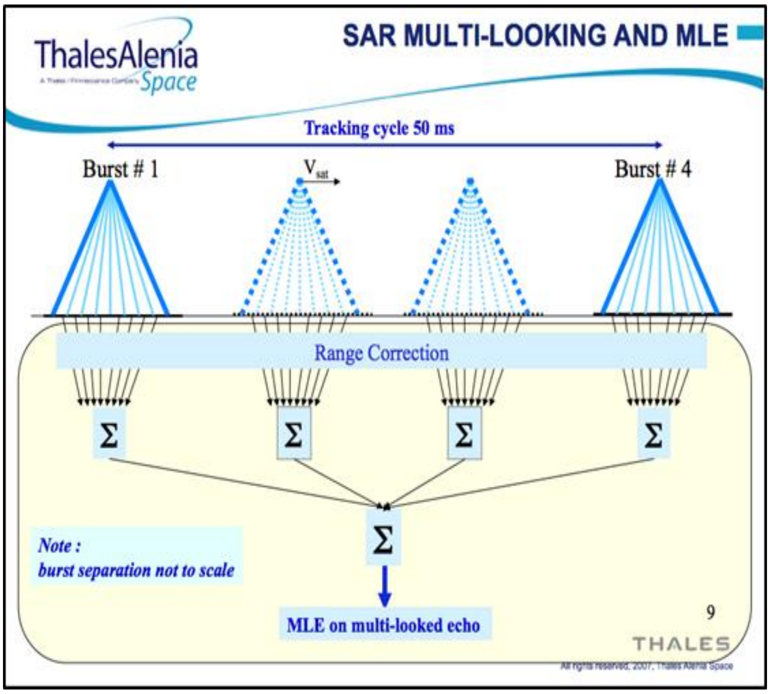

Figure 5: Processing scheme of the LR-RMC processing (credit to Thales)

FORM-NT-GB-7-1

In a nutshell the LR-RMC consists in performing the delay-Doppler processing on the bursts contained within a radar cycle (4 bursts in the Sentinel-3A configuration). Each doppler beam generated are range migrated to account for slant range corrections. The 64 Doppler beams contained in a Delay Doppler Map (DDM) are then summed to produce intermediate waveforms for each burst. Finally, the LR-RMC waveform is the summation of these intermediate waveforms.

The resulting LR-RMC footprint is very different from the SAR unfocused one. In fact, as all the Doppler bands of the Delay Doppler Map are aggregated, it is very similar to the LRM footprint. This is illustrated in the figure below. Nevertheless, as range migrations are applied to the Doppler beams, the across-track surface returns have less influence in LR-RMC compared to LRM.

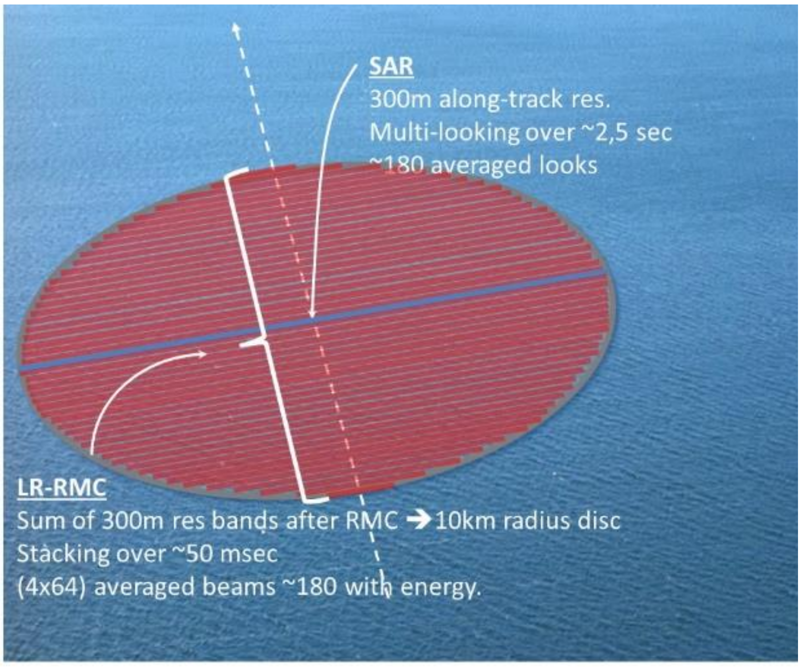

Figure 6: Illustration of SAR & LR-RMC footprints over ocean

First calibration / validation studies performed on two years of Sentinel-3A data have shown extremely promising performances, with a good global agreement with SAR unfocused and:

- Measurement noise reduction in SWH & SSH (~15% for SSH & SWH, at 2 meters SWH)
- In contrast to the SAR unfocused mode, measurement noise is not sensitive to swell conditions. There are ongoing studies regarding potential biases.
- Spectral analysis:
    - Large noise reduction on high frequency content (correlated with first result)
    - Despite its large footprint, no observable short wavelength correlated errors (bump)
    - ⇨ **As a result, mesoscales signal could be better resolved**
- Compared to SAR unfocused mode, a slight degradation is expected over coastal areas. First results show the degradation are negligible.

Studies are still ongoing at CLS/CNES to improve the LR-RMC processing and its level-2 retracker. Products will be generated & distributed to the community in October 2019 for an independent assessment and collecting feedback from users. The processing will also be renamed soon, as its current name is confusing with the “on-board RMC” of Sentinel-6.

The LR-RMC processing is not identified to be implemented in the CRISTAL ground segments. But it could be a relevant option to consider for open ocean, and it will be carefully studied in the following years.

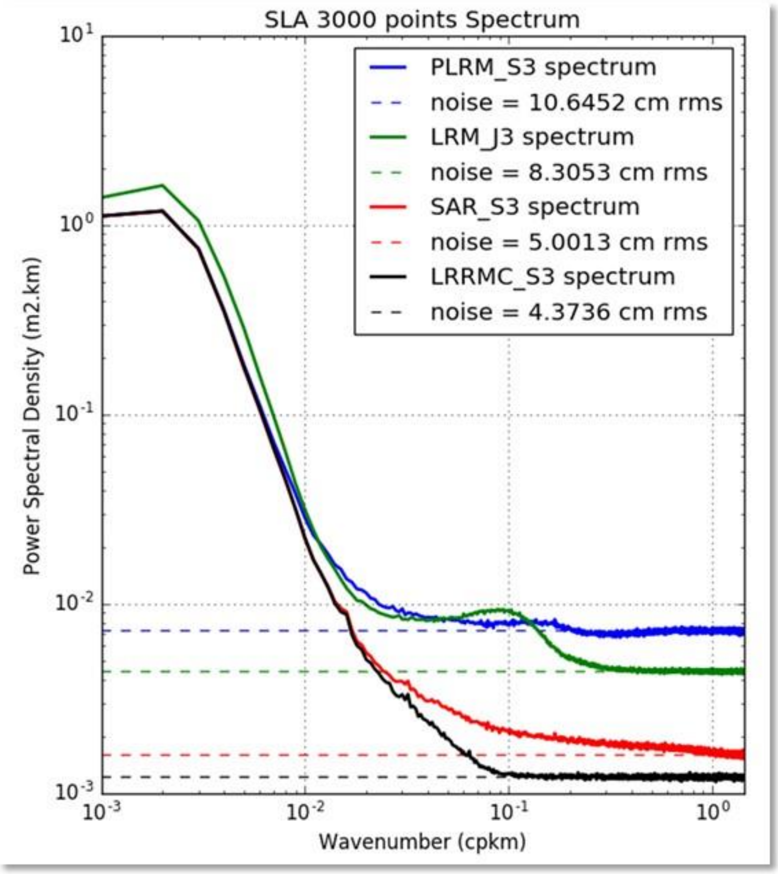

Figure 7: SLA spectrum for the current altimetry modes (LRM / PLRM / SAR & LR-RMC)

We can note, that this processing has been evaluated in the frame of the ESA Sea State CCI project, on Sentinel-3 dataset. It has been evaluated in comparison with other processing solutions and it has been awarded after the Round Robin exercise, as the winner algorithm able to provide the best global performances in terms of accuracy, precision, data availability, spectral analysis, comparison to in-situ dataset (buoys).

2.3.2. Specific level-1 processing

Hamming processing

The main advantage of Delay/Doppler radar altimeters with respect to conventional altimeters is that the along-track footprint size is significantly reduced by exploiting the coherence between the pulses in order to synthesize a narrower antenna. The beam-forming step (azimuth FFT) leads to a sinc-like azimuthal impulse response, as shown in the figure below. This impulse response has relatively high side lobe levels (about -13 dB below the peak power for the first side lobe) and may not be adequate over highly specular surfaces such as sea ice and calm waters. In fact, strong nadir backscattering induces high levels of energy that spread into side lobes and leads to clutter in off-nadir pointing beams. Eventually, waveforms are impacted (especially the leading edge) and it may alter geophysical parameter retrievals.

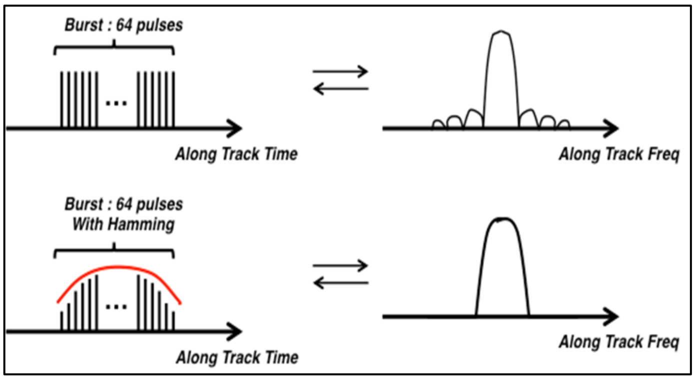

Figure 8: Schematic of the along-track weighting method with a Hamming window

This method has, in turn, the undesirable consequence to degrade the along-track resolution. This drawback is inevitable because reducing side lobes levels of a given window automatically widens its main lobe. However, this degradation remains relatively modest, a factor of 1.486 is mentioned in Scagliola et al. [2017]. For instance, Hamming weighting window applied in the CRISTAL level-1 processing in Ku-band would produce Doppler bands of 446 meters width instead of 300 meters without Hamming weighting applied (see section 5.4.1 for more details regarding along-track resolution).

The figure below shows Sentinel-3A echograms obtained over a sea-ice region in the Arctic in December 2016 with and without Hamming function applied:

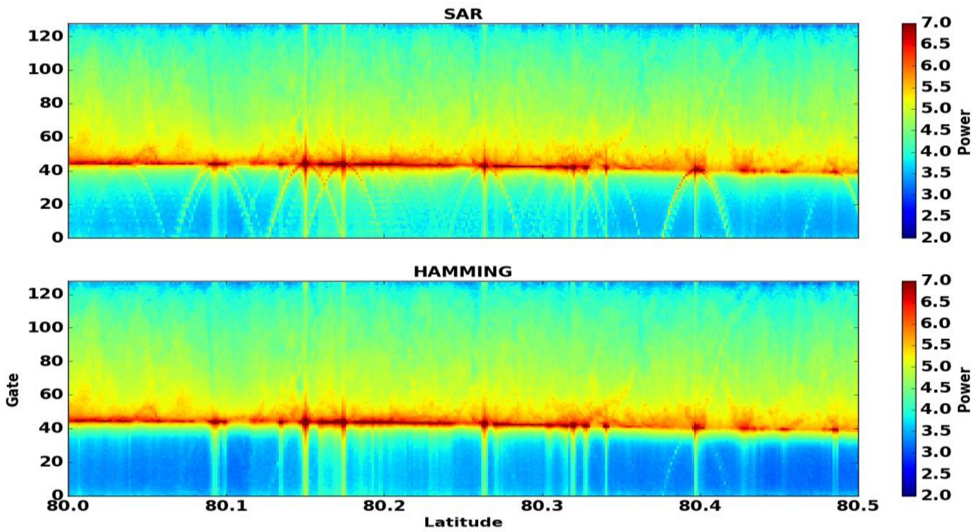

Figure 9: Echograms over a sea-ice region (Arctic pass 604) in December 2016

The echograms contain very energetic and peaky waveforms induced by highly specular surfaces (leads, melted water lakes, etc.). The conventional SAR echogram (top) is affected by the usual spurious effects contaminating the leading edge of waveforms whereas the Hamming echogram (bottom) is not.

Applying along-track Hamming weighting has proved to be beneficial for the observation of regions presenting high contrasts of sigma0, such as sea-ice areas and inland waters.

On the other hand, it has no particular interest over open ocean, and also most probably over ice sheets.

Zero-padding processing

The waveform over-sampling method has been initially mentioned by [Jensen, 1999], who remarked that oceanic waveforms obtained with conventional altimeters may be prone to aliasing artefacts, arising from the magnitude squaring step. It was also suggested that oversampling the complex signals before squaring with a zero-padding method could, to some extent, solve the issue. A recent study by [Smith & Scharroo, 2015], based on CryoSat-2 PLRM data, confirmed that zero-padding improves performances over ocean by reducing the noise level (small but non-zero biases are nevertheless introduced). However, it remains unclear whether the observed improvements are attributable to aliasing removal or simply doubling the number of data points to be fit in the geophysical modelling.

This method is particularly helpful over very specular surfaces (over leads in sea-ice and calm inland waters for instance), and is even more relevant for SAR-mode altimetry, given the peakier nature of SAR waveforms compared to the LRM ones. The zero-padding oversampling method is currently implemented in CryoSat-2 IPF (since Baseline B) to address the poor representation of the waveform peak over sea-ice regions. A clear recommendation from the Sentinel-3 ESL group (output of the S3 ESL meeting held in Toulouse in September 2019) is to implement a zero-padding processing into Sentinel-3 IPF processing chains for optimizing performances over sea ice surfaces and hydrological zones.

Although the sampling rate is doubled with this method, the range resolution remains the same since it is determined by the instrument impulse response. The zero-padding interpolation creates new samples but does not create any additional information. Besides, it could generate unwanted bin-to-bin correlation. Furthermore, over highly specular surfaces, complex I&Q signals may be impacted by aliasing even before the squaring step and therefore oversampling will not help.

2.3.3. Ground segment processing maturity definition

In this technical note, the maturity level of the level-1 / level-2 ground segment processing is addressed. The analysis is based on the Scientific Readiness Levels (SRL) Handbook from ESA [RD5]. The figure and table below provide an overview of the SRLs:

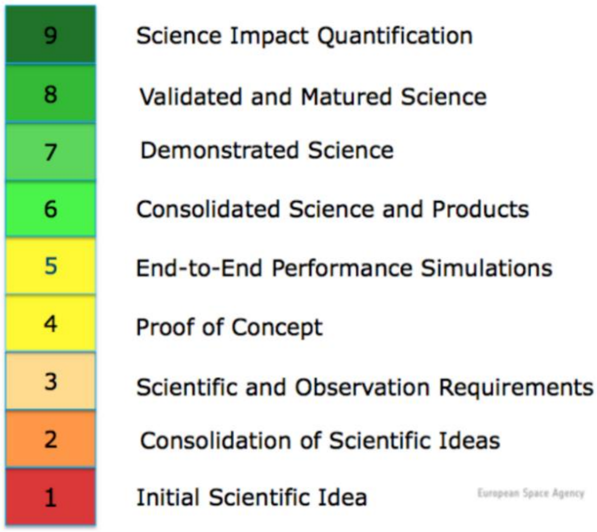

Figure 10: Extracted from the SRL Handbook from ESA: high-level illustration of the SRL scale in the context of the progression from basic research to matured science in (operational) applications in relation to the Phases of an EO mission.

SRL	Name	Experiments	User & requirements
1	Scientific Idea	No observational evidence is required.	- The application area is defined. - Interest of the users is identified. - Start defining high-level scientific requirements.
2	Consolidation of scientific idea	- Experimental evidence supporting the scientific hypothesis.	- Consolidated scientific requirements are established. - A gap analysis with respect to the uniqueness of measurements and observations is performed. - Scientific objective are formulated.
3	Scientific Observation Requirements definition	- Initial capability assessment performed. (Information content analysis) - Conceptual measurement technique is established.	- Scientific objective confirmed and approved. - Scientific goal formulated. - Mission objective(s) formulated.
4	Proof of concept	- First measurement device approximating the instrument is available in case possible for the measurement principle. - Sensitivity of measurements wrt observation is demonstrated.	- Mission objective confirmed and translated into mission requirements and system requirements

FORM-NT-GB-7-1

5	End to end performance simulations	- Demonstrator (e.g. airborne instruments) provides/simulates representative measurements with error budgets, - Draft calibration strategy available.	- First evaluation of observations and / or measurements in applications, - Higher-level products approached.
6	Consolidated science and products	- Test data and sampled data processing - Verification data sets collected - Calibration and validation Plan established	- User studies with simulated or precursor data; - AO call to user community for validation
7	Demonstrated science	- Cal/Val conducted (L1 and L2) - Early release of first data / demonstrational data are provided - Characterisations of measurements and observations; - Performance vs. Specification	- User feedback collected, - Feedback from beta-users received.
8	Validated and matured science	- Systematic validation and quality assurance performed - Operational / nominal processing of measurements and observations	- Science impact quantification, - first performance assessment wrt mission objective - scientific goal evaluation
9	Science impact quantification	- Generation of long-term data sets - Data fusion	- User impact quantification, - Final performance assessment wrt mission objective - Final performance assessment wrt science objective

Table 2: Extracted from the SRL Handbook from ESA: Overview of the Scientific Readiness Levels (SRLs).

Considering that SRLs are established for a satellite mission concept, or a satellite instrument concept, they are not fully transposable to a ground segment algorithm. Therefore, we propose to use the SRLs to define the maturity level of the ground segment algorithms based on:

- The high-level definition of the SRLs (Figure 10)
- The elements mentioned in red color in the table above (Table 2: overview of the SRLs)

2.3.4. Maturity level of the level-1 algorithms

Below are discussed the maturity level of each level-1 processing described before:

- <u>SAR unfocused</u> => <u>SRL 9</u>

SAR unfocused altimetry can now be considered as a complete mature processing mode as it is currently used by two operational missions (Sentinel-3A & Sentinel-3B). Many studies have validated the concept and proved the benefits with Sentinel-3 acquisitions.

- **LR-RMC => SRL 7**

LR-RMC is not yet completely mature as it still requires assessment over long time series by the scientific community and a dedicated publication. Nevertheless, many studies have been conducted by CLS/CNES, with results presented at different scientific conferences (OSTST in particular). As already said, performances are very promising over open-ocean. Recently, a 2-year dataset was processed, followed by an exhaustive CalVal phase. A SGDR dataset will be delivered to scientific users in October 2019, CMEMS will assess the processing in early 2020 and a scientific publication is in preparation.

- **Fully-focused SAR => SRL 6**

FF-SAR cannot be yet considered as mature, as no extensive dataset have been produced from our knowledge, and therefore no exhaustive CalVal has been performed. Nonetheless, several scientific groups have implemented the processing and demonstrated the benefits, with a few scientific publications available. The CPU time remains a challenging aspect to be addressed for an operational implementation.

- **SARIn mode => SRL 9 (for ice sheet margins)**

The SARIn altimetry mode has been successfully introduced in the CryoSat-2 mission. The benefit has been demonstrated over the ice-sheets sloping surfaces and over long time series, providing extremely valuable information for ice sheets mass balance studies. However, the value over sea-ice is not yet clearly demonstrated as CryoSat-2 is not operating in this mode over the ice-covered ocean (except for punctual acquisitions).

- **Zero-padding** => **SRL 8:**

The processing is currently successfully implemented in the CryoSat-2 ground segment in SAR & SARIn modes. A recent study funded by ESA (S3CD contract) and conducted by CLS proves the value of this processing over sea-ice & inland waters. Several scientific publications also corroborate these results. A dedicated study, conducted over a long time period, is probably missing in the literature to shift the SRL maturity at level-9.

- **Hamming** => **SRL 8** => *Same comment than Zero-padding.*

The table below summarizes the maturity levels attributed to the level-1 processing previously described:

	delay Doppler processing				Specific	
Level-1 processing	**SAR unfocused**	**LR-RMC**	**FF-SAR**	**SARIn**	**0-padding**	**hamming**
SRL level of maturity	9	7	6	9	8	8

Table 3: SRL maturity for the level-1 processing

FORM-NT-GB-7-1

2.3.5. Level-1 processing recommendations

The table below summarizes our recommendations for each delay-Doppler processing & specific level-1 processing, depending on the surface:

		Ocean	Ice-sheets	Sea-Ice	Hydrology
Delay Doppler Processing	SAR unfocused				
	LR-RMC				
	FF-SAR				
	SARIn				
Specific L1 processing	Zero-Padding				
	Hamming				

Table 4: Summary table of the level-1 processing relevance for each surface:

Green: recommended; Red: Not recommended; Orange: to be studied; Gray: no specific positive/negative impact

Below, we make a summary of these recommendations:

- For now, **SAR unfocused** is recommended everywhere. The narrow doppler Band (~300m along-track) is definitely valuable over sea-ice, hydrology & ice sheets. Over ocean several limitations exist, in particular the sensitivity to swell, but the measure can be still useful to resolve fine topographic scales.
- **LR-RMC** is recommended only over ocean, because the larger footprint compared to SAR provides degraded performances over heterogeneous surfaces requiring fine spatial sampling (sea-ice & hydrology), or over surfaces subject to large topographic variations (ice sheets)
- **FF-SAR** is clearly valuable over surfaces that require a fine ground sampling (sea-ice to measure leads within floes; hydrology to measure river/lakes). Over ocean & ice sheets the benefit has to be demonstrated.
- **SARIn** should be particularly valuable over ice sheet surfaces, especially the margins, to precisely locate the POCA on ground. Over sea-ice & hydrology it will allow to determine more precisely the location of the specular returns (leads/river) within the footprint. Over ocean first analyses show the interferometric phase measure is too noisy to estimate a precise across-track slope (and derive a potential cm/mm bias due to the oceanic across-track slope), but this deserve more investigations.
- **Zero-Padding** processing is particularly useful for specular waveforms as measured over sea-ice & hydrology surfaces, to better samples peaky waveforms leading edge and avoid waveform aliasing.
- **Hamming** processing is also useful for specular waveforms, over regions presenting high contrasts of Sigma0 (sea-ice & hydrology) to remove spurious energy spread by the azimuthal impulse response on the Delay Doppler Map. On the other hand, it has no particular interest over open ocean, and even slightly degrades the SLA spectrum because of the Doppler band overlap created by the along-track resolution expansion (~450m with hamming instead of ~300m without).

FORM-NT-GB-7-1

2.3.6. Delay-Doppler processing achievability depending on CRISTAL operating modes

The table below summarizes the planned CRISTAL operating modes by Thales, as function of the surface sampled. The operating mode (chronogram) directly condition the delay-Doppler processing possibilities as detailed further. A red cross indicates that the delay-Doppler processing will not be possible (or exploited optimally) with the proposed mode.

		Ocean	Ice-sheets	Sea-Ice	Hydrology
CRISTAL operation modes	Ku band	SAR-CB	SARIn CB	SARIn-OB	SAR-CB
	Ka band	SAR-CB	SAR CB	SAR-OB	SAR-CB
Delay Doppler Processing	SAR unfocused	✓	✓	✓	✓
	LR-RMC	✓			
	FF-SAR	✗	✗	✓	✗
	SARIn	✗	✓ Ku	✓ Ku	✗

Table 5: CRISTAL operating modes as a function of the surface sampled, with colours corresponding to the same recommendations as the above table. Tick/cross indicates the delay-Doppler processing achievability.

CB = Closed Burst; OB = Open Burst (interleaved)

In a nutshell:

- Unfocused SAR mode will be possible over all surfaces and for both Ku/Ka bands
- Unfocussed SARIn mode will be possible in Ku band, over ice sheets & glaciers
- FF-SAR is theoretically possible over all surfaces, but is only efficient with an interleaved chronogram (to avoid replicas, see paragraph below dedicated to FF-SAR). The processing is therefore recommended only over sea-ice areas but could be discussed over other surfaces if the replica problem can be mitigated.
- Moreover, LRM measurements are possible with an interleaved chronogram, while a closed-burst chronogram will provide P-LRM measurements (such as Sentinel-3 or Cryosat-2), because fewer uncorrelated pulses are aggregated within a radar cycle.
- For hydrological surfaces we recommend:
  - Interleaved chronogram: to enable FF-SAR processing without replicas
  - SARIn mode: also recommended with a lower priority

Note: Hamming & level-1 processing are not conditioned by the altimeter chronogram

References

Curlander, J. C., and R. N. McDonough, Synthetic Aperture Radar: Systems and Signal Processing, 647 pp., John Wiley, New York, 1991.

Egido, A., & Smith, W. H. (2016). Fully focused SAR altimetry: theory and applications. *IEEE Transactions on Geoscience and Remote Sensing*, *55*(1), 392-406.

Gray, L., Burgess, D., Copland, L., Cullen, R., Galin, N., Hawley, R., and Helm, V.: Interferometric swath processing of Cryosat data for glacial ice topography, The Cryosphere, 7, 1857–1867, https://doi.org/10.5194/tc-7-1857-2013, 2013.

Guccione, P.; Scagliola, M.; Giudici, D. 2D Frequency Domain Fully Focused SAR Processing for High PRF Radar Altimeters. *Remote Sens.* **2018**, *10*, 1943.

Jensen, J.R "Radar altimeter gate tracking: Theory and extension," IEEE Trans. Geosci. Remote Sens., vol. 37, no. 2, pp. 651–658, Mar. 1999.

McMillan, M., Shepherd, A., Muir, A., Gaudelli, J., Hogg, A. E.,and Cullen, R.: Assessment of CryoSat-2 interferometric andnon-interferometric SAR altimetry over ice sheets, Adv. SpaceRes., 62, 1281–1291, https://doi.org/10.1016/j.asr.2017.11.036,2017.

Scagliola, M.; Tagliani, N.; Fornari, M. Measuring the effective along-track resolution of CryoSat. In Proceedings of the CryoSat Third User Workshop European Space Agency, Dresden, Germany, 12–14 March 2014.

Smith, W., R. Scharroo, "Waveform Aliasing in Satellite Radar Altimetry", IEEE Transactions on Geoscience and Remote Sensing, Vol. 53, No. 4, April 2015

3. Ice sheets

3.1. Definition of level-1 & level-2 products

In this section, we begin by reviewing the User Requirements Documents [AD1; AD2], the Mission Requirements Document [AD3] and the Technical Note that were delivered as part of Task 1 of this study [AD4], in order to identify a list of Level-1b and Level-2 parameters relevant to ice sheets. We define Level-1b and Level-2 parameters according to the MRD [AD3], as:

Level-1b: Level 1A data that have been quality controlled and reformatted but not resampled. Calibration has been applied. Geometric information is computed, appended but not applied.

For CRISTAL, the principal L1b parameters for ice sheets are the multi-looked (SAR) or incoherently averaged (pseudo-LRM; pLRM) detected waveforms, and associated phase difference and coherence information (Ku-band only). Also included within the L1b product are all the parameters required to compute elevation. These include satellite location, range to the nominal tracking point of the range window, satellite altitude, geophysical corrections, quality flags etc. Level-2 data are defined as:

Level-2: Derived geophysical variables at the same resolution and location as Level 1 source data.

For CRISTAL, the User Requirements [AD1; AD2], and associated Mission Requirements [AD3] documents indicate that the principal Level-2 ice sheet parameter is the surface elevation at the echoing point. Also included within the Level-2 product are parameters required to interpret the data, most notably to compute rates of surface elevation change. These include the waveform parameters sigma-0, leading edge width and trailing edge slope, time tag, the location of the ground reflection and quality flags. In this regard, CRISTAL will inherit from the long heritage of product specification, stemming from ESA's previous polar radar altimeters.

All parameters will (as far as possible given the instrument design) be derived for both the Ku-band and Ka-band measurements. Furthermore, it should also be noted that both Level-1b and Level-2 can be provided at a range of different along-track resolutions, depending upon the delay-doppler processing configuration; e.g. fully-focused versus unfocused SAR.

Identification and traceability of ice sheet parameters

In the Polar Expert Group's proceedings [AD1; AD2], the following list of ice sheet parameters relevant to the CRISTAL mission were identified [AD2, Appendix 4]:

- Ice shelf thickness and extent.
- Ice sheet elevation.
- Ice sheet elevation change.
- Ice sheet mass balance.
- Ice sheet grounding line.
- Ice shelf basal melt.

Most of these parameters, with the exception of Ice Sheet elevation, are derived, higher-level (Level-3) products, which can be computed by the expert user from the altimeter Level-2 elevation measurements themselves (as summarised in the Task 1 Technical Note; AD4). Consequently, at Level-2, the fundamental parameter over ice sheets is elevation, and this is reflected by one of the two primary mission objectives that has been defined for the mission:

PRI-OBJ-2. To measure and monitor the surface elevation and changes therein of polar glaciers, ice caps and the Antarctic and Greenland ice sheets.

This primary mission objective in turn motivates the definition of Mission and Geophysical Product Requirements. We have summarised these in Table 6, and linked them to the principal Level-1b and Level-2 parameters that are associated with each requirement.

MRD ID	Requirement	Level-2 parameters	Level-1b parameters
MRD-020	The mission shall acquire measurements of elevation over sea-ice, land ice, polar glaciers, ice caps and ocean.	Ku-band echoing point location. Ku-band echoing point elevation. Ku-band waveform parameters. Ku-band swath elevation. Ka-band echoing point location. Ka-band echoing point elevation. Ka-band waveform parameters.	Satellite ground track location. Satellite altitude. Interferometer orientation. Ku-band waveform. Ku-band phase difference. Ku-band coherence. Ku-band window delay. Ku-band geophysical & instrument corrections. Ka-band waveform. Ka-band window delay. Ka-band geophysical & instrument corrections.
MRD-110	The payload shall include a SAR Radar Altimeter with the capability of interferometry.	Ku-band echoing point location. Ku-band echoing point elevation. Ku-band waveform parameters. Ku-band swath elevation. Across-track surface slope.	Satellite ground track location. Satellite altitude. Interferometer orientation. Ku-band waveform. Ku-band phase difference. Ku-band coherence. Ku-band window delay. Ku-band geophysical & instrument corrections.
MRD-160	The altimeter shall be capable of operating at two frequency channels.	Ku-band echoing point location. Ku-band echoing point elevation. Ku-band waveform parameters. Ka-band echoing point location. Ka-band echoing point elevation. Ka-band waveform parameters.	Satellite ground track location. Satellite altitude. Ku-band waveform.. Ku-band window delay. Ku-band geophysical & instrument corrections. Ka-band waveform. Ka-band window delay. Ka-band geophysical & instrument corrections.
MRD-230	The altimeter shall be able to measure variations of backscatter coefficient ranging from 0dB to 50dB.	Ku-band sigma-0. Ka-band sigma-0.	Ku-band waveform. Ka-band waveform. Ku-band scaling factor to convert from waveform units to dB. Ka-band scaling factor to convert from waveform units to dB
MRD-240	The altimeter in Ku-band shall be able to measure low backscatter coefficient values down to -10dB.	Ku-band sigma-0.	Ku-band waveform. Ku-band scaling factor to convert from waveform units to dB.
MRD-340	The mission shall be capable of retrieving surface	Time of acquisition. Ku-band echoing point location. Ku-band echoing point elevation.	Time of acquisition. Satellite ground track location. Satellite altitude.

	elevation and surface elevation change over ice sheets, glaciers and ice caps.	Ku-band waveform parameters. Ku-band swath elevation. Ka-band echoing point location. Ka-band echoing point elevation. Ka-band waveform parameters.	Ku-band waveform. Ku-band phase difference. Ku-band coherence. Ku-band window delay. Ku-band geophysical & instrument corrections. Ka-band waveform. Ka-band window delay. Ka-band geophysical & instrument corrections.
MRD-360	The system shall be capable of delivering surface elevation with a horizontal resolution of at least 100 m.	Ku-band swath elevation.	Satellite ground track location. Satellite altitude. Interferometer orientation. Ku-band waveform. Ku-band phase difference. Ku-band coherence. Ku-band window delay. Ku-band geophysical & instrument corrections.

***Table 6**. Correspondence between Mission Requirements and principal Level-1b and Level-2 parameters relevant to ice sheets. Note that each parameter can be provided at different along-track resolutions, depending upon the delay-doppler processing applied, for example fully-focused vs unfocused SAR.*

Regarding the parameter list presented in Table 6, we make three additional comments:

1. The Mission Requirement MRD-360 necessitates greater SAR focussing compared to the current CryoSat-2 configuration (i.e. closer towards fully-focussed SAR), together with swath processing.

2. Within the context of the CRISTAL mission, the capability to measure snowpack penetration, defined as the difference between co-located Ku-band and Ka-band ranges, or elevations, is a key motivator of the mission design; hence it is expected that this may be included as an additional, derived, Level-2 parameter.

3. For conciseness, we do not distinguish between different processing modes within Table 6. Nonetheless, we note that for each identified parameter, it is anticipated that there will be several different variations. Namely, (1) an un-focused, conventional SAR product, with along-track resolution of ~ 300 metres, (2) a fully focused SAR product, with along-track resolution to be determined (in theory less than 1 metre, but in practice likely to be greater to reduce noise), and (3) an incoherently-averaged low resolution product, with along-track resolution of ~ 1.5 – 2 km (pLRM).

3.2. Definition of ground processor algorithms

In this section we identify and review the ground processor algorithms that can be used to generate the ice sheet parameters identified in Section 2.1, together with any associated auxiliary products, with the aim of identifying the state-of-the-art, the maturity and any gaps in current processing algorithms.

In every case, we pay particular attention to both the algorithm's current maturity, and also its expected maturity in 2025, based upon the observing system at that time. Broadly speaking, we categorise algorithms as '**mature**' if they have been used by multiple authors, or in multiple ground segments, over an extended period of time; '**immature**' if they have been used by a single author or ground segment, or are still in a development and testing phase; and '**untested**' if there are no cases where an algorithm has been defined or used to date. For all algorithms, we also provide supporting references, to ensure full traceability. The primary objective of this section is to identify where existing algorithms exist, and where new algorithms are required.

3.2.1. Level-1 processing

In this section, we identify the high-level alternatives of SAR processing that are already in use, or are currently being developed. Because Level-1 SAR processing is still in its relative infancy over ice sheets, there are fewer unique options than for the Level-2 processing. The main differentiator is therefore the overarching processing approach, rather than in the component algorithms within each approach; and so we focus on the approaches themselves here. Furthermore, it is clear that all SAR processing is untested for a Ka-band system in Earth orbit, because none has existed to date. The results of this analysis are presented in Table 7, together with references to the associated algorithms, where relevant.

Processing Step	Processing Approach	Description	Maturity (expected maturity at 2025)	Existing SRL	Algorithm reference (where exists)
SAR processing	Unfocused SAR.	Conventional unfocused SAR processing chain applied to a closed-burst system; as implemented in the CryoSat-2 and Sentinel-3 ground segments; principal steps include (1) determination of doppler beam angles, (2) delay-doppler processing, (3) stacking, (4) geometrical corrections, (5) range compression, and (6) multi-looking.	**Ku**: Mature (mature) **Ka**: Untested (untested)	7 2	Raney, 1998; Wingham et al., 2006. -
SAR processing	Fully-focused SAR.	Improvement of the along-track resolution towards its theoretical limit, using the full along-track illumination period of the ground target.	**Ku**: Immature (mature) **Ka**: Untested (untested)	6 2	Edigo et al., 2017 -
LRM processing.	Conventional LRM processing.	Incoherent processing of radar pulses.	**Ku**: Mature (mature) **Ka**: Mature (mature)	9 8	Wingham et al., 1998; Wingham et al., 2006. AltiKa Algorithm Theoretical Baseline Definition: Altimeter Level 1b Processing, Ref. SALP-ST-M2-EA-15884-CN.

Table 7. Level-1 processing approaches, maturity and traceability over ice sheets.

3.2.2. Level-2 processing

The processing workflow for deriving Level-2 ice sheet elevations from L1b waveforms is mature and full details can be found within numerous expositions, for example:

- CryoSat-2 Product Handbook, Baseline-D 1.0, issued 3/4/2018.
- Bouzinac, C., Technical Report of CryoSat Interferometric Level 2 Processing Algorithms, Version 1.8, 14 June 2004.

The principal steps of Level-2 processing over ice sheets can be summarised as (1) retracking, (2) application of geophysical corrections, (3) sigma-0 estimation, and (4) measurement relocation to the true echoing point; usually defined as the 'Point of Closest Approach' – the location on the ice sheet surface that is within the beam footprint and closest to the satellite.

The purpose of this section is therefore to identify where algorithms currently exist for each of these steps; their maturity, their traceability; and to highlight where new algorithms are in need of being developed. The results of this analysis are presented in Table 8. Following this, we then provide a summary of the auxiliary data products needed for ice sheets Level-2 processing, with a particular focus on the current state-of-the-art. This information is presented in Table 9.

Processing Step	Algorithm	Description	Maturity (expected maturity at 2025)	Existing SRL	Algorithm reference (where exists)
Retracking	Threshold Centre of Gravity	'ICE-1' retracker, as applied in ERS-1, ERS-2, Envisat, CryoSat-2 (LRM; baseline-c onwards), AltiKa and Sentinel-3 ground segments; retracks based on a threshold of the Offset Centre of Gravity amplitude.	**Ku**: Mature (mature) **Ka**: Mature (mature)	9 8	Wingham, 1995; Wingham et al., 1998. Yang et al., 2018; Otosaka et al. (*in review*)
Retracking	Threshold First Maximum	Retracks based on a threshold of the first maximum amplitude; has been applied to both LRM and SAR measurements.	**Ku**: Mature (mature) **Ka**: Immature (mature)	9 7	Davis, 1997; Helm et al., 2014; Gray et al., 2015; Nilsson et al., 2015. Yang et al., 2018;
Retracking	ICE-2	'ICE-2' retracker, currently applied to ERS-1, ERS-2, Envisat and AltiKa; fits a Brown model.	**Ku**: Mature (mature) **Ka**: Immature (mature)	9 7	Brown, 1977; Legresy et al., 2005. Yang et al., 2018; Suryawanshi et al., 2019.
Retracking	SARIn retracker	6-parameter functional fit used to retrack CryoSat-2 SARIn mode echoes; designed to mimic the theoretical echo shape.	**Ku**: Mature (mature) **Ka**: Untested (untested)	8 1	Bouzinac, C., 2004; Wingham et al., 2006. -
Retracking	β-parameter retracker	An empirical formulation, but shows some similarity to the theoretical shape	**Ku**: Mature (mature) **Ka**: Untested (untested)	9 1	Martin et al., 1983. -

		of the Brown-Hayne model.			
Retracking	CFI ocean retracking, based on analytical model fit.	CFI MLE retracking; used to retrack CryoSat-2 land ice LRM echoes.	**Ku**: Mature (mature) **Ka**: Immature (mature)	9 7	Hayne et al., 1980. Yang et al., 2018.
Sigma-0 calculation	Sigma-0 from retracker amplitude.	Standard approach based on the amplitude calculated by each retracker.	**Ku**: Mature (mature) **Ka**: Mature (mature)	9 8	CryoSat L2 Processor Design Summary Document, Issue 6.0, 22nd Nov. 2012, Mullard Space Science Laboratory. AltiKa Algorithm Theoretical Baseline Definition: Altimeter Level 2 Processing SALP-ST-M2-EA-15886-CN.
Echo relocation	Non-interferometric echo relocation using linear slope.	Uses a DEM-based estimate of the linear slope at nadir to relocate the echoing point to the point where the surface is orthogonal to the incident radar beam; used in LRM ground segment processing for ERS-1, ERS-2, Envisat and CryoSat-2 (LRM), and in SAR processing for Sentinel-3.	**Ku**: Mature (mature) **Ka**: Immature (mature)	9 7	Bamber, 1994. Suryawanshi et al., 2019.

Echo relocation	Non-interferometric echo relocation using point of closest approach within the beam footprint.	Uses a DEM to identify the point of closest approach within the beam footprint, and thus relocate the echoing point; advantageous over the previous approach because it accounts for non-linear topography.	**Ku**: Mature (mature) **Ka**: Immature (mature)	9 7	Roemer et al., 2007. Otosaka at al., (*in review*).
Echo relocation	Interferometric echo relocation.	Point of closest approach identified using interferometric phase difference at the retracking point.	**Ku**: Mature (mature) **Ka**: Untested (untested)	8 1	Bouzinac, 2004; Wingham et al., 2006. -
Geophysical corrections	Based on physical model simulations	Typically, corrections are derived from physical models and applied to the range measurement.	**Ku**: Mature (mature) **Ka**: Mature (mature)	9 8	Wingham et al., 2006; CryoSat-2 Product Handbook, Baseline-D 1.0, 3/4/2018; see also summary provided in Table 9. SARAL/AltiKa Products Handbook, SALP-MU-M-OP-15984-CN, Issue 1.2, 12/12/2011.
Swath processing	Interferometric swath processing	Uses interferometric phase difference and coherence at delay times beyond the point of closest approach to map	**Ku**: Mature (Mature) **Ka**: Untested (untested)	8 1	Gray et al., 2013; Gourmelen et al., 2018. -

		elevation across a swath.			
Ku radar penetration	Ku-Ka range difference.	Use range difference between Ku and Ka-band to estimate the Ku-band penetration into the near surface snowpack.	Untested (tested for airborne systems).	4	-

Table 8. Level-2 processing algorithms, maturity and traceability over ice sheets.

Given that the Ku radar penetration may be a novel parameter within the CRISTAL Level-2 product, we discuss this in more detail here. Specifically, assuming that both Ku and Ka reflections occur from the same location on the ice surface, then the difference in the Ku and Ka range – once all instrument and geophysical corrections have been applied – will provide a measure of the Ku radar penetration into the snow surface. This makes the assumption that Ka-band scatters from the air-snow interface, which needs to be confirmed across a wide range of snowpack characteristics, either using simulations or airborne campaigns. It also needs to be assessed whether an estimate of the firn density is needed, in order to account for the change in radar wave velocity within the snowpack at Ku-band; if so, firn densification models may be used for this purpose.

Given the different beam widths of the Ku-band and Ka-band instruments, it is important to note that the assumption that ***both Ku and Ka reflections occur from the same location on the ice surface*** may not always hold, for example in the case where there is a surface reflection that is both (1) within the Ku beam footprint, but (2) out with the Ka footprint, and that this represents the closest point to the satellite. In this case Ku POCA and the Ka POCA will not be the same, leading to an incorrect calculation of the penetration depth (Figure 11), and so a flag must be included within the Level-2 product to indicate such occurrences.

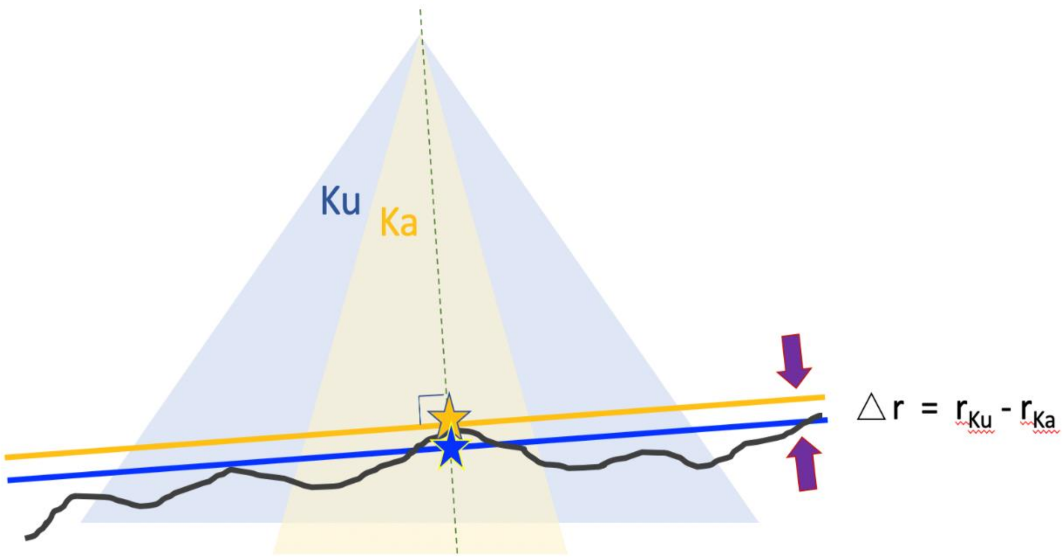

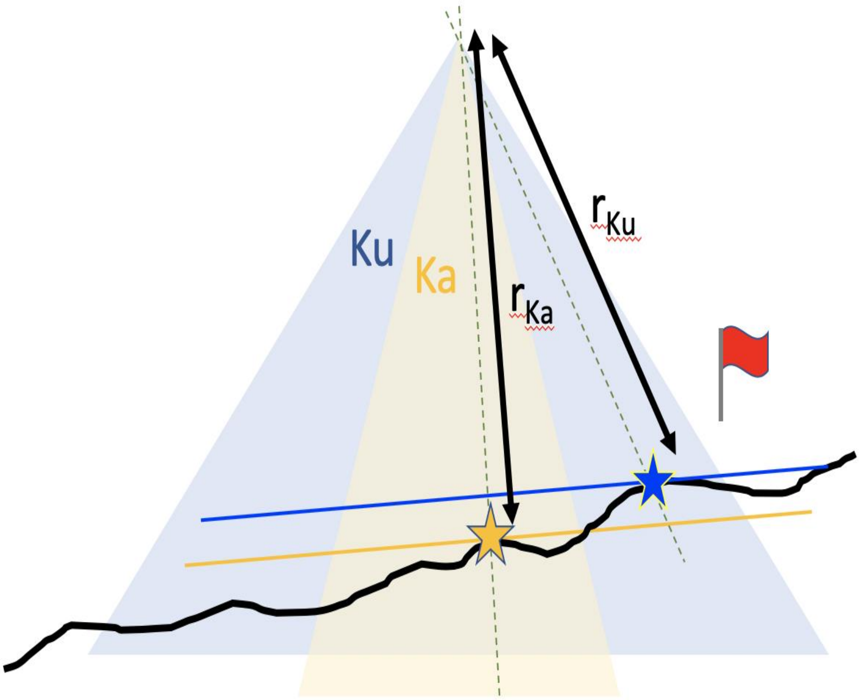

Figure 11. Different topographic configurations for computing the 'Penetration Depth' parameter. In the top panel, the point of closest approach lies within both the Ku-band and the Ka-band footprint, and therefore the penetration depth can be computed as the difference between the Ku and Ka range, once all instrument and geophysical corrections have been applied. In the bottom panel, the point of closest approach within the Ku footprint is different from the point of closest approach within the Ka footprint; leading to an invalid penetration depth estimate, that must be flagged within the Level-2 product.

Finally, it is clear that the Level-2 processing relies on a range of auxiliary models and datasets, to correct for various geophysical effects. The models used are, of course, in a constant evolution, but we provide a summary of the current state of the art within Table 9.

Correction	Description	Typical magnitude	Auxiliary Product	Reference
Dry Tropospheric Correction	Accounts for the effect of non-polar gases such as oxygen and nitrogen.	1.7 – 2.5 metres	Derived from ECMWF surface pressure fields.	CryoSat-2 Product Handbook, Baseline-D 1.0, issued 3/4/2018.
Wet Tropospheric Correction	Accounts for the effect of polar gases, mainly water vapour.	0 – 0.5 metres	Sourced from ECMWF.	CryoSat-2 Product Handbook, Baseline-D 1.0, issued 3/4/2018.
Inverse Barometer Correction	Accounts for variations in ocean height due to atmospheric pressure variations; for ice sheets,	-0.15 – 0.15 metres.	Sourced from ECMWF.	CryoSat-2 Product Handbook, Baseline-D 1.0, issued 3/4/2018.

	applicable over ice shelves only.			
Ionospheric Correction	Accounts for free electrons in the Earth's ionosphere slowing the radar pulse.	0.06 – 0.12 metres.	The Global Ionospheric Map.	http://iono.jpl.nasa.gov/gim.html.
Ocean Tide	Accounts for ocean tide; for ice sheets, applicable over ice shelves only.	-0.5 – 0.5 metres.	FES2014 ocean tide model.	Lyard F., L. Carrere, M. Cancet, A. Guillot, N. Picot: FES2014, a new finite elements tidal model for global ocean, in preparation, to be submitted to Ocean Dynamics in 2017.
Ocean Loading Tide	Accounts for the deformation of Earth's crust due to ocean tides.	-0.02 – 0.02 metres	FES2014 ocean tide model.	Lyard F., L. Carrere, M. Cancet, A. Guillot, N. Picot: FES2014, a new finite elements tidal model for global ocean, in preparation, to be submitted to Ocean Dynamics in 2017.
Solid Earth Tide	Accounts for the deformation of Earth due to direct tidal forces.	-0.30 – 0.30 metres.	Cartwright model.	D.E. Cartwright and A.C. Edden, Corrected tables of tidal harmonics. Geophysical Journal of the Royal Astronomical Society, Volume 33, 1973, 253-264.
Geocentric Polar Tide	Accounts for the distortion of Earth's crust due to movement of Earth's rotational axis.	-0.02 – 0.02 metres.	Pole location files sourced from Système au Sol d'ALTimétrie et d'Orbitographie.	CryoSat-2 Product Handbook, Baseline-D 1.0, issued 3/4/2018.
Echo relocation.	Echo relocation, or slope correction; applied to account for the echoing point being upslope of the nadir track.	Variable depending upon method and topography within the beam footprint.	CryoSat-2 DEM ArcticDEM REMA DEM	Helm et al., 2014.; Slater et al., 2018. Porter et al., 2018. Howat et al., 2019.

Table 9. Summary of Geophysical Corrections, and the auxiliary products from which they are derived, as anticipated for the CRISTAL mission.

FORM-NT-GB-7-1

3.2.3. Level-3+ processing

Whilst not the main focus of this Task, for completeness, we conclude this section by listing the principal Level-3+ gridded products that may be derived by the CRISTAL mission over ice sheets. All of these are computed from the 20 Hz elevation parameter within the Level-2 product.

1. Ice sheet Digital Elevation Models. Computed using established techniques that either grid data over a short time period of acquisition (e.g. Helm et al., 2014) or use a longer time period to improve measurement density and simultaneously account for rates of elevation change through time (e.g. Slater et al., 2018). Typically posted at 1km-5km resolution, although swath offers capability to improve this by an order of magnitude.

2. Ice sheet slope models. Computed using Digital Elevation Models.

3. Ice sheet penetration depth. A new gridded product based upon gridding a Level-2 'Ku penetration depth' parameter; calculated as the difference between Ku and Ka elevation.

4. Rate of elevation change. Gridded rate of elevation change computed from a timeseries of elevation data. Several well-established techniques exist for computing elevation change (e.g. Wingham et al., 1998; McMillan et al., 2014; Helm et al., 2014), and gridded products are currently produced as part of CCI+ and C3S contracts.

3.3. Observation concept

3.3.1. Altimeter characteristics, modes and expected performances

In terms of the overall observation concept, we recall the principal novel characteristics and modes of operation for the CRISTAL mission over ice sheets, as these are most relevant for further discussion:

- Over ice sheet margins CRISTAL will operate in Open Loop tracking mode; within the ice sheet interior the satellite will operate in Closed Loop.
- Over all ice sheet surfaces CRISTAL will operate a Ku-band SARIn Closed Burst configuration.
- Over all ice sheet surfaces CRISTAL will operate a Ka-band SAR Closed Burst configuration.

In the following sections, we describe each of the modes in turn, and evaluate what is known about their expected performance.

Ice Margin Open Loop Tracking

The selection of Open Loop tracking over the ice sheet's margins is driven by the following mission requirement:

MRD-150. The altimeter shall include tracking ability over steep terrain and as a minimum be able to track ice surfaces/glaciers with slopes <1.5°.

It has been estimated (Helm et al., 2014) that 96% of the Antarctic Ice Sheet exhibits slopes that satisfy this constraint. Whereas Closed Loop tracking is well-established for multiple previous missions, Open Loop tracking is not, and limited experiences to date have not been successful in allowing the range window to track the ice surface. Notably, Sentinel-3A operated in Open Loop tracking for the first 6 months of its lifetime, but was subsequently switched to Closed Loop over the ice sheet margins, because Open Loop performance was not satisfactory. Figure 12 shows loss of coverage around the steeper coastal regions of Antarctica for Sentinel-3A operating in Open Loop during cycle 10. It should be noted that CRISTAL has a larger range window than Sentinel-3 over ice sheets (256 m for CRISTAL as compared to 60 m for Sentinel-3); however, the experiences with Sentinel-3 indicate that a conservative approach should be taken, and the need to fully evaluate the performance of the Open Loop approach, which is still immature.

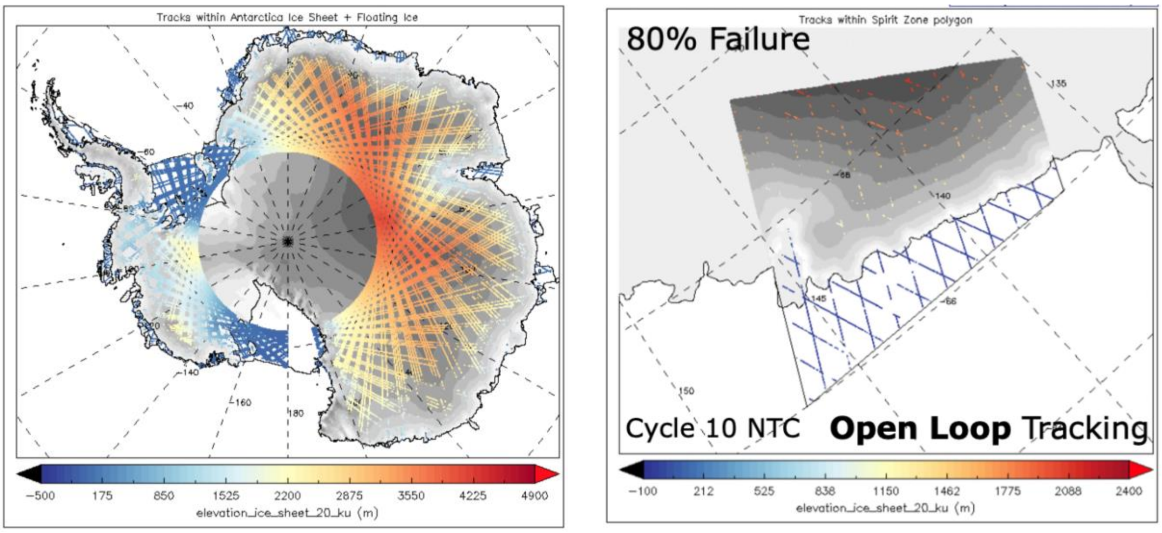

Figure 12. Example of loss of coverage in coastal regions for Sentinel-3A Open Loop tracking, for the whole of Antarctica (left panel) and for the Spirit site in East Antarctica (right panel). Coloured tracks show elevations retrieved during Cycle 10; with a lack of measurements in the high sloped margin regions, where the altimeter lost track of the ice surface.

More detailed analysis of the Sentinel-3 Open Loop Tracking Command (OLTC) over complex glaciological terrain; this time in Peru and the Himalaya illustrates the current limitations for Sentinel-3 (Figure 13). It is clear that both the accuracy of Sentinel-3A's OLTC, and the frequency with which the OLTC updates, are insufficient to keep the surface consistently within the range window, given a 20 Hz measurement sampling. This provides important lessons to be learned for the CRISTAL mission and suggests that, with its current level of maturity, further investigation into Open Loop tracking is required. This should include assessment of the improvements that can be offered by using a state-of-the-art of DEM for the OLTC. High resolution DEM's of both ice sheets now exist; REMA for Antarctica (Howat et al., 2019) and ArcticDEM for Greenland (Porter et al., 2018) and are likely to give much better performance than the historical ACE-2 DEM currently utilised for Sentinel-3 Open Loop tracking. Furthermore, the frequency with which the OLTC updates needs to be assessed, to understand feasibility given the hardware constraints of the mission, and the expected long repeat cycle.

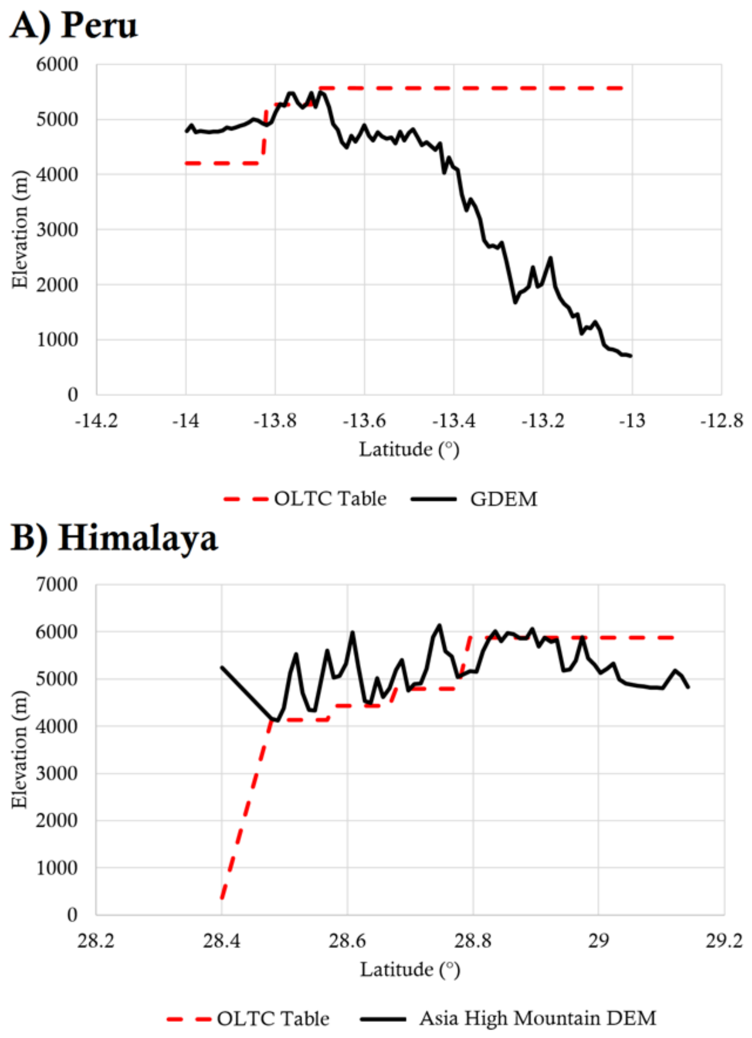

Figure 13. Examples of Sentinel-3 Open Loop Tracking Command over mountainous terrain in Peru (top panel) and the Himalaya (bottom panel). The accuracy and sampling frequency are insufficient to adequately track the complex variations in surface elevation [Credit: L. Taylor].

<u>Closed Burst Ku-band SARIn</u>

Closed Burst Ku-band SARIn is now mature as a technique, given the ~10 years of operation by CryoSat-2 in this mode. The performance of this mode is well-evaluated over coastal regions with complex topography (e.g. Helm et al., 2014; McMillan et al., 204; McMillan et al., 2016), across both Greenland and Antarctica. It should be noted however, that the accuracy of CryoSat-2 should be bettered by CRISTAL, due to the larger 500 MHz bandwidth of the latter, which will provide an improved range resolution (31 cm for CRISTAL compared to 47 cm for CryoSat-2). Although this mode of operation is untested over inland regions, given that SAR has been shown to perform well (McMillan et al., 2019) and that the topography tends to be simpler than at the coast, it is reasonable to expect good performance here. Nonetheless, several orbits of SARIn have been acquired by CryoSat-2 and so further assessment could be performed in anticipation of CRISTAL, using these dedicated acquisitions.

Closed Burst Ka-band SAR

As described previously, Ka-band SAR is untested in an Earth orbit. Therefore, its performance is currently unknown. Given our experiences of comparing Ku LRM and Ku SAR, it is reasonable to expect Ka SAR to be equivalent or better than Ka LRM, as operated by AltiKa. Analysis of AltiKa elevation measurements over the low slope Lake Vostok site in East Antarctica (Aublanc et al., 2017), indicates a median bias of several 10's of cm (relative to *in situ* data and ICESat observations), and a dispersion of around 10 cm. Analysis of AltiKa measurements in the Amundsen Sea sector of West Antarctica (Otosaka, *in review*) suggests that in complex ice margin regions, the median bias in elevation (relative to airborne data) is of the order of several metres and the dispersion is several tens of metres. When rates of elevation change are computed, the agreement with airborne data improves (Otosaka, *in review*), with a median difference of the order of 1 cm/yr, and a dispersion of several 10's of cm/yr. These statistics represent our best current estimate of Ka performance. However, they should be treated as a 'worst-case' lower bound on the performance of the CRISTAL Ka-band altimeter; the switch from LRM to SAR, improvements to onboard tracking and a larger range window all offer the potential to further enhance measurement quality.

3.3.2. Impact of radar wave polarization

Legresy et al. [1999] were the first ones to notice unexpected differences on the LRM waveforms shape between ascending & descending tracks over some parts the Antarctic ice sheets. In particular they reported differences on the waveform leading edge width, resulting in crossover biases in Sigma-0, and more critical: crossover biases in the surface elevation estimated by the retracking. They map this effect over the whole Antarctic ice sheet using ERS & Envisat data, and found maximum variations up to 2dB and elevation by about 1 m. These variations were retrieved using the Ice-2 retracker, sensitive to the snow volume scattering [Remy et al.,2012].

More recently, Armitage et al. [2014] did a similar analysis with CryoSat-2 data, using a 50% offset center of gravity (OCOG) retracker. They also reported static crossover differences of up to ±1m in elevation and more than ±2dB in the backscattering coefficient. *(Static difference refers to the crossover difference after removing the time-varying signal due to mass-balance instability).* The following figure shows the static part of the elevation and σ0 crossover difference observed by CryoSat-2.

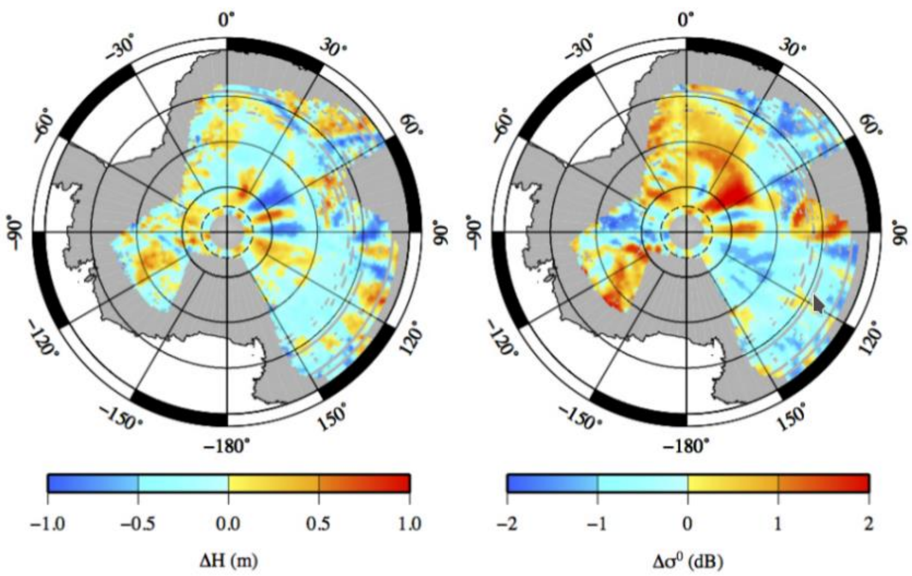

Figure 14: Elevation (left) and σ-0 (right) ascending minus descending crossover difference observed by CryoSat-2 in LRM over the Antarctic ice sheet. Credits to Armitage et al. [2014]

FORM-NT-GB-7-1

This error is complex and two explanations of this phenomenon have been suggested in the literature:

- Legrésy et al. [1999] interpreted this phenomenon as an effect of the interaction of the linearly polarized radar signal with wind-induced surface structures. These features may include erosion, snow drift or snow deposition figures due to the persistent and strong katabatic winds. They are found on various scales, from the centimeter scale (microroughness) to the sastrugi scale (1-m scale), up to the megadune scale (100-m scale).

- The second one by Arthern et al. [2001] suggested an anisotropic effect within the snowpack, over the previous mentioned features. Indeed, contrary to the study of Legresy et al., their methodology allows distinguishing the subsurface- echo part due to a snow extinction. They conclude that this anisotropic effect is controlled by the direction of the antenna polarization relative to a buried, wind-induced anisotropy in the structure of the snowpack.

Over ocean, in LRM, there is no evidence of differences at crossovers over specific surface features such as swell. Note this is complicated to demonstrate regarding the ocean dynamic movement and the sea state modification between ascending & descending track. Nonetheless, this element tends to support the second assumption, and would confirm an anisotropic effect of the snowpack internal scattering. The second hypothesis would be confirmed if the radar wave polarization effect is not (or weakly) noticeable on AltiKa measurements. In fact, the Ka band does not penetrates deeply into the snowpack depth, the energy measured by the satellite mostly comes from the air/snow interface (or several cm in depth). Therefore the Ka measure should not be sensitive to a potential snowpack anisotropy. Unfortunately, we do not have knowledge of such an analysis with AltiKa data.

Both assumptions mainly concord on the effect dependency, directly linked to the angle made between the radar polarisation direction and the wind-induced firn azimuthal anisotropy direction.

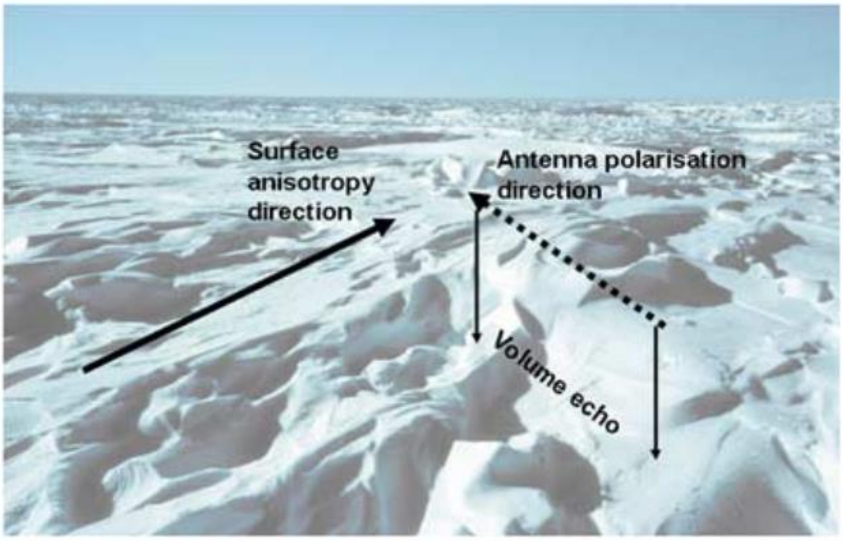

Figure 15: Sastrugi field suggesting the wind effect on the surface and snowpack and a schematic explanation. These sastrugi are wind-driven erosion features, and the direction of the field follows the prevailing wind direction. Credits to Remy et al. [2006].

Helm et al. [2014] showed that the crossovers differences can be largely mitigated when the retracker focuses on the bottom part of the waveform leading edge. The figure below, extracted from their paper, shows CryoSat-2 bias at crossovers depending on different retracking algorithms. The “L2” retracker refers to ESA Ice-2 retracker (from the official products), GSFC to “Goddard

Space Flight Center" retracker [NASA,2006], the offset center of gravity re-tracker (OCOG) uses a threshold of 0.25 of the OCOG amplitude [Wingham et al.,1986] and TFMRA [Helm et al.,2014] employs a threshold of 0.25 of the first waveform maxima.

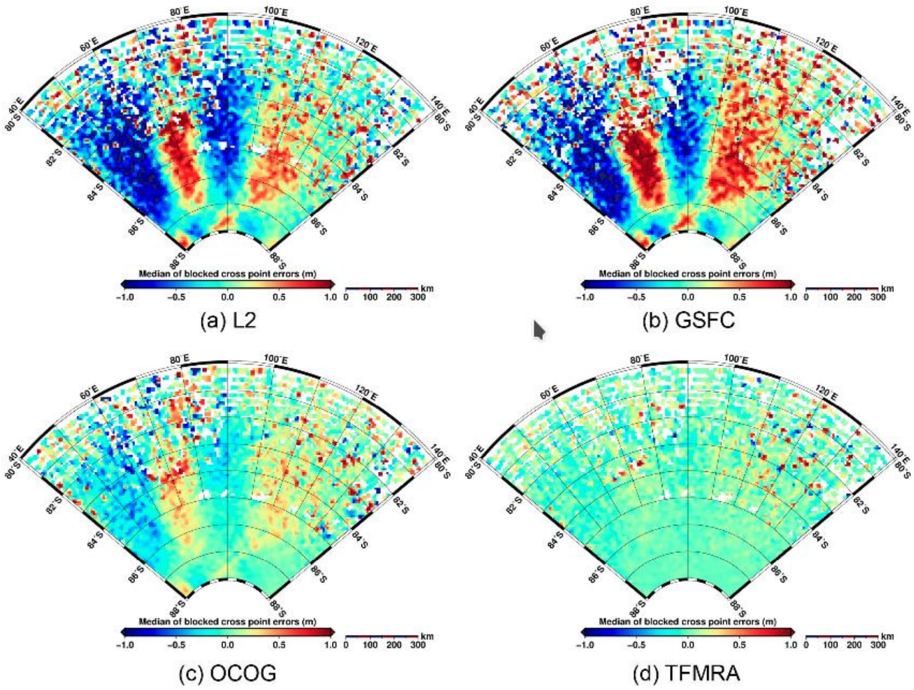

Figure 16: Results of the LRM crossover analysis in East Antarctica using different re-trackers. Credits to Helm et al. [2014]

Among the 4 retrackers evaluated, TFMRA estimates the altimeter range at the lowest location/position on the waveform leading edge (25% of first energy peak). This allows to remove almost entirely the static patterns.

Finally, even if the causes of theses static crossover differences are globally understood, the effect on the altimetry measurements and its correction remains a challenge. For now there is no specific ground segment level-2 processing dealing with this effect. In the frame of the CRISTAL mission the following problematics should be addressed:

- **What are the potential impact in SAR altimetry mode?** *As demonstrated by Aublanc et al. [2018], SAR waveform leading edge is dominated by surface echo, therefore the effect could be minor if the phenomena origin confirms to be an anisotropic effect within the snowpack (affecting the volume echo only).*

- **In P-LRM, this effect will be another source of discrepancies between Ku and Ka measurements.**
    - Firstly, the potential impact should be assessed and quantified in Ka band, as there is no published study addressing this topic for now.
    - Secondly, methods will have to be set up to account/correct for this effect in Ku band (and potentially in Ka band). It could be a dedicated retracking algorithm or an empirical correction as proposed by Armitage et al. [2014].

3.3.3. Spatial & temporal sampling required

Over ice sheets, the spatial and temporal correlation length scales of elevation change are dependent upon the climatic forcing mechanisms that drive change. Here we summarise the principal length-scales of variability, providing traceability to the glaciological studies upon which they are based. We consider each ice sheet in turn, because they exhibit different modes of variability. It is anticipated that, within the proposed CCN, these glaciological requirements will be fully confronted by the potential orbit configurations outlined in Section 3.3.4, to arrive at a fully-justified selection for the optimal CRISTAL orbit.

Antarctica: In Antarctica, signals of elevation change are either meteorological (essentially snowfall accumulation) or dynamical (i.e. related to ice flow) in origin. The former has a typical spatial length scale of the order 100 km (Wingham et al., 1998), whereas the latter has a length scale of the order of 10 km – 100 km, depending on the size of the glacier and the timescale over which the dynamical imbalance has persisted (McMillan et al., 2014; Konrad et al., 2017). In terms of persistence through time, meteorological effects typically span annual to several years (e.g. Lenaerts et al., 2013), whereas dynamical imbalance persists for decades (e.g. Shepherd et al., 2018; Konrad et al., 2017). To satisfactorily capture both meteorological and dynamical signals, and thus the Antarctic contribution to sea level rise, it requires measurements of elevation change of the order of 10 km in space and sub-annual (monthly-quarterly) in time.

Greenland: In Greenland, signals of elevation change are again either meteorological or dynamical in origin. However, due to the different climatological setting, and typical size of outlet glaciers, both the spatial and temporal scales of variability are different from Antarctica. Meteorologically driven changes in elevation are primarily driven by ice melting and accumulation; with the dominant periodicity being the seasonal cycle of mass loss (summer melt) and gain (winter accumulation) (Kuipers-Munneke et al., 2015; McMillan et al., 2016). Therefore, for Greenland it is crucial to resolve the elevation changes at monthly timescales, to adequately capture summer melting. Spatially, meteorologically driven changes have typical length scales of the order of 100's of km (e.g. Tedesco et al., 2013). The dominant dynamical signal affecting mass imbalance tend to persist for a wide range of timescales; from seasonal to multi-decadal periods (Shepherd et al., 2009; Tedstone et al., 2015), whereas spatially they are limited to ~10 km length scales, reflecting the smaller nature of outlet glaciers on the Greenland Ice Sheet (McMillan et al., 2016). Therefore, an observational system needs to be able to resolve spatial length scales of the order 1-10 km, to be able to adequately capture the signals of dynamical imbalance which contribute to Greenland's ice loss.

3.3.4. Orbit configuration

Over ice sheets the orbital configuration is driven by the following mission requirements:

1. **MRD-040.** The mission shall measure ice and ocean surface elevations over Polar Regions (Arctic and Antarctic) with an omission not exceeding 2° of latitude around the poles.
2. **MRD-050.** The mission shall have an orbit sub-cycle of less than 10 days.
3. **MRD-350.** The system shall be capable of delivering surface elevation with a temporal sampling of at least 30 days.

This has led to 3 proposed orbit configurations, which are currently under consideration:

- Case 1, 365_5268: Sub-cycles of 2 / 7 / 30 / 67 / 365 days.
- Case G2, 372_5297: Sub-cycles of 5 / 14 / 33 / 113 / 372 days.
- Case 3, 365_5204: Sub-cycles of 4 / 31 / 66 / 365 days.

In the scope of Task 2, we have undertaken a preliminary analysis of each of these candidate configurations, to evaluate the coverage they provide over Antarctica. The analysis is based upon the 1 month of orbit data that were provided by ESA, and we anticipate that this provisional analysis will form the basis of a more in-depth study, should ESA decide to issue a CCN to this effect. The following figures (Figure 17 - Figure 19) show the coverage provided by each orbit's ground tracks over varying-length periods, ranging from 2 days to 1 month. Figure 17 shows the coverage over all of Antarctica, whereas Figure 18 and Figure 19 shows zooms of sectors of East and West Antarctica.

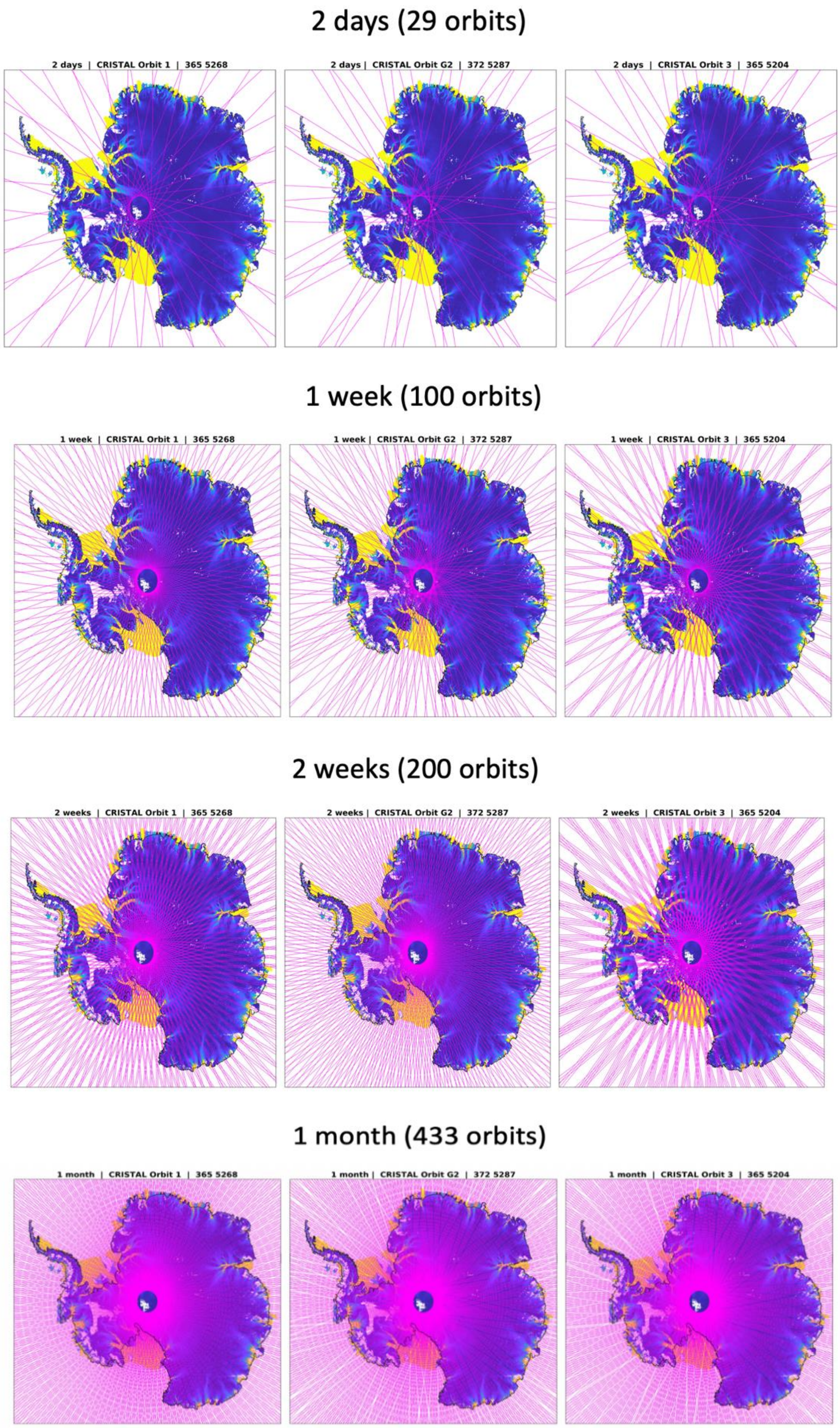

Figure 17. Coverage of ground tracks over Antarctica for orbit configuration 1 (left), G2 (centre) and 3 (right); rows show (from top to bottom), coverage over 2 days, 1 week, 2 weeks, and 1 month.

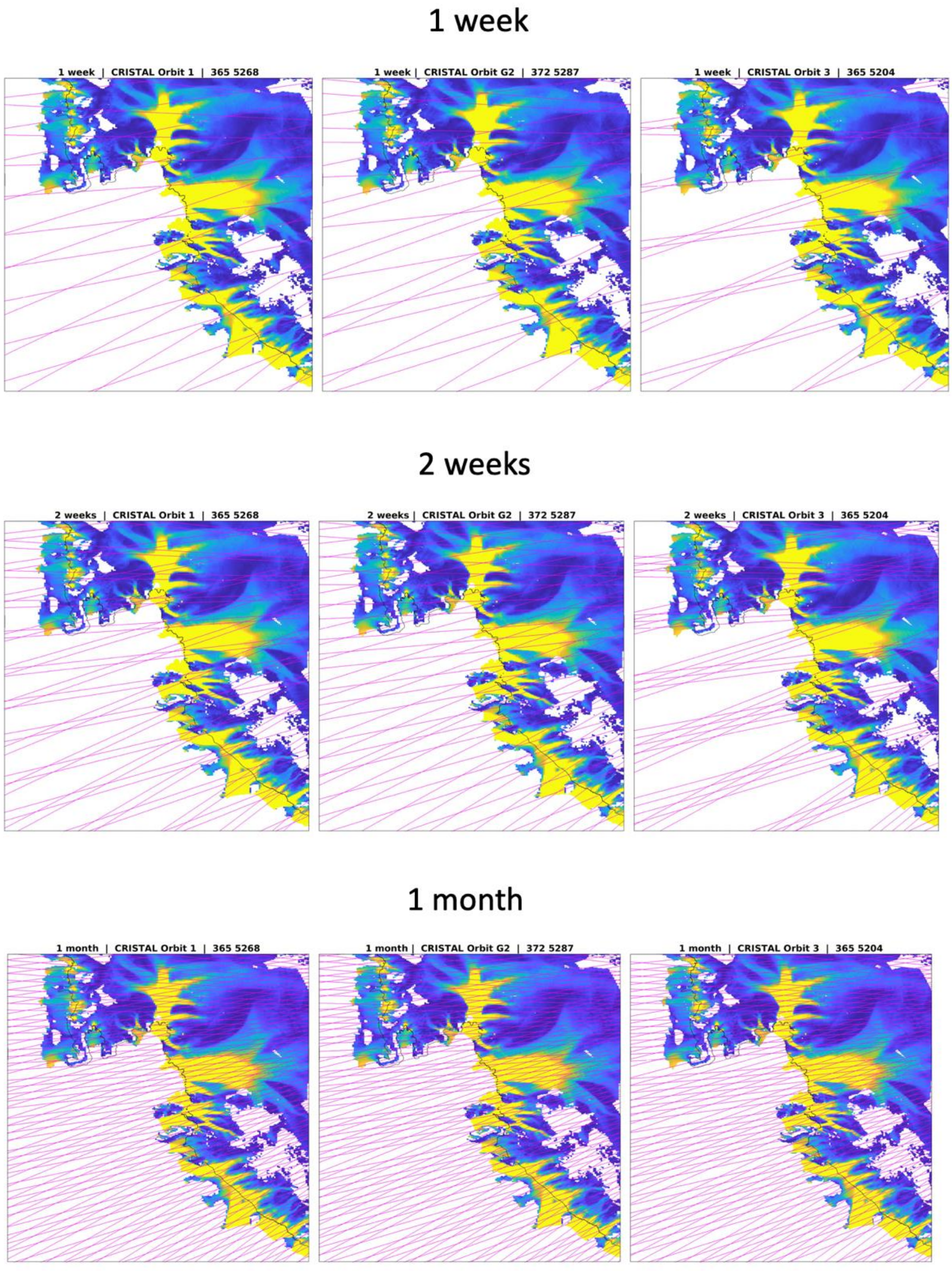

Figure 18. Coverage of ground tracks over the Amundsen Sea Sector of West Antarctica for orbit configuration 1 (left), G2 (centre) and 3 (right); rows show (from top to bottom), coverage over 1 week, 2 weeks, and 1 month.

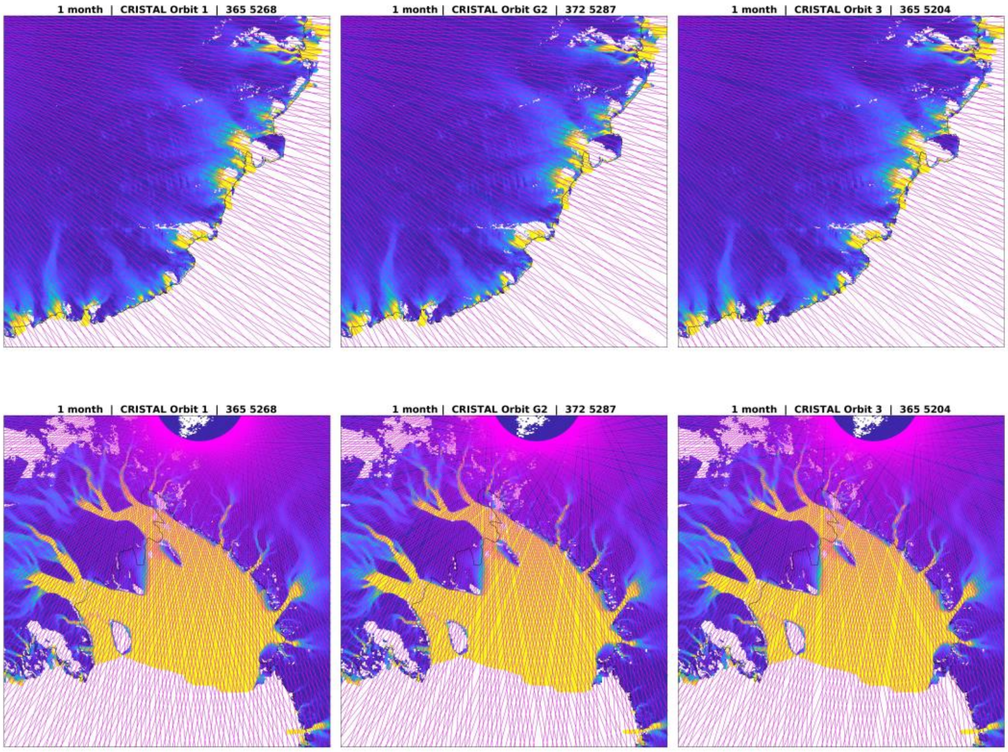

Figure 19. Coverage by 1 month of ground tracks over the Wilkes Land Sector of East Antarctica (top row) and the Ross Ice Shelf (bottom row) for orbit configuration 1 (left), G2 (centre) and 3 (right).

The preliminary analysis of 1 month's worth of orbit data shows, qualitatively, that there are differences between the 3 candidate orbits at short (weekly) timescales (Figure 18 and Figure 20). However, bearing in mind the monthly or longer timescales over which dominant patterns of change occur over ice sheets (Section 3.3.3), and the associated specification in the mission requirements (MRD-350), our preliminary analysis indicates that there is no clear difference between the 3 orbit configurations at this timescale (Figure 17 - Figure 19). This is to be expected, given that all 3 configurations have been designed to have a ~30 day sub-cycle.

To provide a more detailed evaluation of the ability of each orbit to fully sample ice sheet mass loss, we next assessed the extent to which each orbit configuration sampled the different flow velocities of the Antarctic Ice Sheet. Such analysis is important because elevation change and mass loss tend to be correlated with ice flow (i.e. rapid surface lowering preferentially occurs in areas of fast ice flow). Therefore in judging an orbit configuration, it is important to assess how well it samples areas of ice flow; not just its overall sampling of the entire ice sheet. We therefore used the MEASURES dataset of Antarctic Ice Velocity, downloaded from the US National Snow and Ice Data Centre (nsidc.org), to analyse this proportion of different velocity bands that were sampled by each configuration. The results of this analysis are shown in Figure 20 (2 week's worth of acquisitions) and Figure 21 (1 month's worth of acquisitions).

For ice velocity up to ~ 1500 m/yr, all 3 configurations sample approximately 25% and 50% of the total area over a 2-week and 1-month period, respectively. At flow speeds in excess of 1500 m/yr the sampling of any given velocity band becomes more variable, typically ranging from around 20% to 80% coverage during 1 month. The variability in the percentage coverage is in part driven by the small number of 5 x 5 km pixels that fall within these higher velocity bands. Again though, there is no obvious 'best' or 'worst' performer amongst the 3 configurations at these higher flow speeds.

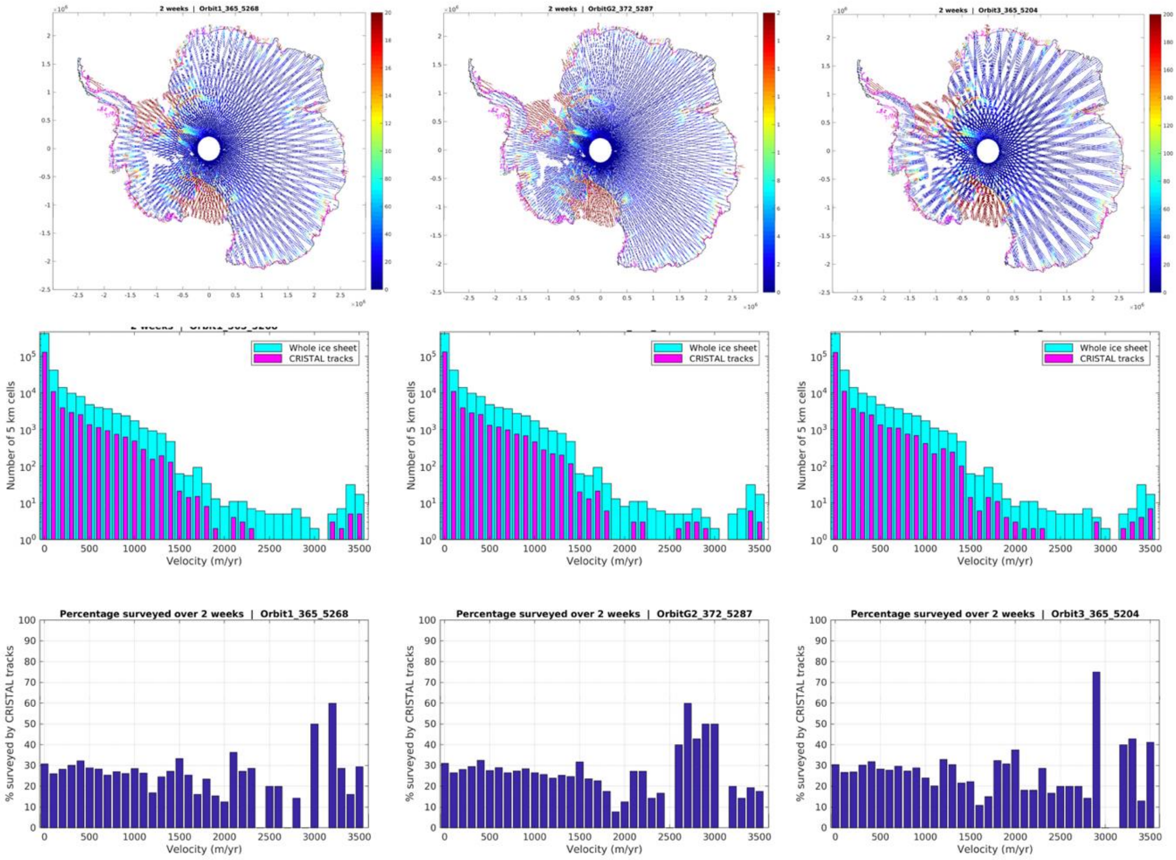

Figure 20. Sampling of Antarctica's ice velocity field over 2 weeks for orbit configuration 1 (left), G2 (centre) and 3 (right). The top row shows visually the sampling. The centre row shows the distribution, according to velocity, of 5 x 5 km ice sheet pixels (turquoise), and those sampled by 2 weeks of data (pink); note the log scale. The bottom row shows the percentage of the ice sheet sampled by 2 weeks of data, broken down according to velocity band.

FORM-NT-GB-7-1

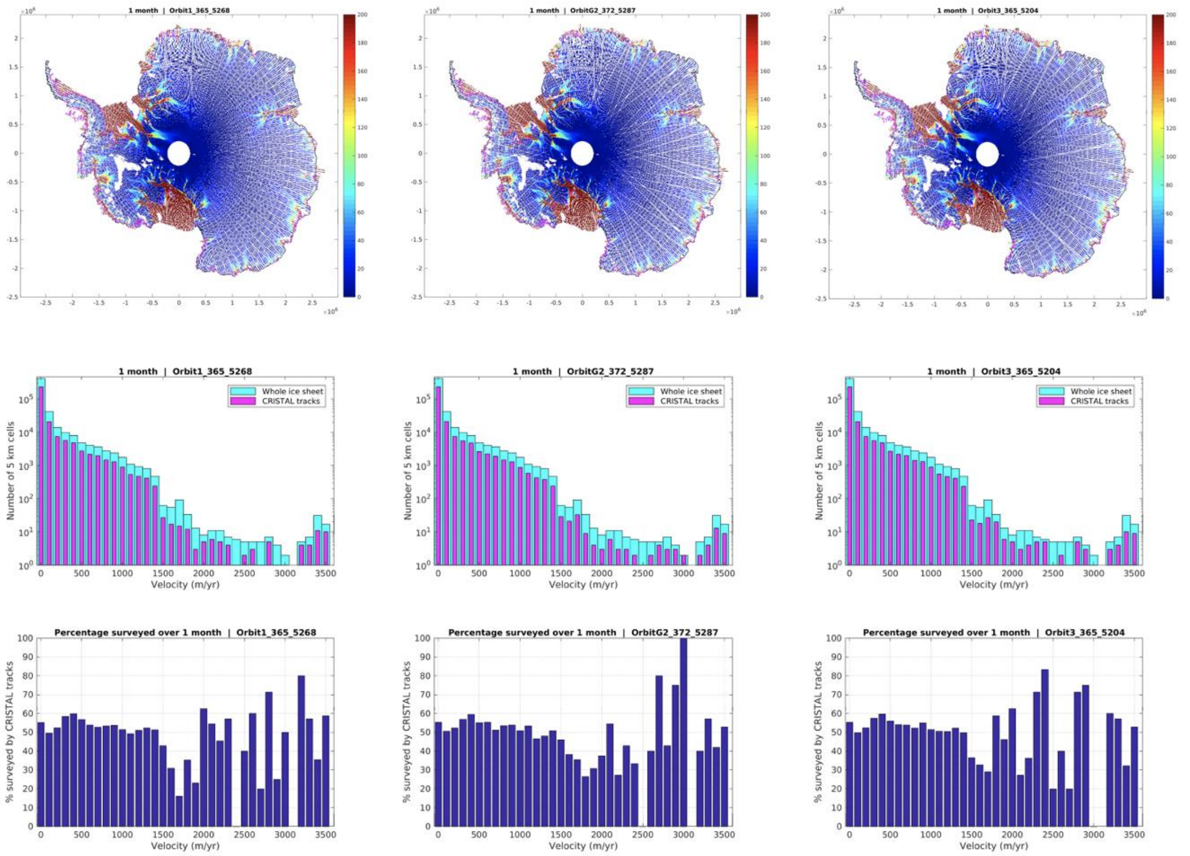

Figure 21. Sampling of Antarctica's ice velocity field over 1 month for orbit configuration 1 (left), G2 (centre) and 3 (right). The top row shows visually the sampling. The centre row shows the distribution, according to velocity, of 5 x 5 km ice sheet pixels (turquoise), and those sampled by 1 month of data (pink); note the log scale. The bottom row shows the percentage of the ice sheet sampled by 1 month of data, broken down according to velocity band.

Based upon this preliminary analysis, we recommend the following more detailed analysis to fully understand the implications for ice sheet sampling of the different orbit configurations:

- An assessment of the proportion of the current mass balance signal sampled; to enable firm conclusions to be reached about which orbit configuration best samples the current imbalance.
- An analysis of a longer period of orbits; for Antarctica, a quarterly ice sheet sampling frequency is commonly chosen, and so performance of the 3 orbits at this timescale should also be assessed.
- A quantitative statistical assessment of whether there are significant differences between the 3 orbit configurations.
- An assessment for Greenland; the same analysis should also be performed for Greenland.

3.3.5. Analysis of the need of a microwave radiometer

With regard to the microwave radiometer, the mission requirement is as follows:

MRD-120 The mission shall embark a microwave radiometer to support wet tropospheric correction for ocean applications and ice/snow type classification.

Over ice sheets, the wet tropospheric correction required for radar altimetry measurements is derived from model output, rather than from microwave radiometer observations (e.g. Product Data Format Specification - SRAL/MWR Level 2 Land products, Sentinel-3 Mission Performance Centre, Ref. S3IPF.PDS.003.2, Issue 2.12, 05 March 2018). Therefore, in order to meet the ice sheet mission requirements, there is no specific need in terms of a microwave radiometer.

3.3.6. Potential synergy with contemporaneous missions

By 2025, we will be approaching 35 years of near-continuous radar altimeter measurements over polar regions. At that time, the ongoing continuity of the record will be reliant upon Sentinel-3, which provides coverage up to 81.35° latitude, together with a relatively short revisit timed of 27 days. ICESat-2 was launched on 15th September 2018, with a lifetime goal of 5 years, and is therefore not expected to form part of the observation system at 2025. CRISTAL will complement Sentinel-3, and enhance overall polar observation capability, by:

1. Providing coverage up to 88° latitude, thereby completing the coastal coverage of Greenland and Antarctica that is missed by Sentinel-3's lower orbital inclination.
2. Providing a complementary long-repeat orbit cycle of ~ 1 year; which will fill in the gaps in coverage between Sentinel-3 ground tracks, particularly around the ice sheets' margins.
3. Providing more accurate measurements in the complex ice margin regions, due to the Ku-band interferometer.
4. Providing more accurate measurements of elevation change in the interior of the ice sheets, due to the ability of the dual frequency configuration to resolve time variations in the depth distribution of the backscattered Ku-band signal.
5. Improving the Sentinel-3 measurements themselves; for example, crossing CRISTAL Ka with Sentinel-3 Ku will yield information relating to Sentinel-3 penetration, and the CRISTAL Ku interferometric slope can assist the Sentinel-3 echo relocation step during the Level-2 processing.
6. Providing redundancy for the long-term Ku-band record; should Sentinel-3 unexpectedly fail.

3.4. Synthesis

In summary, the closed burst, dual frequency Ku-SARIn and Ka-SAR proposed to operate on CRISTAL, will provide a unique platform for making measurements of ice sheet elevation change that satisfy the User Requirements [AD1; AD2], and associated mission requirements [AD3]. Inheriting much of the heritage of CryoSat-2, the proposed system builds upon the success of this Earth Explorer mission in the following principal ways:

1. CRISTAL adds a dual frequency altimeter to address one of the major uncertainties associated with resolving ice sheet change, namely determination of changes in the depth distribution of Ku-band backscattering.

2. CRISTAL operates globally in delay-doppler mode, thereby providing continuity with Sentinel-3 in terms of high-resolution measurements in the ice sheets interior, and delivering the first spaceborne Ka delay-doppler observations.
3. CRISTAL provides the first routine acquisition of SARIn measurements over the ice sheet interior, thereby generating innovative ice-sheet-wide datasets, such as high-resolution swath processing.

It is also worth noting that CRISTAL offers other innovations which are expected to improve measurement quality, such as improved range precision and Open Loop tracking around the ice sheet margins.

In terms of geophysical products, CRISTAL will inherit much of the processing workflow developed over many years across the ERS-1/2, Envisat, CryoSat-2, Sentinel-3 and AltiKa missions. However, there will be several innovations that will further improve performance. In particular, the combination of swath processing and fully-focussed SAR can be expected to provide a step change in the accuracy, resolution and quantity of Level-2 available to the user; CRISTAL will truly be a high-resolution radar altimeter. In terms of products, the most important new Level-2 product made available to the scientific community will be the routine estimation of the Ku-band penetration into the snowpack. This is a critical parameter for accurately constraining ice sheet mass balance and the associated sea level contribution.

Finally, regarding the orbit, several candidates have been identified which, based upon a preliminary analysis, all look promising. Further, more detailed study is now required to understand their more subtle differences; to reach robust statistical conclusions and to decide on which will best meet the overall mission requirements. Whichever orbit configuration is ultimately chosen, CRISTAL will provide clear synergy with the Earth Observing system at 2025, and bring far greater capability for monitoring Earth's ice sheets than can be achieved with Sentinel-3 alone.

4. Sea-Ice

4.1. Definition of level-1 and level-2 products

This section identifies of a list of Level-1b and Level-2 parameters associated with sea ice. Similar to ice sheets chapter 3.1, the applicable documents here are the User Requirements Documents [AD1; AD2], the Mission Requirements Document [AD3] and the Technical Note from Task 1 of this study [AD4]. The data product parameters for Level-1b and Level-2 are described in MRD [AD3] as:

Level-1b: Level 1b products are fully calibrated, geolocated containing averaged (pulse-width limited processing) or multi-looked waveforms (focussed or unfocussed SAR processed) but not corrected for geophysical effects.

For sea ice, the main L1b parameters for CRISTAL data products are the multi-looked SAR waveforms, along with satellite altitude, geolocation, measurement time, window delay, geophysical corrections, measurement confidence data flag and surface type model flag.

Level-2: Level-1b measurement data converted into geophysical quantities, maintaining the same time structure and sampling, and combined with auxiliary input data from other sources to yield geophysical parameters.

A comprehensive list of geophysical parameters needed in the Level-2 processing is listed in the ice sheets section in Table 9), and these apply for sea ice as well. In addition to the geophysical corrections applicable for all surfaces (e.g. atmospheric and tidal corrections, mean sea surface and geoid) and common measurement parameters (e.g. frequency ranges for Ka and Ku, sigma0, locations of echoing point and surface elevation), the requested content for sea ice Level-2 product as defined in the MRD [AD3] is:

- local sea level (instantaneous sea surface height, via interpolation between leads)*,
- ice floe elevation (interpolation between sea ice height),
- surface type (from altimeter; lead/floe/open ocean/undefined)
- ice type (from altimeter + radiometer; FYI/MYI/mixed)*,
- distance to the closest lead along-track (used for freeboard computation)
- radar freeboard for both frequencies and uncertainties*
- radar-derived snow depth*
- snow load correction
- correction for slow propagation in snowpack (Ku-band)
- sea ice freeboard (radar freeboard corrected for snow depth)*
- sea ice thickness*
- sea ice volume*
- auxiliary data needed for freeboard to sea ice thickness conversion:
    - snow density*
    - sea ice density
    - water density
    - sea ice type
    - sea ice concentration

The parameters pointed out with an asterisk(*) are those also mentioned in the PEG report [AD1]. In addition to these, there were some requested parameters that are not retrievable by altimetry with current knowledge or are better provided by other products, such as salinity, surface albedo and temperature, and sea ice drift. Vice versa, those parameters from the list above that did not appear in the PEG reports are crucial e.g. for converting L1b data to geophysical quantities. For sea ice volume it was especially pointed out that the 88 degrees latitude is fundamental for the correct estimation of the ice-volume trends [AD2].

The main L2 parameter, sea ice thickness, is derived from radar freeboard and snow load. Nevertheless, estimates of water, snow and ice densities are required in the conversion of radar freeboard to thickness. These densities will be acquired from an auxiliary source.

One of the variables requested by MRD is sea ice volume. By definition, sea ice volume is not a reasonable parameter at footprint scale, but should only be provided as a gridded (L3) product.

Snow depth was mentioned by the PEG in its role in the assessment of snow loading and freeboard measurements, but also important for evolution of sea ice cover. The role of these two parameters, sea ice thickness and snow depth is embodied in the first of the CRISTAL primary objectives:

PRI-OBJ-1. To measure and monitor variability of Arctic and Southern Ocean sea-ice thickness and its snow depth.

Which in turn guides the definition of the Mission and Geophysical Product Requirements, which are summarized in Table 10 and linked to the principal Level-1b and Level-2 parameters associated with each requirement.

MRD ID	Requirement	Level-2 parameters	Level-1b parameters
MRD-020	The mission shall acquire measurements of elevation over **sea-ice**, land ice, polar glaciers, ice caps and ocean.	Ku-band echoing point location. Ku-band echoing point elevation. Ku-band waveform parameters. Ka-band echoing point location. Ka-band echoing point elevation. Ka-band waveform parameters.	Satellite ground track location. Satellite altitude. Interferometer orientation. Ku-band waveform. Ku-band phase difference. Ku-band coherence. Ku-band window delay. Ku-band geophysical & instrument corrections. Ka-band waveform. Ka-band window delay. Ka-band geophysical & instrument corrections.
MRD-110	The payload shall include a SAR Radar Altimeter with the capability of interferometry.	Ku-band echoing point location. Ku-band echoing point elevation. Ku-band waveform parameters. Across-track surface slope.	Satellite ground track location. Satellite altitude. Interferometer orientation. Ku-band waveform. Ku-band phase difference. Ku-band coherence. Ku-band window delay. Ku-band geophysical & instrument corrections.
MRD-120	The mission shall embark a microwave radiometer to support wet tropospheric	Surface type flag.	Brightness temperatures Instrument and geophysical corrections

FORM-NT-GB-7-1

	correction for ocean applications and ice/snow type classification.		
MRD-160	The altimeter shall be capable of operating at two frequency channels.	Ku-band echoing point location. Ku-band echoing point elevation. Ku-band waveform parameters. Ka-band echoing point location. Ka-band echoing point elevation. Ka-band waveform parameters.	Satellite ground track location. Satellite altitude. Ku-band waveform.. Ku-band window delay. Ku-band geophysical & instrument corrections. Ka-band waveform. Ka-band window delay. Ka-band geophysical & instrument corrections.
MRD-230	The altimeter shall be able to measure variations of backscatter coefficient ranging from 0dB to 50dB.	Ku-band sigma-0. Ka-band sigma-0.	Ku-band waveform. Ka-band waveform. Ku-band scaling factor to convert from waveform units to dB. Ka-band scaling factor to convert from waveform units to dB
MRD-260	The mission shall be capable of retrieving year-round elevation measurements of the sea ice-covered oceans.	Time of acquisition. Ku-band echoing point location. Ku-band echoing point elevation. Ku-band waveform parameters. Ka-band echoing point location. Ka-band echoing point elevation. Ka-band waveform parameters. Sea level anomaly.	Time of acquisition. Satellite ground track location. Satellite altitude. Interferometer orientation. Ku-band waveform. Ku-band phase difference. Ku-band coherence. Ku-band window delay. Ku-band geophysical & instrument corrections. Ka-band waveform. Ka-band window delay. Ka-band geophysical & instrument corrections.
MRD-280	The system shall be capable of retrieving sea ice freeboard to an accuracy of 0.03 m along orbit segments ≤ 25 km.	Ku-band echoing point location. Ku-band echoing point elevation. Ka-band echoing point location. Ka-band echoing point elevation. Snow thickness on sea ice. Mean sea surface height. Surface type flag. Sea level anomaly. Radar freeboard. Sea ice freeboard.	Satellite ground track location. Satellite altitude. Interferometer orientation. Ku-band waveform. Ku-band phase difference. Ku-band coherence. Ku-band window delay. Ku-band geophysical & instrument corrections. Ka-band waveform. Ka-band window delay. Ka-band geophysical & instrument corrections.
MRD-330	The system shall be capable of delivering sea ice thickness measurements with a vertical	Ku-band echoing point location. Ku-band echoing point elevation. Ka-band echoing point location.	Satellite ground track location. Satellite altitude. Interferometer orientation. Ku-band waveform. Ku-band phase difference. Ku-band coherence.

	uncertainty less than 0.1 m.	Ka-band echoing point elevation. Snow thickness on sea ice. Mean sea surface height. Surface type flag. Sea level anomaly. Radar freeboard. Sea ice freeboard. Sea ice thickness.	Ku-band window delay. Ku-band geophysical & instrument corrections. Ka-band waveform. Ka-band window delay. Ka-band geophysical & instrument corrections.
MRD-380	The mission shall be capable of retrieving the depth of dry snow on sea ice.	Ku-band echoing point location. Ku-band echoing point elevation. Ka-band echoing point location. Ka-band echoing point elevation. Snow thickness on sea ice.	Satellite ground track location. Satellite altitude. Interferometer orientation. Ku-band waveform. Ku-band phase difference. Ku-band coherence. Ku-band window delay. Ku-band geophysical & instrument corrections. Ka-band waveform. Ka-band window delay. Ka-band geophysical & instrument corrections.
MRD-460	The vertical uncertainty in sea level anomaly retrieval from Ku band (including sea-ice leads) shall be 0.02 m.	Surface type flag. Sea level anomaly.	Satellite ground track location. Satellite altitude. Interferometer orientation. Ku-band waveform. Ku-band phase difference. Ku-band coherence. Ku-band window delay. Ku-band geophysical & instrument corrections.

Table 10. Correspondence between Mission Requirements and principal Level-1b and Level-2 parameter relevant to sea ice.

4.2. Level-2 ground processor algorithms

4.2.1. Overview

This section presents the sea ice algorithms. The section is divided into three parts - first the derivation of radar freeboard ie. freeboard without correction for signal propagation speed in snow. Second subsection discusses the conversion of radar freeboard into sea ice freeboard and further into thickness. Finally, the retrieval algorithms of snow on sea ice is presented in the third subsection.

Algorithms for radar freeboard, sea ice freeboard and thickness retrieval for delay-Doppler algorithms are well settled due to past CryoSat-2 work. These are described in several ESA documents (Paul et al., 2017; Sallila et al., 2019) and research papers [eg. Laxon et al., 2013; Kurtz et al., 2014; Paul et al., 2018; Tilling et al., 2018]. They will be only briefly repeated in this document. Emphasis shall be put onto snow on sea ice retrieval with dual frequency altimeters.

Figure 22 below shows the schematic of altimeter sea ice thickness processing.

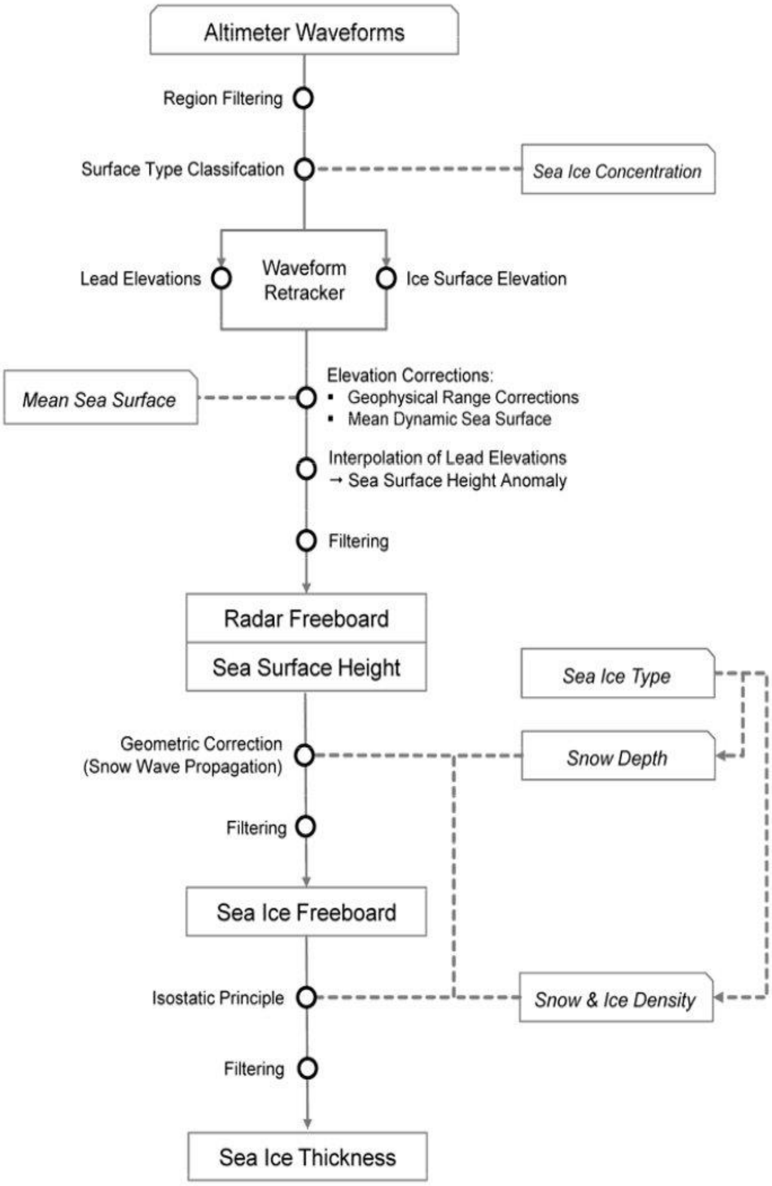

Figure 22: Flow chart for the Sea Ice Thickness Processor [SICCI+ ATDB]

4.2.2. Radar freeboard

The radar freeboard is the distance between local sea level and the surface on the ice floes as measured by the altimeter without compensating for lower propagation speed of radar signal in snow. Radar freeboard is a variable that can be measured with altimeters such as CryoSat-2 without external estimate on snow. In short, elevation measurements recognised to originate from leads are interpolated to ice floe locations and then deducted from ice floe elevations. Comparisons of Ka- (AltiKa) and Ku-band (CryoSat-2) radar freeboards show that Ka-band retrieves consistently greater elevations over sea ice. This difference increases throughout the ice growth season, with mean difference of 4.4 cm in October, up till 6.9 cm in March, for the overlap area up to 81.5°N of AltiKa and CryoSat-2. (Armitage and Ridout, 2015).

Two major steps in radar freeboard retrieval are waveform retracking and surface type classification. In retracking phase, the range to the main scattering horizon is estimated for each waveform. There are several algorithms available, outlined in Table 11. These include mainly empirical and physical retrackers. Common steps include applying the corrections, provided for example with the CryoSat-2 L1b product files, for the elevation: wet and dry tropospheric delay time, ionospheric delay, oscillator drift, inverse barometer effect, dynamic atmospheric correction, ocean equilibrium tide, long period ocean tide, load tide, solid Earth tide, and geocentric pole tide. Also, the surface elevation is computed relative to an ellipsoid (e.g. WGS84, EGM08) by subtracting the retrieved range from the altitude of the satellite. The various retrackers mention snow as one of the greatest uncertainties, and for simplicity assume snow to be dry.

Retracker Type	Method	Current SRL	Algorithm reference
Empirical	Surface-type specific retrackers	9 9	Tilling et al., 2018 Armitage and Ridout, 2015
	Threshold First Maximum Retracker Algorithm	9 9	Ricker et al., 2014
	Waveform centroid retracker	9 1	Kwok and Cunningham, 2015
Physical	Waveform fitting using waveform model	9 1	Kurtz et al., 2014
	SAMOSA+	7 1	Dinardo et al., 2017
	ALES+	7 1	Passaro et al., 2018
	Neural network supervised classification	6 6	Poisson et al., 2018
	K-medoids clustering	6 1	Müller et al., 2017
Numerical	Facet-based model	6 2	Landy et al., 2019

: Different retrackers and classifier with their maturity level, which is assessed based on the adjusted Scientific Readiness Level (SRL) Handbook from ESA [RD5], introduced in Figure 8.

Empirical retrackers are based on the detection of the leading edge position with applying statistical methods on the waveform. The difference in the radar echo shapes from ice floes and leads means that the retracking point is different for these two and requires the determination of a relative bias. E.g. the surface-type specific retracking in Tilling et al. (2018) chose to use two different retrackers for these two different surfaces.

In TFMRA the range estimation is done by computing the time when the power of the smoothed leading edge has risen to a defined percentage of the peak power value. The time is then converted into range by assuming speed of light in a vacuum as the wave propagation velocity.

Waveform centroid retracker of Kwok and Cunningham (2015) is suggested to be less sensitive to scattering from the air-snow interface and snow layer (Kwok, 2014), compared to the range estimation with leading edge. In this method the retracking point is defined by the centroid of the waveform area and this is used as the range to the surface.

Physical retrackers fit a mathematical model to the waveform, trying to capture the backscatter process. The possible advantages over empirical retrackers are that these are independent of empirical thresholds.

Using two different physical models applied to the different shapes of waveforms can result into bias between the two, which needs to be taken care of. Also, using a single physical retracker for different surfaces sets requirements on the model, and it is suggested that it should be based on a shape model able to accommodate for both specular and diffuse waveform (Quartly et al., 2019). Such approaches have been implemented to LRM missions by Poisson et al. (2018) and Passaro et al. (2018).

The Adaptive Leading Edge Subwaveform (ALES) retracker (Passaro et al., 2014) selects part of the returned echo and models it with Brown functional form (Brown, 1977; Hayne, 1980), with least square estimation. While ALES was designed for open ocean and coastal waters, Passaro et al. (2018) created an ALES+ retracker that adapts the fitting of signal depending on the sea state and includes handling the sea level in leads.

For SAR waveforms a physical retracker SAMOSA+ (tailored SAR Altimetry MOde Studies and Applications model, Dinardo et al., 2017), capable of discriminating between waveforms from diffusive and specular scattering surfaces, has been successfully applied to retrieve sea-ice freeboard from CryoSat-2 SAR data (Quartly et al., 2019).

The physical retracker of Kurtz et al. (2014) adapts to both sea-ice and lead echoes with the variation of two parameters. One parameter models the efficiency of backscattering from a surface as a function of the incidence angle. Another parameter models the standard deviation of the heights illuminated by the footprint. The physical model has been used to fit CryoSat-2 waveforms for surface elevation retrieval by using lookup tables and bounded trust region Newton least-squares fit approach. The retracker results were validated against Operation IceBridge data, showing significantly better consistency for freeboard and thickness retrievals when compared with an empirical retracker. However, for a longer time period comparison, sea ice thickness retrieved with empirical retrackers resulted in better agreement with Operation IceBridge (Sallila et al., 2019).Most of the published empirical algorithms (such as Kurtz et al. 2014, Paul et al. 2018, Guerreiro et al. 2017 and Tilling et al. 2018) follow the surface type classification scheme of Laxon et al. (2013) that relies on few waveform parameters, namely Pulse Peakiness (PP) and Stack Standard Deviation (SSD). Kwok and Cunningham (2015) had a slightly different approach using the power of the pulse peak and the width of the centroid of the waveform area relative to the range location of the peak to differentiate ice and water.

The surface is traditionally classified to belong to one of the following classes:

1. sea ice surface, which will be used for freeboard and thickness retrieval
2. leads, which will be used for sea surface height estimation
3. mixed surface/unknown, which will be discarded from further processing

The parameters describing the waveform shape (e.g. PP and SSD) have distinct properties for ice surface and leads, and this property is used for classification. An example of classified waveforms from CryoSat-2 can be seen in Figure 23.

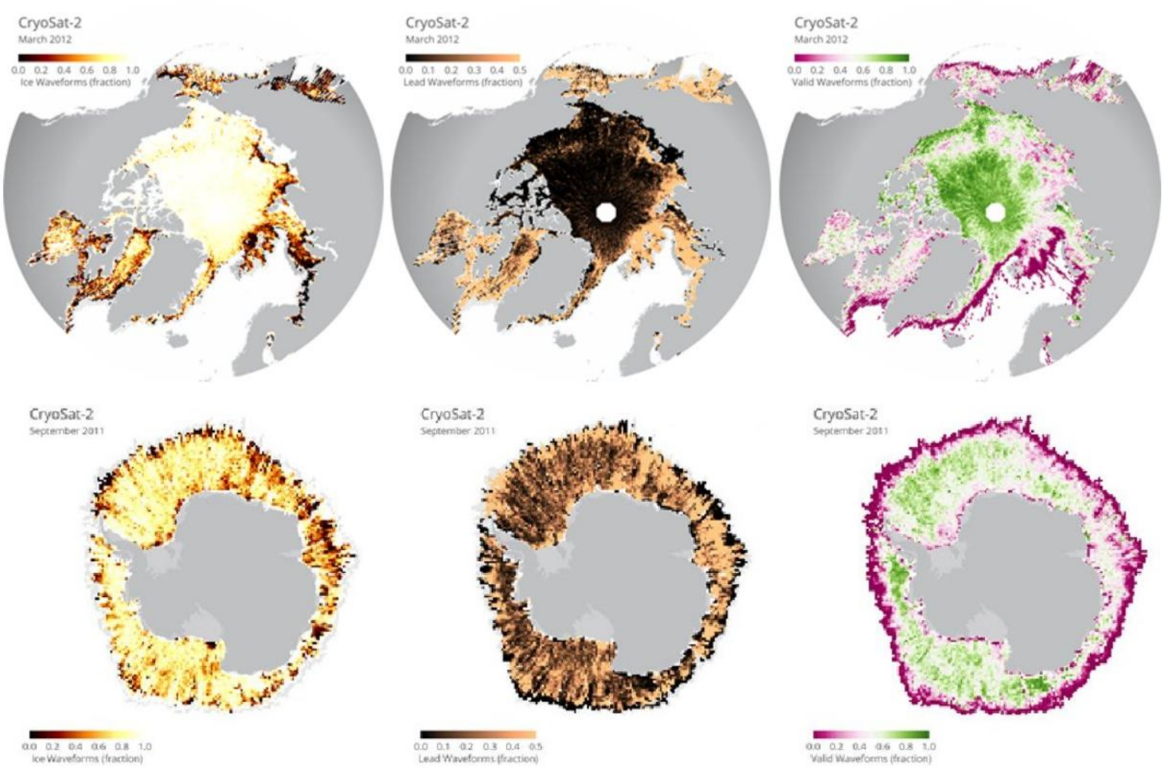

Figure 23: Examples of classified waveforms for a month, left column fraction of waveforms classified as ice, middle for leads and right the fraction of valid waveforms. Figure from SICCI-ATBD (Paul et al., 2017).

Traditionally, as in most of the methods mentioned above, the waveform is classified to sea ice and leads, or specular and diffuse reflections, based on simple thresholds, which are user made limits. The sea ice community has recently adopted machine-learning and data-mining methods, that could challenge the more conventional retrackers. These statistical approaches are commonly divided into supervised classification algorithms and unsupervised classification algorithms.

The supervised classification algorithms require a classified training data set, which is used to link the received waveforms to surface types or geometrical shapes of the echoes based on predefined characteristics. Neural network classification, as in Gommenginger et al. (2011) and Poisson et al. (2018) uses user-defined classes to train the neural net to associate particular waveform shapes with the predefined classes. A neural network method method has been used to classify Envisat waveforms to 12 possible classes by Poisson et al. (2018) as well as expanded to AltiKa and Sentinel-3 waveforms (Longépé et al., 2019).

Unsupervised classification algorithms assign the waveform without pre-classified echoes. Müller et al. (2017) used six waveform parameters and partitioned the data using k-medoids clustering. This method results into k classes of waveforms, which can then be assigned to different surfaces (possible various categories of “ocean, “ice floe”, and “lead”) using reference dataset, which contains examples of majority of all possible scatter/surface types.

The facet-based model for SAR altimeter echoes by Landy et al. (2019) seems to perform well at separating the backscatter sources between different surfaces. In addition to SAR echoes, the model works for pulse-limited echoes as well, and in other frequencies in addition to Ku-band. This model could be used to evaluate the effects of surface roughness and snow properties on the waveform shape, and these theoretical corrections could be then used to improve the empirical corrections, e.g. those made for AltiKa and CryoSat-2 for the snow depth product by Lawrence et al. (2018). Sea ice freeboard and thickness

Sea ice freeboard is the distance between local sea level and upper surface of ice. Sea ice freeboard is obtained from the radar freeboard after applying geometric correction that accounts for the slower wave propagation speed of the radar signal in the snow layer.

Sea ice thickness is estimated from freeboard by assuming hydrostatic equilibrium according to Archimedes' principle:

$$sit = \frac{s + \rho_s - fb \cdot \rho_w}{\rho_w - \rho_i}$$

Where, sit is sea ice thickness, s snow depth, fb freeboard and $\rho_{s/w/i}$ the densities for snow, sea water and ice, respectively. The parameters are illustrated in Figure 24.

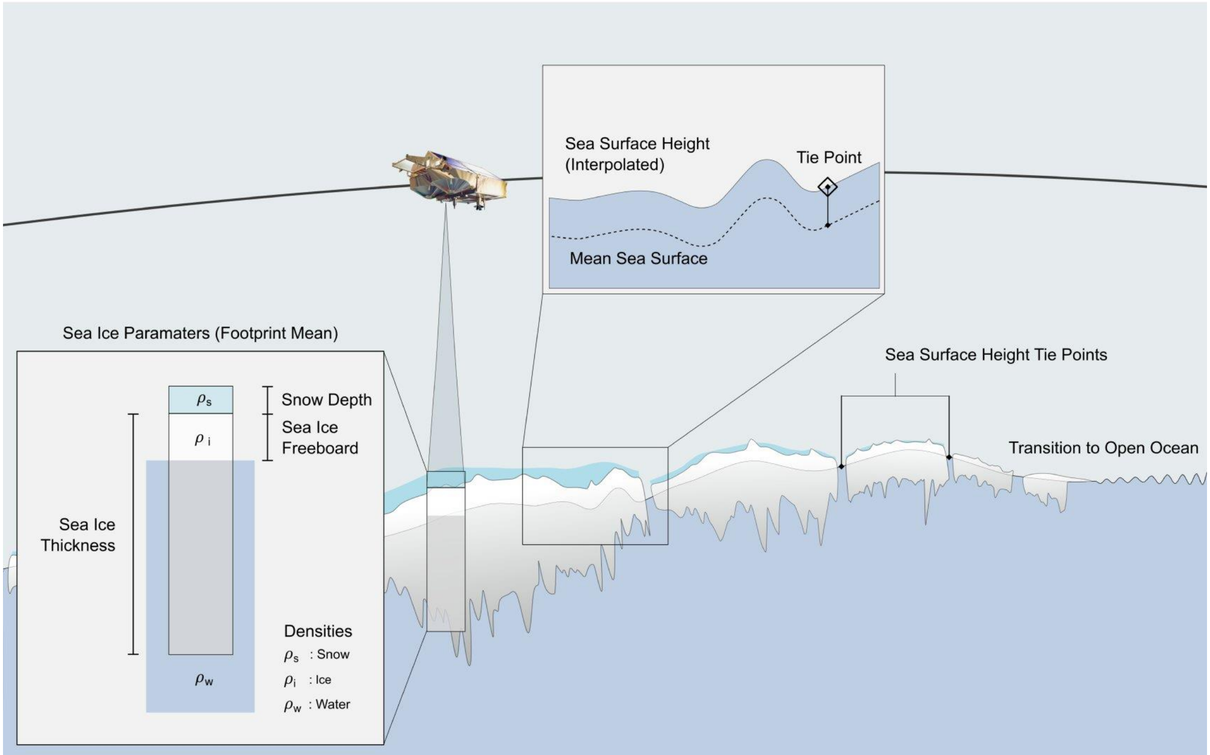

Figure 24: A schematic portraying how an altimeter measures the distance to the ice surface, and the sea ice parameters that need to be accounted for when calculating sea ice thickness. Figure 17 from Quartly et al., 2019.

4.2.3. Snow on sea ice

The planned configuration of a dual frequency altimeter is expected to measure snow thickness on sea ice, needed to convert radar freeboard into sea ice thickness. The background for the snow depth retrieval algorithms is given in this section and summarised in Table 12.

The backbone of the algorithm is different penetration depths of Ka- and Ku-bands. However, it has been demonstrated that the Ku band rarely penetrates all the way into the snow-ice interface whereas the Ka-band measured elevation is not that of snow-air interface. Guerreiro et al. (2016) studied the penetration depths with a model simulation of Ka- and Ku-band radar altimeters, mapping the penetration depth as a function of grain size. Based on these simulations they suggested that Ka-band stops within the first few centimeters into snow, and Ku-band signal can be reflected before the snow-ice interface for large snow grains. The study of Guerreiro et al. replicated AltiKa and CryoSat-2, which were studied previously by Armitage and Ridout (2015) with similar findings for freeboard differences, with Arctic basin-mean freeboard difference of 4.4 cm in October 2013 growing up till 6.9 cm in March 2014.

The most recent study of AltiKa and CS-2 penetration depths by Lawrence et al. (2018) suggests, with the support from radar theory of Rapley et al., (1983) and recent findings of Guerreiro et al. (2017) that the freeboard differences found in Armitage and Ridout (2015) might have been partly due to differences in sampling area and processing technique, in addition to difference in physical snow penetration. Lawrence et al. define the freeboard bias as the proportion of AltiKa minus CS-2 freeboard difference that does not originate from the difference in snow penetration. Due to the larger footprint of AltiKa, its waveforms are more likely to be ambiguous, not clearly identifiable as leads or floes, and thus to be discarded from the study data set compared to those of CS-2. This discarding results in bias towards higher freeboards for AltiKa, as only the larger, thicker floes are captured. Also off-nadir ranging leads are more likely to show in AltiKa than in CS-2 due to its larger footprint, and although dicarding AltiKa waveforms based on their backscatter per unit area, Lawrence et al. expect freeboard bias due to snagging to be higher for AltiKa.

When creating their dual-altimeter snow thicknesses Lawrence et al. assume that these two effects of snow penetration and sampling area bias, are not separable, and calibrate different satellite freeboards with independent freeboard data, correcting for both snow penetration and sampling area simultaneously. In their study this independent freeboard data was snow depth and laser freeboard from Operation IceBridge. They use pulse peakiness, similarly to Guerreiro et al. (2017), to characterize the surface and then compare the satellite's deviation from its expected dominant scattering horizon against the pulse peakiness. This relationship is then used to calibrate for Ka-freeboards to snow surface and Ku-freeboards to snow-ice interface.

The dual-altimeter snow thickness (DuST) from Lawrence et al. (2018) was used in the ESA Support To Science Element product for snow on drifting sea ice. As part of the project study, the impact of using this novel snow product in sea ice thickness processing was assessed and compared with thicknesses processed using the usual Warren climatology. An example of results using DuST versus Warren snow (Figure 25) in sea ice thickness processing can be seen In Figure 26.

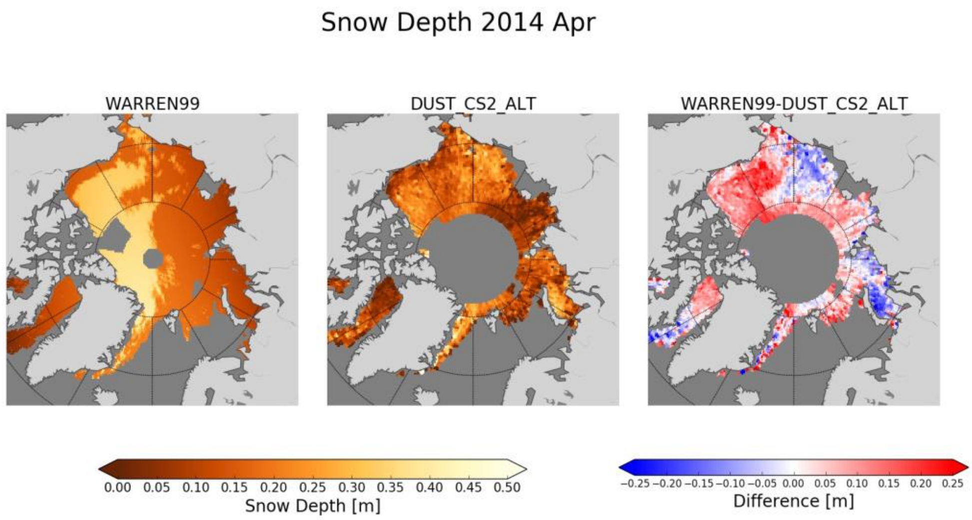

Figure 25: Examples of snow depth from Warren climatology (left), DuST product with CryoSat-2 and AltiKa (middle) and their difference (right).

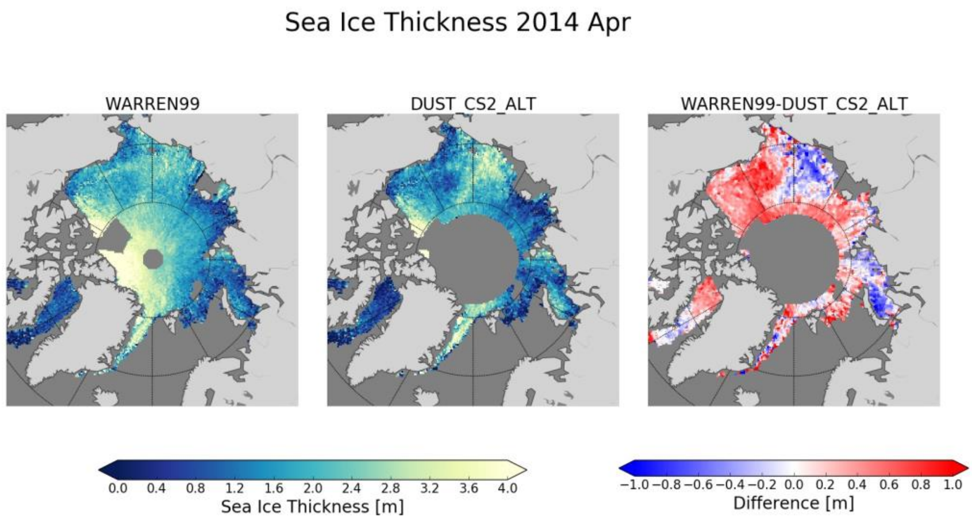

Figure 26:Examples of sea ice thickness, processed with AWI pysiral v0.2 using snow depth from Warren climatology (left), DuST product with CryoSat-2 and AltiKa (middle) and the difference of the sea ice thicknesses (right).

The current concept of the IRIS altimeter is to operate in delay-Doppler mode for both Ku- and Ka-bands. This will make the difference in footprint size much smaller than is the case with AltiKa and CryoSat-2. However, the effect of ambiguous penetration depths still stands even if the footprints would be identical (which, even for IRIS, is not the case). Thus in order to build and validate a snow thickness algorithm shall still require coincident, large scale airborne measurements of snow thickness.

Snow density is needed to account for the change of velocity within the snow for Ku-band signal. The densities provided in the Warren climatology are generally used. However, the contribution of snow density on the total sea ice thickness error budget, assessed in Tilling et al., 2019, varies between 9.2/10.0 and 11.1/11.3 percentages, for spring and autumn FYI/MYI, respectively. For snow depth these percentages are 15.1/16.4 and 16.6/16.9, which are higher, but show that the error from snow density estimates is not negligible.

Method	Current SRL	Algorithm reference
Altimetric Snow Depth (ASD)	7 7	Guerreiro et al., 2016
Dual-altimeter snow thickness (DuST)	7 7	Lawrence et al., 2018

Table 12: Two existing dual-altimeter snow depth retrieval algorithms with their maturity level, which is assessed based on the adjusted Scientific Readiness Level (SRL) Handbook from ESA [RD5], introduced in Figure 8.

4.2.4. Need for external data

Even with snow on sea ice retrieval from the dual frequency altimeter, external data source for sea ice concentration and type as well as mean sea surface will be still required. Near real time products for sea ice concentration and type are provided for example by the EUMETSAT OSISAF (available at: http://osisaf.met.no/p/ice/) as well as EU Copernicus Climate Change Service (available at: https://cds.climate.copernicus.eu/cdsapp#!/dataset/satellite-sea-ice). For sea ice concentration, also the NSICD Near-Real-Time DMSP SSMI/S Daily Polar Gridded Sea Ice Concentrations (Maslanik and Stroeve, 1999) have been used (Tilling et al., 2018; Kurtz and Harbeck, 2017). Similarly, mean sea surface height estimates such as the DTU18 (Andersen et al., 2018), UCL13 (produced by University College London), CLS15 (produced by CLS and distributed by Aviso+, with support from Cnes, https://www.aviso.altimetry.fr/), are readily available and, based on the past product versions (e.g. DTU15, DTU13, DTU10), frequently updated. The list of auxiliary products in Table 13 is not exhaustive but covers only the products we found most potential and most validated. These auxiliary products are needed e.g. for providing sea ice thickness, which is listed to be provided in the CRISTAL Level-2 data.

Parameter	Auxiliary Product	Source/reference
Sea ice concentration	OSI-SAF	EUMETSAT (http://osisaf.met.no/p/ice/)
	C3S	C3S (https://cds.climate.copernicus.eu/cdsapp#!/dataset/satellite-sea-ice)
	NSIDC NRT DMSP SSMI/S	Maslanik and Stroeve, 1999
Sea ice type	OSI-SAF	EUMETSAT (http://osisaf.met.no/p/ice/)
	C3S	C3S (https://cds.climate.copernicus.eu/cdsapp#!/dataset/satellite-sea-ice)

Mean sea surface height	DTU18 UCL13 CLS15	Andersen et al., 2018 Provided in ESA CryoSat-2 baseline-C data products (ftp://science-pds.cryosat.esa.int) https://www.aviso.altimetry.fr/

Table 13. Possible options for auxiliary data needed for a few Level-2 products.

4.2.6 On the maturity levels of the ground segment algorithms

Most of the aforementioned algorithms (Tables 11 and 12) are in a high level of maturity, and there are several long-term datasets created with these methods, undergone various validation and with a long user history, possible operational products, as well as a place in the scientific community. Another set of algorithms have been published and shown their skills in the presented use cases, but might not have as established status in the community, for example due to the lack of data releases. However, these algorithms have a great potential to take place among the older ones, once they have undergone more validation and dataset publication.

While the high level of maturity holds true for Ku-band studies, Ka-band should be given some attention to bring it to a matching level of maturity. This could be done e.g. by choosing a set of existing algorithms, adapting them to Ka-band and comparing these results. In addition, reaching some of the accuracy requirements demands additional efforts in dual-altimeter method for snow depth retrieval. The snow depth retrieval methods mentioned in Table XX are developed with data from altimeters on separate platforms, and the fact that the measurements with CRISTAL will be done from a single satellite, will certainly improve the accuracy of the snow depth product compared to the existing ones. However, this improvement could be demonstrated with a flight campaign, perhaps with results from MOSAiC.

4.3. Observation concept

4.3.1. Altimeter characteristics, modes and expected performances

CRISTAL is planned to be operated over sea ice in:

- Sea-Ice and Icebergs (SII) open-burst or SARIn mode over potentially sea ice covered areas for Ku-band
- Land-Ice and Glacier (LIG) closed-burst SARIn mode over ice caps, potentially covering some coastal sea ice areas e.g. around Greenland and Canadian Archipelago
- Open-burst SAR mode in Ka-band for improving snow depth retrieval over SII and closed-burst over LIG

The interferometric capabilities correspond straight to the mission requirement:

MRD-110. The payload shall include a SAR Radar Altimeter with the capability of interferometry.

which brings added value over sea ice as it is used to locate the echoing point over leads, improving the detection of across-track leads in particular, as stated in MRD-080 (The along-track resolution shall be sufficient to distinguish ocean (open ocean) from sea ice surfaces.). Furthermore, more accurate detection of leads improves the elevation retrieval, relating to MRD-260: The mission shall be capable of retrieving year-round elevation measurements of the sea ice-covered oceans. Similarly, open-burst timing improves sea-ice lead discrimination, leading to improved elevation and polar sea level anomalies (Kern et al., 2020).

CRISTAL will have a large bandwidth (500 MHz), which will improve the range resolution from 0.5 m (CryoSat-2) to ~0.3 m, which will improve the accuracy of sea-ice freeboard retrieval.

The 500 MHz bandwidth in Ka-band further supports discriminating ice and snow interfaces, which ought to improve not only the snow depth retrieval but reduce the overall uncertainties in freeboard and sea ice thickness retrieval.

4.3.2. Spatial & temporal sampling required

The vertical accuracy for freeboard is stated in:

MRD-280. The system shall be capable of retrieving sea ice freeboard to an accuracy of 0.03 m along orbit segments ≤ 25 km.

As freeboard is derived in Ku-band from the elevation of the ice surface and lead sea level elevation, the accuracy is dependent on the error budget of the ocean sea level retrieval, which is stated in MRD-480. The dependency on lead retrieval also means that for freeboard the accuracy cannot be beyond about 12 km, an estimate distance from the nearest lead.

MRD-290. The horizontal resolution of sea ice thickness measurements shall be 80 m.

This, strictly interpreted, requires the instrument to operate in SARIn mode over sea ice. With delay doppler processing only, horizontal resolution in the across-track direction shall be much poorer than 80 m.

Another requirement for spatial resolution is:

MRD-080. The along-track resolution shall be sufficient to distinguish ocean (open ocean) from sea ice surfaces.

with the note that this refers also to lead detection. Even if the MRD is ambiguous because no size of the lead to be detected is given, this is the driver for delay doppler processing allowing ~ 100 m scale along track resolution. This requirement could be clarified in this sense so that a minimum width for a lead to be tracker would be given.

For temporal sampling, there are no strict requirements for sea ice. As sea ice moves at speeds up to several m/s, absolute revisit times are not as relevant as for land ice since no same sea ice is measured at the same location twice. However, for users interested in a single sea area (such as for example Kara sea or Canadian Arctic waters) even distribution of ground tracks in the area of interest over one week is preferable. Ice services, such as the Canadian Ice Service and Russian Arctic and Antarctic Research Institute (AARI) update their ice charts of remote areas with little ship traffic only once a week. For snow depth on sea ice there was a request [AD2] that temporal sampling would be the same as for ice thickness.

As discussed, the requirements for temporal sampling are not detailed, and with altimetry it would be peculiar to claim a strict sea ice-oriented sampling scheme. There are requests [AD2] for pan-

Arctic daily samplings for sea ice thickness, which will never be possible with single-satellite altimetry. Currently, there are data products for Level-3 with 2 week or monthly satellite tracks gridded and interpolated, and this should be the aim for sea ice products on a full pan-Arctic coverage temporal sampling rate. However, the requirement for year-round sampling:

MRD-260. The mission shall be capable of retrieving year-round elevation measurements of the sea ice-covered oceans.

is not currently met as first of all the melt ponds remain problematic. In the MRD [AD1] it was mentioned that even though it is not possible to measure freeboard all year-round, this may evolve in the coming years and that year-round measurements are necessary for improving sea level estimation. It is not clear, whether this requirement will be met in time for CRISTAL, hence either major efforts should be made to meet the requirement and first of all studies made that it is possible to reach the requirements year-round, or the phrasing of the requirement should be relaxed.

In addition, for latency there are clear requirements in:

MRD-100. The mission shall be capable to deliver products in near real time or longer latency periods as required by the relevant application and depending on the quality and availability of auxiliary/ancillary data needed in their generation.

For which product specific latencies are specified as 6 hours (MRD-310) for sea ice freeboard, 24 hours (MRD-300) for sea ice thickness and 24 hours for snow depth on sea ice. The freeboard requirement depends on the sea level retrieval, and as operational ocean altimetry products are available within 3 hours at NRT, the 6 hour latency should be reachable for sea ice freeboard. There is a goal of 6 hour latency for sea ice thickness [AD1], and certainly sea ice thickness and snow depth can be retrieved within 24 hours considering freeboard retrieval is done in 6. It is to note that the latency depends on the availability of auxiliary data products.

4.3.3. Orbit configuration

Detailed analysis of orbit configuration for CRISTAL is suggested to be carried out in a separate CCN. However, here are listed the main mission requirements related to the orbit:

MRD-040. The mission shall measure ice and ocean surface elevations over Polar Region (Arctic and Antarctic) with an omission not exceeding 2° of latitude around the poles.

MRD-050. The mission shall have an orbit sub-cycle of less than 10 days.

MRD-070. The orbit spatial sampling pattern shall be repetitive to achieve discrimination of trends of first and multi-year sea-ice thickness and land ice elevation.

MRD-040. means in practice the small pole hole, which is a key driver for sea ice. This requirement means in practice a similar inclination to CryoSat-2. MRD-050 is necessary for solving the tides and for capturing the snowfall variability on sea ice.

The orbit options are listed in Section 3.3.4, and as suggested, will be discussed in a separate CCN.

4.3.4. Analysis of the need of a microwave radiometer

The sea ice within the microwave radiometer footprint will dominate the measured brightness temperature. An example of this can be seen in the calculated mean sea level anomalies in Figure 27, where the MWR based WTC causes unrealistic values north of the Canadian Arctic Archipelago where sea ice is heavily present. In consequence, retrieval of wet troposphere correction (WTC) from the radiometer data is not feasible over sea ice and the correction must be derived from other sources. For CryoSat-2 sea ice products this correction is provided from Meteo-France via SSALTO (Segment Sol multi-missions dALTimetrie, d'orbitographie et de localisation précise) and based on data from the European Centre for Medium-range Weather Forecasts (ECMWF). The accuracy of this WTC product version is not discussed further in the related documentations, but the results computed with ECMWF model fields indicate error of 0.02-0.03 m in the polar regions (Figure 28). The microwave radiometer based WTC values in the previous ESA missions (namely EnviSat and ERS-½) may reach -0.5 m over high latitudes, where ice is present, which is far from the expected values in the range of -0.1-0.0 m. Errors in the magnitude of several decimetres make such products unusable for polar regions (Fernandes et al., 2015). However, MRD-120 states that the radiometer shall support sea and snow type classification:

MRD-120. The mission shall embark a microwave radiometer to support wet tropospheric correction for ocean applications and ice/snow type classification.

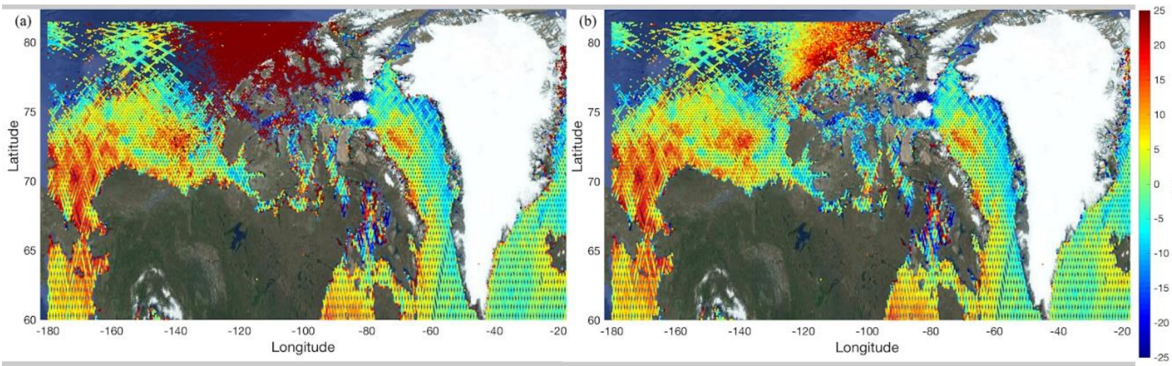

***Figure 27**: An example of the mean sea level anomaly for Sentinel-3A calculated using the WTC from (a) the on-board MWR and (b) the ECMWF model. Figure from Quartly et al., 2019.*

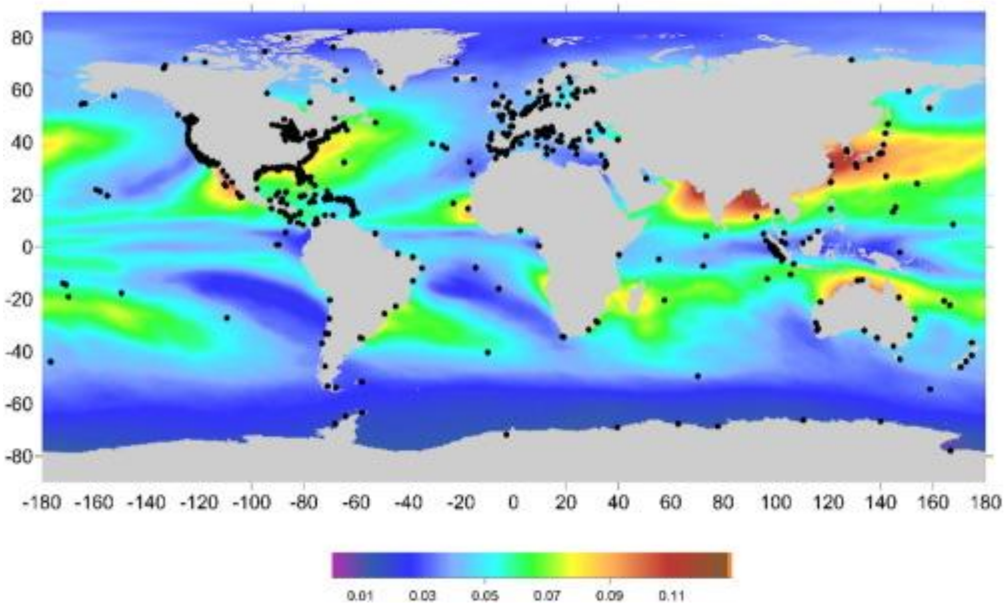

***Figure 28**: Standard error of the wet tropospheric correction, in metres, computed from two years of ECMWF model fields. Figure from Fernandes et al., 2015.*

Which is why we briefly discuss some possibilities that MWR might bring. One of these use cases is in sea ice type classification. Sea ice type classification utilising MWR has been studied e.g. by Tran et al. (2009), who presented a sea ice type classification algorithm for EnviSat MWR and RA-2. The utilise Ku and S-band backscatter and pulse peakiness from RA-2 in combination with MWR brightness temperatures for 23.8 and 36.5 GHz to as features in a classifier to derive sea ice type as well as wetness of snow. However, CCI+ RA-2 sea ice sea ice thickness processor today (Paul et al. 2017) relies on external sources for ice type since the S-band side of RA-2 was not available throughout the mission. Tran et al. (2008) also studied retrieving snow conditions with Ku and S-band backscatter and brightness temperatures and were able to identify e.g. dry and wet snow zones, but this was only done over ice sheets.

Markus and Cavalieri (1998) created and algorithm capable of using passive microwave data to retrieve snow depth over smooth first year ice with thin, less than 0.2 m, snow cover, based on AMSR-E retrieved snow depth and in situ comparisons. However estimates of snow depth over rough and thick sea ice are not successful with this method (Markus et al., 2006; Brucker and Markus, 2013). In conclusion, MWR can bring additional value in sea ice type classification and possibly in snow conditions, but to reach a mature level, further studies would be needed and the issues with sea ice dominance in brightness temperatures would still remain.

Based on the current state of the WTC and surface type classification with microwave radiometry, and given the fact that model based WTC seems to be good enough to fulfil the mission requirements, it would be recommended to favour ocean application performance, and keep the ice domain application as a secondary objective in MRD-120. However, the alternative WTC sources should still be investigated and the accuracy over polar regions confirmed.

4.3.5. Potential synergy with contemporaneous missions

There are major synergies between the sea ice observations from Sentinel-3. Sentinel-3 will provide radar freeboard measurements up to 82 degrees latitude. Furthermore, the track spacing of Sentinel-3 will be dense close to its latitude limit. Sentinel-3 will also benefit from the snow estimates from CRISTAL. An example of the capabilities of Sentinel-3 in retrieving freeboard, in comparison with CryoSat-2 is in Figure 29: Comparison of Sentinel-3 and CryoSat-2 derived freeboards.:

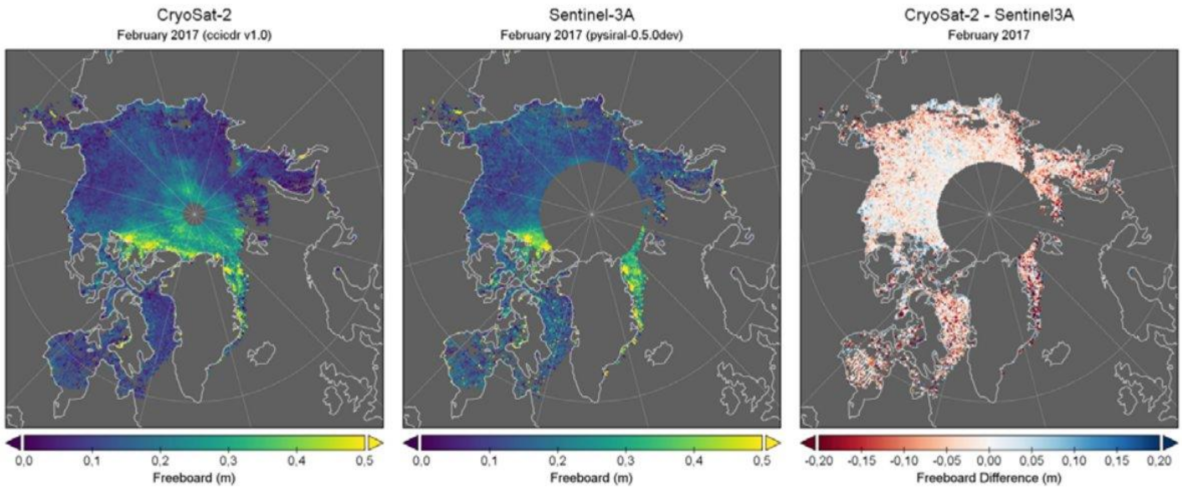

Figure 29: Comparison of Sentinel-3 and CryoSat-2 derived freeboards.

ICESat-2, which in principle measures the elevation from the snow-air interface, has been successfully orbiting transmitting data since its launch in September 2018. ICESat-2 measures elevations with the Advanced Topographic Laser Altimeter System (ATLAS) with six photon-counting beams and footprint of ~17 m. It has a 91-day exact orbit and latitudinal coverage up to 88 degrees. There are not yet publications of ICESat-2 retrieved sea ice thickness, for freeboard an example retrieval can be seen in Figure 30: Examples of total freeboard for beam 5 from ATL10 for months a) November, b) January and c) March. Figure adapted from Kwok et al., 2019., but these will certainly be useful for future synergies. In addition ICESat-2 measurements could be helpful in CRISTAL Ka-band validation and snow depth estimation.

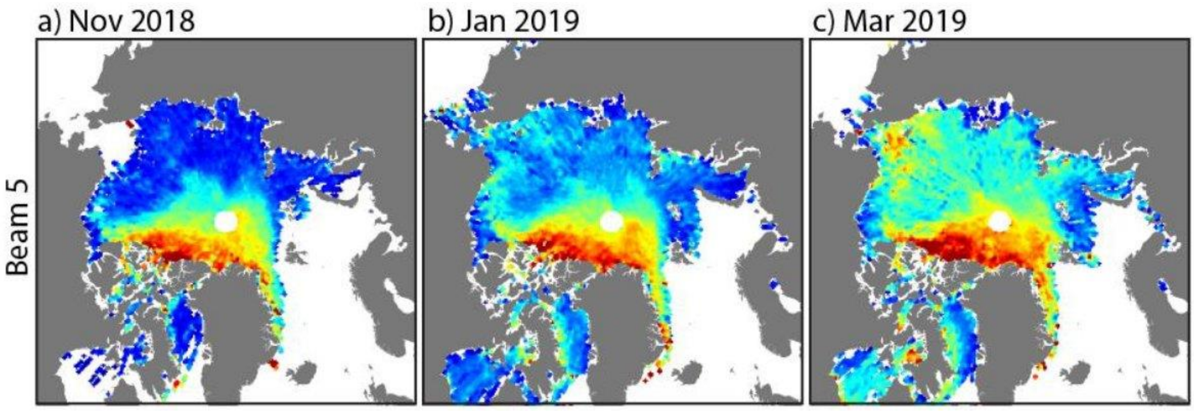

Figure 30: Examples of total freeboard for beam 5 from ATL10 for months a) November, b) January and c) March. Figure adapted from Kwok et al., 2019.

CRISTAL sea ice information can also be combined with operational SAR sea ice frames from Sentinel-1 and other imaging SAR satellites. Imaging SAR will support the extrapolation of sea ice thickness between the altimeter ground tracks.

Furthermore possible future L-band passive microwave instruments, most importantly CIMR, will open a possibility for joint CRISTAL / CIMR sea ice product, where CIMR shall provide the low resolution thickness of thin sea ice, similarly as SMOS data is merged with CryoSat-2. Furthermore, as SIC information is required in surface classification of altimeter waveforms, satellites providing SIC will be of high importance to the CRISTAL mission.

4.4. Synthesis

- **In order to achieve 80 m horizontal resolution (MRD-290), SARIn mode is required over sea ice.**
- **The sea ice products shall include sea ice thickness, freeboard and snow on sea ice thickness with uncertainty estimates as well as parameters required for snow correction and freeboard to thickness conversion.**
- **For sea ice applications, major orbit requirement is high inclination. Also, ~ weekly orbit pattern giving even coverage on ice covered seas is desirable.**
- **CRISTAL mission shall have major synergies with Sentinel-3 and CIMR as well as several imaging SAR missions including Sentinel-1.**

References

Andersen, O., Knudsen, P. and Stenseng, L. 'A New DTU18 MSS Mean Sea Surface – Improvement from SAR Altimetry' 25 years of progress in radar altimetry symposium, Portugal, 24/09/2018 - 29/09/2018, pp. 172, 2018.

Armitage, T. W. K. and Ridout, A. L.: Arctic sea ice freeboard from AltiKa and comparison with CryoSat-2 and Operation IceBridge, Geophys. Res. Lett., 42, 6724–6731, https://doi.org/10.1002/2015GL064823, 2015.

Brown, G.: The average impulse response of a rough surface and its applications. IEEE Trans. Antennas Propag., 25, 67–74, 1977.

Brucker, L., Markus, T., Arctic-scale assessment of satellite passive microwave-derived snow depth on sea ice using Operation IceBridge airborne data. J. Geophys. Res. Oceans 118, 2892–2905. http://dx.doi.org/10.1002/jgrc.20228, 2013.

Dinardo, S., Fenoglio-Marc, L., Buchhaupt, C., Becker, M., Scharroo, R., Fernandes, M. and Benveniste, J.: "Coastal SAR and PLRM altimetry in german bight and west baltic sea," Adv. Space Sci., 62(6), 2017.

Fernandes, M. J., Lázaro, C., Ablain, M. & Pires, N.: Improved wet path delays for all ESA and reference altimetric missions. Remote Sens. Environ. 169, 50–74, 2015.

Gommenginger, C., Thibaut, P., Fenoglio-Marc, L., Quartly, G., Deng, X., Gómez-Enri, J., Challenor, P., Gao, Y.: Retracking Altimeter Waveforms Near the Coasts. In Coastal Altimetry; Vignudelli, S., Kostianoy, A.G., Cipollini, P., Benveniste, J., Eds.; Springer: Berlin/Heidelberg, Germany, pp. 61–101, 2011.

Guerreiro, K., Fleury, S., Zakharova, E., Rémy, F., and Kouraev, A.: Remote Sensing of Environment Potential for estimation of snow depth on Arctic sea ice from CryoSat-2 and SARAL / AltiKa missions, Remote Sens. Environ., 186, 339–349, https://doi.org/10.1016/j.rse.2016.07.013, 2016.

Guerreiro, K., Fleury, S., Zakharova, E., Kouraev, A., Rémy, F., and Maisongrande, P.: Comparison of CryoSat-2 and ENVISAT radar freeboard over Arctic sea ice: toward an improved Envisat freeboard retrieval, The Cryosphere, 11, 2059–2073, https://doi.org/10.5194/tc-11-2059-2017, 2017.

Hayne, G. Radar altimeter mean return waveforms from near-normal-incidence ocean surface scattering. IEEE Trans. Antennas Propag., 28, 687–692, 1980.

Kern, M., Cullen, R., Berruti, B., Bouffard, J., Casal, T., Drinkwater, M. R., Gabriele, A., Lecuyot, A., Ludwig, M., Midthassel, R., Navas Traver, I., Parrinello, T., Ressler, G., Andersson, E., Martin Puig, C., Andersen, O., Bartsch, A., Farrell, S. L., Fleury, S., Gascoin, S., Guillot, A., Humbert, A., Rinne, E., Shepherd, A., van den Broeke, M. R., and Yackel, J.: The Copernicus Polar Ice and Snow Topography Altimeter (CRISTAL): Expected Mission Contributions, The Cryosphere Discuss., https://doi.org/10.5194/tc-2020-3, in review, 2020.

Kurtz, N. T., Galin, N., and Studinger, M.: An improved CryoSat-2 sea ice freeboard retrieval algorithm through the use of waveform fitting, The Cryosphere, 8, 1217–1237, https://doi.org/10.5194/tc-8-1217-2014, 2014.

Kurtz, N. and Harbeck, J.: CryoSat-2 Level-4 Sea Ice Elevation, Freeboard, and Thickness, Version 1 [October-April, 2010–2018], NASA National Snow and Ice Data Center Distributed Active Archive Center, Boulder, Colorado USA, https://doi.org/10.5067/96JO0KIFDAS8, 2017.

Kwok, R. Simulated effects of a snow layer on retrieval of CryoSat-2 sea ice freeboard. Geophys. Res. Lett. 41, 5014–5020. doi:10.1002/2014GL060993, 2014.

Kwok, R. and Cunningham, G. F.: Variability of Arctic sea ice thickness and volume from CryoSat-2, Philos. T. Roy. Soc. A., 373, 20140157, https://doi.org/10.1098/rsta.2014.0157, 2015.

Kwok, R., T. Markus, N. Kurtz, A. Petty, T. Neumann, S.L. Farrell, G.F. Cunningham, D. Hancock, A. Ivanoff, J.T. Wimert. Surface height and sea ice freeboard of the Arctic Ocean from ICESat-2: Characteristics and early results. Journal of Geophysical Research Oceans, https://doi.org/10.1029/2019JC015486, 2019.

Landy, J. C., Tsamados, M., Scharien, R. K.: A Facet-based numerical model for simulating SAR altimeter echoes from heterogeneous sea ice surfaces. IEEE Transactions on Geoscience and Remote Sensing 57 (7):4164–4180, 2019.

Lawrence, I. R., Tsamados, M. C., Stroeve, J. C., Armitage, T. W. K., and Ridout, A. L.: Estimating snow depth over Arctic sea ice from calibrated dual-frequency radar freeboards, The Cryosphere, 12, 3551–3564, https://doi.org/10.5194/tc-12-3551-2018, 2018.

Laxon S. W., Giles, K. A., Ridout, A. L., Wingham, D. J., Willatt, R., Cullen, R., Kwok, R., Schweiger, A., Zhang, J., Haas, C., Hendricks, S., Krishfield, R., Kurtz, N., Farrell, S., and Davidson, M.: CryoSat-2 estimates of Arctic sea ice thickness and volume, Geophys. Res. Lett., 40, 732–737, https://doi.org/10.1002/grl.50193, 2013.

Longépé, N., Thibaut, P., Vadaine, R., Poisson, J.C., Guillot, A., Boy, F., Picot, N., Borde, F.: Comparative Evaluation of Sea Ice Lead Detection Based on SAR Imagery and Altimeter Data. IEEE Trans. Geosci. Remote Sens., 57, 4050–4061, 2019.

Markus, T. and Cavalieri, D. J. Snow depth distribution over sea ice in the Southern Ocean from satellite passive microwave data. In Antarctic Sea Ice: Physical Processes, Interactions and Variability, 19--39. Washington, DC: American Geophysical Union, 1998.

Markus, T., Cavalieri, D.J., Gasiewski, A.J., Klein, M., Maslanik, J.A., Powell, D.C., Stankov, B.B., Stroeve, J.C., Sturm, M., Microwave signatures of snow on sea ice: Observations. IEEE Trans. Geosci. Remote Sens. 44, 3081–3090. http://dx.doi.org/10.1109/ TGRS.2006.883134, 2006.

Maslanik, J. and Stroeve, J. Near-Real-Time DMSP SSMIS Daily Polar Gridded Sea Ice Concentrations, Version 1. Boulder, Colorado USA. NASA National Snow and Ice Data Center Distributed Active Archive Center. doi: https://doi.org/10.5067/U8C09DWVX9LM, 1999.

Müller, F.L., Dettmering, D., Bosch, W., Seitz, F.: Monitoring the Arctic seas: How satellite altimetry can be used to detect open water in sea-ice regions. Remote Sens., 9, 551, 2017.

Passaro, M.;,Cipollini, P., Vignudelli, S., Quartly, G.D., Snaith, H.M. ALES: A multi-mission adaptive subwaveform retracker for coastal and open ocean altimetry. Remote Sens. Environ., 145, 173–189, 2014.

Passaro, M., Rose, S.K., Andersen, O.B., Boergens, E., Calafat, F.M., Dettmering, D., Benveniste, J. ALES+: Adapting a homogenous ocean retracker for satellite altimetry to sea ice leads, coastal and inland waters. Remote Sens. Environ., 211, 456–471, 2018.

Paul, S., Hendricks, S., and Rinne, E.: Sea Ice Climate Change Initiative Phase 2, D2.1 Sea Ice Thickness Algorithm Theoretical Basis Document (ATBD), SICCI-P2-ATBD(SIT), v.1.0, 50 pp., 2017.

Paul, S., Hendricks, S., Ricker, R., Kern, S., and Rinne, E.: Empirical parametrization of Envisat freeboard retrieval of Arctic and Antarctic sea ice based on CryoSat-2: progress in the ESA Climate Change Initiative, The Cryosphere, 12, 2437–2460, https://doi.org/10.5194/tc-12-2437-2018, 2018.

Poisson, J.C., Quartly, G.D., Kurekin, A.A., Thibaut, P., Hoang, D., Nencioli, F.: Development of an ENVISAT altimetry processor providing sea level continuity between open ocean and Arctic leads. IEEE Trans. Geosci. Remote Sens. 56, 5299–5319, 2018.

Quartly, G. D., Rinne, E., Passaro, M., Andersen, O. B., Dinardo, S., Fleury, S., Guillot, A., Hendricks, S., Kurekin, A. A., Müller, F. L., Ricker, R., Skourup, H., and Tsamados, M.: Retrieving Sea Level and Freeboard in the Arctic: A Review of Current Radar Altimetry Methodologies and Future Perspectives, Remote Sens., 11, 881, https://doi.org/10.3390/rs11070881, 2019.

Rapley, C., Cooper, A. P., Brenner, A. C., and Drewry, D.: A Study of Satellite Radar Altimeter Operations Over Ice-covered Surfaces, Tech. Rep. July 2015, European Space Agency, 1983.

Ricker, R., Hendricks, S., Helm, V., Skourup, H., and Davidson, M.: Sensitivity of CryoSat-2 Arctic sea-ice freeboard and thickness on radar-waveform interpretation, The Cryosphere, 8, 1607–1622, https://doi.org/10.5194/tc-8-1607-2014, 2014.

Sallila, H., Rinne, E. and Hendricks, S. Sea Ice Climate Change Initiative+ Phase 1, D2.1 Sea Ice Thickness Algorithm Theoretical Basis Document (ATBD), v1.0, 2019.

Tilling, R. L., Ridout, A., and Shepherd, A.: Estimating Arctic sea ice thickness and volume using CryoSat-2 radar altimeter data, Adv. Space Res., 62, 1203–1225, https://doi.org/10.1016/j.asr.2017.10.051, 2018.

Tilling, R., Ridout, A., and Shepherd, A.: Assessing the impact of lead and floe sampling on Arctic sea ice thickness estimates from Envisat and CryoSat-2, J. Geophys. Res.-Oceans, 124, https://doi.org/10.1029/2019JC015232, 2019.

Tran, N., Rémy, F., Feng, H., and Fémenias, P.: Snow facies over ice sheets derived from Envisat active and passive observations. IEEE Trans. Geosc. Remote Sens., 46 (11):36943708, 2008.

Tran, N., Girard-Ardhuin, F., Ezraty, R., Feng, H., & Femenias, P. Defining a Sea Ice Flag for Envisat Altimetry Mission. IEEE Geoscience and Remote Sensing Letters, 6(1), 77–81. doi:10.1109/lgrs.2008.2005275, 2009.

5. Level-2 products & processing for Ocean

5.1. Definition of level-2 & higher-level products

5.1.1. Level-2 products

All information available in the level-1 products should be reported in the level-2 products. In addition, the table below describes the different categories of parameters that will present in the level-2 products.

Parameters(s)	Comment
Retracking outputs	Outputs from the different retracking algorithms
Radiometer outputs	Related to the radiometer instrument & derived information
Geophysical corrections	Geophysical corrections applied to derive SSH / SLA
Auxiliary data	Information collected from external datasets that can be useful for users
Waveforms parameter	Related to the waveform shape
Oceanic Geophysical parameters	List of all geophysical parameters derived from the altimetry measurements

Table 10: Level-2 parameters categories

Retracking outputs

Variables in output of the physical level-2 retrackers:

- **Epoch**: Position in the window analysis where the altimeter range is estimated, located in the waveform leading edge.
- **Thermal noise:** Measured on the waveform first samples, where the altimeter does not receive any energy from surface
- **Amplitude:** Allow to derive the backscatter coefficient (Sigma-0)
- **Antenna mispointing**: Estimation of the global mispointing (roll & pitch) of the antenna. *Estimated only from (P)LRM measurements*.
- **Mean Quadratic Error**: Quantify the agreement between measured waveform and the final retracking model
- **Quality flag**: To inform if retracking was successful
- ***Significant Wave Height (SWH)***: *See geophysical parameters category*

Radiometer outputs

Variables relative to the microwave instrument & geophysical information derived:

- **Brightness temperatures** for each channel
- **Surface type** derived from radiometer measurements
- **Quality flags**
- ***Liquid water content:*** *See geophysical parameters category*
- ***Water vapor content:*** *See geophysical parameters category*
- ***Wet tropospheric correction:*** *see geophysical corrections category*

Geophysical corrections:

Include all geophysical parameters that allow to derive the Sea Surface Height (SSH) & Sea Level Anomaly (SLA):

- **Dry Tropospheric Corrections:** The dry tropospheric correction compensates for the effect of non-polar gases such as oxygen and nitrogen.
- **Wet Tropospheric Corrections:** The wet tropospheric correction compensates for the effect of polar gases, mainly water vapor. Wet tropospheric corrections are derived thanks to the on-board microwave measurements or models if there is no on-board microwave.
- **Inverse barometric correction**: it compensates for variations in sea surface height due to atmospheric pressure variations, known as atmospheric loading.
- **Dynamic atmospheric correction**: it compensates for variations in sea surface height due to atmospheric pressure and winds.
- **Ionospheric correction**: it compensates for the free electrons in the Earth's ionosphere slowing the radar pulse.
- **Ocean tide correction:** it removes the effects of local tides i.e. those caused by the Moon, and the long--period equilibrium ocean tide correction removes tidal effects due to the Sun.
- **Ocean loading tide correction:** it removes the deformation of the Earth's crust due to the weight of the overlying ocean tides.
- **Solid Earth tide correction:** it removes the deformation of the Earth due to tidal forces from the Sun and Moon acting on the Earth's body.
- **Geocentric polar tide correction:** it removes a long--period distortion of the Earth’s crust caused by variations in centrifugal force as the Earth’s rotational axis moves its geographic location.
- **Mean Sea Surface (MSS) correction:** The mean sea surface grid used corresponds to the mean sea surface elevation computed with all altimetry estimations since Jason-1. It allows to derive a Sea Level Anomaly (see *geophysical parameters category)*, the difference between the measured sea surface height (SSH) and the MSS.
- **Atmospheric attenuation:** Correction to apply on Sigma-0 accounting for atmospheric losses. The correction will be different between Ku/Ka bands.
- **Sea State bias:** See section 5.2.4.

<u>**Auxiliary data:**</u>

The following list is taken from Sentinel-3A auxiliary data available in the NTC products. Usually the auxiliary data also comprised dataset used to derive geophysical information. These are not present below, as all the geophysical information used to derive the oceanic SSH/SLA are already listed in the previous section:

- **Orbit POE:** Contain precise orbit information
- **Sea-Ice concentration**: Providing the ratio of ice present per pixel grid.
- **Sea ice concentration climatology**
- **Snow depth climatology:** snow depth data is available from the National Snow and Ice Data Centre
- **Surface classification mask:** to discriminate between open ocean, land, continental water, aquatic vegetation, continental ice snow, floating ice, salted basin
- **Marine/Land mask**
- **Geoid height map**
- **Map of the slopes of the MSS/geoid with respect to the ellipsoid**
- **Bathymetry/Topography map**
- **Surface slope models:** Used to derive slope-induced error over Antarctic & Greenland ice sheets
- **Distance to shore**
- **Look Up Tables / correction tables / empirical tables:** Different LUT or tables must be available in the products:
    - SAMOSA retracker
    - MLE4 retracker
    - SSB correction table
    - Wind table
    - Rain rate correction table
    - Sigma-0 tables in LRM/SAR

<u>**Waveforms parameter:**</u>

- Waveform classification depending on shape parameters & retracking outputs (see Poisson et al., 2018)
- Waveform peakiness

<u>**Altimetry geophysical parameters:**</u>

Finally, below is the list of all the geophysical parameters derived directly or indirectly from altimetry measurements over ocean:

- **Sea Surface Height (SSH):** From the estimated altimeter range, with all necessary geophysical corrections applied
- **Sea Level Anomaly (SLA):** Difference between SSH & Mean Sea Surface
- **Significant Wave Height (SWH):** Directly from the retracking outputs
- **Sigma-0:** Backscattering coefficient of the surface, derived from the waveform amplitude
- **Wind speed:** Derived from the Sigma-0 & SWH
- **Liquid water & water vapor content:** Derived from radiometer measurements
- **Rain rate & probability:** Derived from radiometer measurements

On the MRD, the ocean observables include: **"sea level anomaly, significant wave height, wind speed, sea state bias, geostrophic current"**. All these parameters are listed above, except for the "geostrophic current". In fact, the geostrophic currents estimated in altimetry are retrieved from gridded Absolute Dynamic Topography (ADT) products [Arbic et al., 2012], usually generated from multi-missions measurements. Therefore, providing such an estimation at level-2 looks irrelevant.

5.1.2. Higher level products

Currently, Copernicus Marine Environment Monitoring Service is producing and distributing several higher level products in Near Real Time (NRT) & delayed time (reprocessing). Below is the list of the distributed products, as also listed in the Polar Monitoring TN-1. Level-3 refers to mono-sensor, along-track products & level-4 to multi-sensors, gridded products.

- ***Sea Level Anomaly (SLA)***

See definition in the previous section. Products are available at level-3 & level-4.

- ***Absolute Dynamic Topography (ADT)***

The absolute dynamic topography is obtained by adding the SLA to the Mean Dynamic Topography. Products are available at level-4 (multi-missions gridded products).

- ***Surface Geostrophic Current Velocity***

The geostrophic current products disseminated to users are computed by geostrophy using the ADT estimations. More details are available in Arbic et al. [2012] & Pujol et al. [2016]. Products are available at level-4.

- ***Significant Wave Height (SWH)***

SWH is commonly used as a measure of the height of ocean waves. Products are available at level-3, and a level-4 product will be available soon.

5.2. Level-2 ground processor algorithms

The level-2 processing contains mainly 2 blocks of algorithms;

- One dedicated to the estimation of the geophysical parameters. It is essentially composed by a retracking algorithm.
- One dedicated to the correction of the geophysical estimates including instrumental corrections, sea state bias corrections, geophysical and environmental corrections, …

5.2.1. Retracking algorithms

The retracking is a key algorithm of the altimeter processing chain on which depends a significant part of the altimeter performances, not only over open ocean but over all surfaces.

Over open ocean, the retracking provides three or four geophysical parameters from the SAR unfocused & (P)LRM waveforms:

- the Sea Surface Height (SSH) (indirect output via the epoch parameter)
- the Significant Wave Height (direct output)
- the backscattering coefficient of the surface (Sigma-0, indirect output via the amplitude parameter)
- In addition, in (P)LRM the retracking is also capable of estimating the antenna mispointing angle

The retracking algorithm used over open-ocean can be split in three modules:

- **The signal modelling**, that must fit the acquired waveform. A physical model is considered in the SAMOSA retracker and in the CNES S3 processing prototype retracker.
- **The estimation process:** usually Newton-Raphston or Levenberg-Marquardt or or Nelder-Mead solution are used. The SAMOSA retracker uses an analytical modelling of the signal, with a Levenberg-Marquardt Least-Squares Estimation Method [Ray et al., 2014].
- **The cost function** (usually maximum likelihood or least square), which is the mathematical function used to fit the model to the data. It can account or not for the real characteristics of the noise distribution. Great benefits have been found when using a Maximum Likelihood criterion (ADAPTIVE retracker from CLS) instead of a Least Square criterion (SAMOSA retracker from ESA).

Different solutions are currently existing, developed by different teams and providing various performances.

CRISTAL altimeter is planned to operate in closed-burst mode over open ocean, in both Ku and Ka bands. Hence, it will be possible to produce SAR & P-LRM waveforms, using the unfocused processing such as the Sentinel-3 missions. Currently, in P-LRM, the retracking algorithm implemented in the Sentinel-3A IPF is the classical Maximum Likehood Estimator (MLE4), using the analytical Brown model [Amarouche, 2004]. This algorithm is employed for all the LRM historical missions.

One advantage of the SAMOSA retracker is the fast CPU time computation thanks to the analytical expression of the SAR model. However, simplifications are employed on this analytical expression, in particular regarding the Pulse Target Response (PTR) & and the Azimuth impulse response. In the SAMOSA retracker, the PTR are considered Gaussian, while they are more similar to a sinus cardinal in reality. This creates biases in the final geophysical estimations. To account for this effect, Look Up Table (LUT) are applied during each iteration of the processing.

Recently, this drawback has been highlighted during Sentinel-3 ESL council meeting (Sept 2019). A drift of the instrumental PTR width has been detected. It occurs since the beginning of the Sentinel-3A mission and is not taking into account in the SAMOSA LUT. The estimated impact on the SSH is an error of ~0.3 mm/year in SAR mode, which could prevent the mission to be used for climate studies. Due to a similar approximation in the analytical Brown model, a similar error is estimated in PLRM: ~0.36 mm/year.

The solution that has been chosen right now, is to update the SAMOSA LUT to account for the drift, but if the drift is non-linear errors will still occur. Another option is to use a **numerical retracker**, which can integrate the real PTR & Azimuth impulse response and thus account for all evolutions of the PTR. This second option will be studied carefully. Nevertheless, one drawback of current numerical retrackers is the CPU time. A recent very promising study shows that this problem can be tackled. Investigations are currently done to analyse the impacts in terms of CPU and in terms of performances of the algorithm.

Continuity between open-ocean & sea-ice/coastal regions

Recently, CLS has developed and successfully validated a new solution called "Adaptive Retracker" for LRM or SAR measurements, implementing a new waveform model (accounting for the mean surface roughness parameter) and a Nelder Mead optimization method with exact likelihood criteria.

This solution has been already implemented in the ground processing chains of the CFOSAT mission, and will be implemented for the future GDR-F Jason-3 reprocessing. For Delay-Doppler altimetry, a similar version has been developed at CLS for Sentinel-3 and Cryosat-2. As written previously in this chapter, the results over open ocean are excellent for LRM altimeters but some progresses have still to be done for Delay-Doppler. The results are currently under investigation.

However, **an additional characteristic of this algorithm has also to be emphasized**. It concerns the capability of this algorithm to maintain the continuity of SLA observations between open ocean measurements and sea level measurements in the leads. Trying to extend the SLA estimation to the pole is indeed crucial for polar observation and it is linked to our ability to recognize the measurements coming from the leads and to process them. The Adaptive retracker has the great advantage to guaranty this continuity of observation as illustrated in the following figures for LRM and SAR. We clearly see in these two figures that open ocean SLA values (green points on the left of the plot) are consistent with SLA in the leads (red points on the right of the plot) while values provided by empirical retrackers in purple (retrackers that are currently used over these regions) are clear biased and noisier.

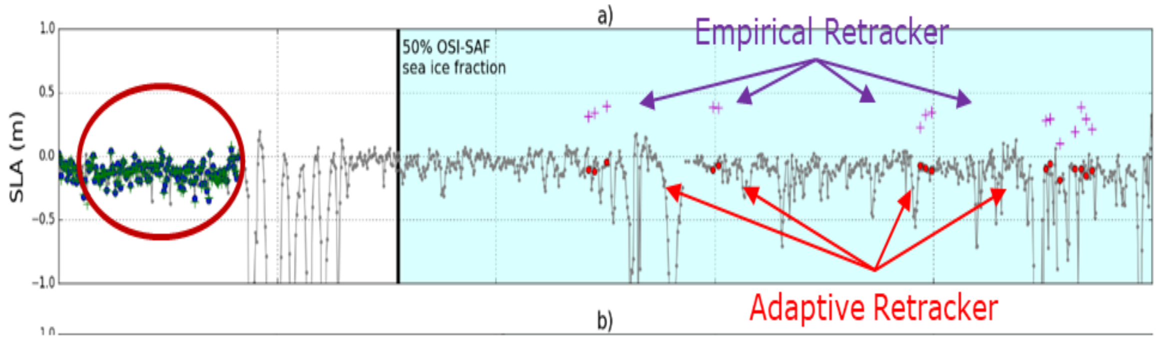

Figure 27: Envisat/RA-2 Cycle 64, P 788 in December 2007.

FORM-NT-GB-7-1

As well for Sentinel-3 Sar data, the same SLA continuity is observed.

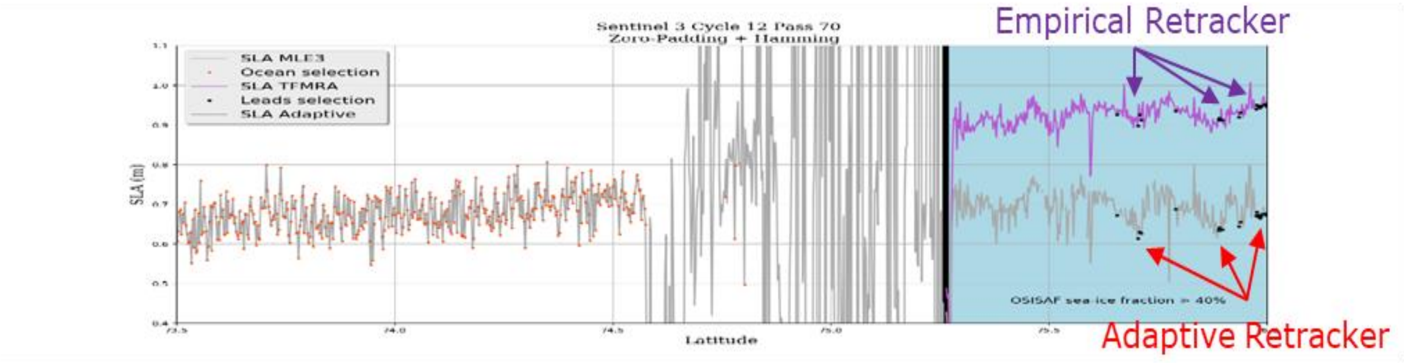

***Figure 28: Sentinel-3 Cycle 12, P 70 in December 2016*.**

We must note that similar adaptations of the open ocean retracker have been done on the GPOD service provide by ESA with an extension of the SAMOSA retracking algorithm named SAMOSA+ [Dinardo & al, 2017]. We recall that the SAMOSA retracker is the retracker currently used operational in the Sentinel-3 IPF.

The adaptive solution (CLS/CNES solution or SAMOSA+ solution) is thus fully recommended:
- To ensure the continuity of estimations from open-ocean waveforms to peaky waveforms acquired over the leads in the Arctic ocean for example.
- To provide consistent estimations of the sea-ice surfaces (floes & leads), which are necessary to achieve the best possible accuracy for the freeboard. On the other hand, the current retrackers, such as Thresholf First Maximum Retracker (TMFRA), are based on empirical thresholds which does not account for instrumental characteristics (PTR) and variation of surface roughness.

Recent progress made in SAR modelling over open ocean

Calibration/validation studies demonstrate that there are still some slight discrepancies remaining between LRM & SAR unfocused estimations. In particular there is a 10cm to 15cm bias on the estimated SWH between SAR & (P)LRM. Recent efforts have been made to understand and correct this bias. In particular, Buchhaupt shown in his PhD work that wave orbital velocity as an impact on the altimetry Doppler processing, which is currently not taken into account in the operational ground processing. In particular, it could explain the positive bias observed in SWH compared to (P)LRM. Internal studies conducted at CLS with numerical simulators also reach the same conclusions.

More studies will be necessary to confirm these first results, and potentially to find a solution to include the wave orbital velocity parameter in a future retracking algorithm.

Conclusions

To conclude, the following recommendations for the choice of the retracking algorithm in SAR & P-LRM over open ocean can be given:

- **A numerical retracker** solution should be considered, as 1) level-2 estimates will not be impacted by potential instrumental drift, such as those observed in Sentinel-3A. 2) CPU time resources will be improved by 2025 & already new algorithmic solutions exist to reduce the high computational effort required
- Accounting for the **roughness of the ocean surface (MSS)** is critical for improving the SLA continuity between open ocean & sea-ice regions. A significant improvement can be made on our knowledge of the Mean Sea Surface at high latitudes. Moreover, more accurate estimations of the freeboard are expected with a physical retracker including the mss, compared to current empirical retrackers (see section 3, dedicated to Sea-Ice).
- *It is clear from our experience that great benefits can be found to use optimization methods that account for the speckle noise statistics corrupting the waveforms. It has been already demonstrated in conventional altimetry. Such a solution is already implemented in the CFOSAT ground processing and will be used for the Jason-3 GDR-F reprocessing that will be done in 2020.*
- Studies relative to the effects of wave orbital velocity in delay Doppler altimetry should be closely followed
- For the sake of continuity with the historical missions **a classical Brown MLE4 retracker cannot be discarded in P-LRM. However, all historical missions are currently reprocessed using more efficient algorithms like the Adaptive retracker (the ESA FDR4ALT project will reprocess ENVISAT/RA-2 and ERS1/2 missions using an Adaptive solution, Jason1/2/3 and SARAL missions will be as well reprocessed with the Adaptive retracker)**

5.2.2. Wind speed retrieval

The estimation of the wind speed is performed thanks to a mathematical relationship with the backscattering coefficient (Sigma-0) and the Significant Wave Height (SWH) [Witter & Chelton, 1991; Abdalla, 2012]. The model functions developed to date for altimeter wind speed have all been purely empirical. The wind speed model function is evaluated for 10 meters above the sea surface and is considered to be accurate to 2 m/s.

The CRISTAL altimeter will have the capability to provide two wind speed estimates, one in Ku-band another in Ka-band. Even if Ka-band is sensitive to atmospheric factors like liquid water and water vapor, AltiKa wind speed is completely usable [Abdalla, 2015; Kumar et al., 2015]. Therefore, studies should be conducted to assess how a dual Ku/Ka wind speed estimation could be efficiently used.

5.2.3. Additional algorithms using dual Ku/Ka measurements

CRISTAL will be the first mission to operate with dual frequency bands over Ocean. As it will be presented in the next sections, the along-track footprint in Ku band should be around 268 meters (~25Hz regarding satellite velocity) & 100 meters in Ka band (~66Hz regarding satellite velocity). An algorithm could be developed, combining Ku & Ka estimations for the SSH/SLA & SWH parameters, with the purpose to provide an optimal estimation at 20Hz rate.

Prior to that, it will be essential to assess the differences between Ku/Ka estimations and understand any possible discrepancies. In addition, Ku band & Ka band will respond differently to small surface roughness due to their different wavelengths (2.2cm Ku vs 0.8cm Ka). Acquiring simultaneous measurements in Ku and Ka bands will provide for sure interesting information regarding the sea state.

5.2.4. Sea State bias estimation

The sea state bias (SSB) is an altimeter cm-level range error due to the presence of ocean waves on the surface. For operational purposes, empirical satellite based SSB look-up tables are built to describe the SSB amplitude as a two-dimensional function of the SWH and the wind speed [Gaspar et al. 1994; Gaspar and Florens; 1998] because these parameters are concurrently measured by radar altimeters. Different aspects of the empirical determination have been analyzed and improved through the years. It was shown that operational wave modeling can now support improved ocean altimetry. Tran et al. [2006, 2010] pointed out that the addition of the mean wave period (Tm) from a numerical wave model to build a three-dimensional global SSB model, can significantly improve the SSB estimates regionally and can reduce the altimeter range error budget by approximately 7.5%. The empirical modeling remains still a challenging topic in the context of new operational modes for recent and future nadir altimeter missions (e.g. SAR and SARin modes) or wide-swath topography interferometers for instance, because of the anisotropic nature of their measurements that might add another layer of complexity to the isotropic footprint of a traditional altimeter.

5.2.5. High Frequency Adjustment (HFA)

The observation of small ocean scales lower than 100 km by altimeters is limited by cm-scale measurement noise. Lately, an empirical high-frequency adjustment (called HFA) was developed for Jason-3 to reduce 20-Hz correlated noises observed between range and SWH data [Tran et al., 2019] and that arises from the altimeter measurement process itself, the retracking algorithm. This follows the work of Zaron and DeCarvalho [2016] and needs to be determined specifically for each mission and processing mode. This additional empirical correction applied to standard SSH computation aims at improving the signal-to-noise ratio. SSB and HFA are two empirical terms that play together to improve the SSH estimations. Equivalent HFA correction can also be applied on SWH estimations [Tran et al., 2019].

5.3. Level-2 processing maturity

The maturity of the level-2 algorithms previously described is now discussed, based on the Scientific Readiness Levels (SRL) Handbook from ESA [RD5] (see section 2.3.2).

- **MLE4 Brown retracking (LRM/PLRM) => SRL 9**

  The classical LRM MLE4 retracker using Brown model was adopted since the Jason-1 mission [Thibaut et al., 2010] and is implemented on all altimetry ground segments processing LRM data. The algorithm is therefore fully mature.

- **SAMOSA retracking (SAR mode) => SRL 8**

  SAMOSA retracker is employed to operationally process the Sentinel-3 waveforms since the beginning of the Sentinel-3 era, in 2016. Deep assessments have been performed by the Sentinel-3 Mission Performance Center team, proving the good performances of SAR altimetry mode over open ocean. And implicitly the expected behavior of the SAMOSA retracker. Nevertheless, the processing still have known drawbacks, in particular the inability to account for a real Pulse Target Response (PTR) prevent to use SSH/SLA estimations for climate objectives.

- **Numerical retracking => SRL 7**

Compared to SAMOSA, which rely on an analytical computation, the value of the numerical retracker is to fully take into account all instrumental effect that impact the measurement, in particular the PTR and its potential drift. Even if a CalVal analysis is available in the literature [Raynal et al. 2018], CPU time is currently a barrier for an operational implementation. Nonetheless, recent studies prove to tackle this issue.

- **Retracking accounting for mean square slope => SRL 7**

As previously detailed, objectives of such retrackers is to provide more accurate estimations over the ice covered ocean and maintain a continuity between open-ocean and sea-ice. From our knowledge two retracking solutions exists: the CLS Adaptive (numerical approach) & the GPOD SAMOSA+ (analytical approach). While the CLS adaptive approach has been validated in LRM [Poisson et al., 2018], this is not yet the case in SAR. There is no exhaustive CalVal of the SAMOSA+ retracker from our knowledge.

- **Retracking accounting for orbital wave => SRL 5**

First developments were performed by C.Buchhaupt during his PhD studies. The obtained results are promising as it would remove the +10/15cm SWH bias in SAR mode (wrt LRM), but the method is not yet valid for all waves range and must be matured.

- **Wind speed retrieval => SRL 9**

Algorithm is fully mature and implemented on all altimetry ground segments. Among its usage, The parameter is required for the Sea State Bias computation.

- **Sea State Bias => SRL 9**

Algorithm is fully mature and implemented on all altimetry ground segments, as it is not possible to retrieve an accurate sea level estimation without it. Note the algorithm itself has been refined over time. For instance, CLS proposes to implement a new computation for the ESA FDR4ALT project (ERS and Envisat RA-2 reprocessing), including a new parameter: the wave mean period.

- **HFA => SRL 7**

The High Frequency Adjustment algorithm has been tuned for the SWH parameter, and for different modes (LRM / SAR / LR-RMC). It has also been tuned for the range parameter, only in LRM for now. Long time series of data were processed, along with dedicated CalVal. There is currently no immediate plan to include it in a ground segment.

The table below summarizes the maturity levels attributed to the oceanic level-2 processing previously described:

	Retracking algorithms				
Level-2 processing	**Brown MLE4**	**SAMOSA**	**Numerical retracker**	**with Mean Square Slope**	**with orbital wave**
SRL level of maturity	**9**	**8**	**7**	**7**	**5**

	Others processors		
Level-2 processing	**Wind speed retrieval**	**Sea State bias**	**HFA**
SRL level of maturity	**9**	**9**	**7**

Table 11: SRL maturity for the oceanic level-2 processing

5.4. Observation concept

5.4.1. Altimeter characteristics, modes and expected performances

Based on the proposition made by Thales, the instrumental configuration should be the following one:

- Closed-bursts of 64 pulses emitted at 18 kHz, in both Ku & Ka bands
- Ku & Ka bandwidth 500MHz, leading to a vertical resolution of ~30cm
- Range window size of 256 samples / 64 meters
- Closed-loop tracking mode

Based on this configuration, the along-track resolution will be (width of unfocused Doppler bands):

<u>500km satellite altitude - such as ICESat-2</u>

- Ku band: **184m** along-track resolution
- Ka band: **69m** along-track resolution

<u>725km satellite altitude - such as CryoSat-2</u>

- Ku band: **268m** along-track resolution
- Ka band: **101m** along-track resolution

<u>1300km altitude - such as Jason serie</u>

- Ku band: **491m** along-track resolution
- Ka band: **185m** along-track resolution

To anticipate the performances of the altimeter, the following aspects have to be considered:

- The **number of individual looks** contained in the stack:
  - In Ku band this number should be close to Sentinel-3A one (180), as both altimeters configurations are similar over open ocean. However, thanks to the 256-points length of the analysis window, more looks of the same Doppler band on ground can be accumulated with CRISTAL. Nevertheless, we have to consider that these lateral looks are less energetic than central ones, and therefore will contribute to a smaller extent to the multi-looking noise reduction.
  - In Ka band, the antenna aperture is narrower, hence the number of individuals of looks should be divided by a factor of two approximately compared to Ku-band, providing a less efficient noise reduction from multi-looking.
- **Ka band is supposed to provide a better noise level reduction compared to Ku band** thanks to a smaller and statistically more homogeneous footprint [Bonnefond et al., 2017]. Nevertheless, the noise reduction provided by this unique effect remains unquantified, and in the CRISTAL vase, Ku/Ka footprint will be the same, because of the identical 500MHz bandwidth.
- **Vertical resolution of the range gates** also impacts the noise levels of the geophysical parameters estimated. In this respect, the CRISTAL altimeter will be the first one providing a 500MHz Bandwidth in Ku band, leading to a vertical resolution of ~30cm. Therefore, a better noise level reduction is expected compared to Sentinel-3. Note that Ka band will also have the same ~30cm vertical resolution.
- The along-track spatial resolution in Ka-band (100m with the CryoSat-2 orbit) will allow to provide estimations at ~**66Hz frequency rate,** compared to ~25Hz in Ku band.

Finally, in terms of noise level on the 20Hz estimates, and considering the altimeter configuration retained, the following conclusions can be drawn over open ocean:

- In SAR Ku band, CRISTAL noise level will be lower than Sentinel-3* thanks to a better vertical resolution (30cm vs 47cm), and more individual looks contained in the stack (second order effect). Without a robust study it is difficult to precisely quantify the potential gain.

- It is not straightforward to determine which band between Ku & Ka will provide the lowest noise level in SAR mode:
  - In Ku band more individual looks will be collected due to the wider antenna aperture, providing a more efficient noise reduction by multi-looking. The -3dB antenna aperture ratio is 2.4 (0.43° in Ka vs 1.4° in Ku).
  - Thanks to a thinner along-track resolution (100m vs 260m) Ka band will be ideally able to provide a single estimate out of 2.6 estimates in Ku band. Nonetheless, this will depend on the chosen on-ground sampling.
  - Ka band is supposed to be less noisy due to a smaller and statistically more homogeneous footprint, but in the CRISTAL case Ku & Ka will have the same footprint.

=> In conclusion, the different advantages/disadvantages of both bands could cancel each other out, and perhaps a similar noise level in the estimated geophysical parameters will be reached. This will also depend on the chosen on-ground sampling. A dedicated study would be necessary to investigate the Ku & Ka noise levels. Finally, note that the measure in Ka band will be more sensitive to swell because of the smaller along-track footprint.

Discussions about MRD requirements (RD-3)

Here, we discuss briefly some recommendations made over open ocean in the MRD:

MRD 460 - The vertical uncertainty in sea level anomaly retrieval from Ku band (including sea-ice leads) shall be 0.02 m.

Discussed in section 6 (Specific MRD analyses required by MAG)

MRD 480 - The standard deviation of the 1-second along-track averaged corrected measurements of sea surface height shall be less than 0.0294 m.

Discussed in section 6 (Specific MRD analyses required by MAG)

MRD 510 - The uncertainty of 1-second averaged measurements of significant wave height in the range 0.5 to 8 m shall be less than 0.15 m plus 5% of the significant wave height

Here we suppose that "***The uncertainty of 1-second averaged measurements***" refers to the "***standard deviation of the 1-second along-track***", similarly to the requirement relative to SSH. The SAR Sentinel-3A 1Hz **SWH** noise is currently estimated at **0.09m** (from CLS Cal/Val studies). This results was presented at the Sentinel-3 Validation Team meeting (March 2018), by M.Raynal. The presentation is available here:
https://www.eumetsat.int/website/home/News/ConferencesandEvents/DAT_3645214.html

Considering the close configuration of CRISTAL over open ocean (detailed before), the 0.15 m (plus 5% of the significant wave height) requirement should be easily achieved.

Moreover, the better waveform sampling (~30cm vertical resolution for CRISTAL) should provide a lower noise level compared to Sentinel-3A. As discussed before the Ka-band estimates should be at least at the same noise level than Ku-band ones, potentially even lower. But this is partly conditioned by the ground sampling choose for both bands.

5.4.2. Spatial & temporal sampling required

The MAG recently made the following recommendations for open ocean:

- Regular, homogeneous sampling is generally favorable.
- The orbit must complement Sentinel-3 orbit pattern.
- A 15 days sub-cycle for mid-latitude mesoscale is desirable for oceanographic purposes and objectives but the lack of such sub-cycle should not be a criterion to reject an orbit.

We globally agree with this, and add the following recommendations from G.Dibarboure analysis, even if we fully understand that ocean is not the highest priority for CRISTAL:

- A 2 to 3 days sub-cycle will be beneficial for wave assimilation & polar meso-scale
- 90 or 120 or 180 days sub-cycle will allow to remove seasonal biases in polar MSS
- A 365 days cycle will be beneficial for global & polar Mean Sea Surface

Discussions about MRD requirements (RD-3)

MRD-420 - The mission shall be capable of retrieving sea level anomaly at an along-track resolution better than 10 km.

Current altimeters are already capable of delivering SLA at 20Hz rate, corresponding to ~330m on-ground. Considering the CRISTAL configuration, the finest sampling achievable will depend on the SAR along-track resolution:

- Ku band: ~300 meters along-track sampling
- Ka band: ~100 meters along-track sampling

Note that the closed-burst configuration over open ocean will prevent to perform FF-SAR, therefore we cannot expect a better sampling than the one provided by the SAR unfocused.

In addition, the SLA along-track resolution should also be considered with respect to its noise level. In fact, over open ocean 20Hz estimations are usually not exploit by users, and are averaged over a longer time (1Hz estimations & even more) to reduce the inherent noise measurement.

MRD-430 - The temporal resolution of sea level anomaly (including in ice covered water) shall be less than 10 days.

MRD-440 - The mission shall be capable of retrieving mean dynamic topography (MDT) at an along-track resolution better than 10 km

MRD-450 - The temporal resolution of absolute dynamic topography (ADT) retrieval shall be less than 10 days

Several comments can be made regarding these requirements:

- The SLA temporal resolution must be discussed on a multi-missions context, where CRISTAL will be included in a 4-5 satellites constellation
- The same remark goes for the Absolute Dynamic Topography
- The MDT is not available as an along-track product, as it averaged over grids. We believe Mean Dynamic topography in requirements MRD-440 refers here at Absolute Dynamic Topography.
- SLA & ADT/MDT spatial/temporal resolution are discussed in section 0

5.4.3. Orbit configuration

First analyses were performed over ocean and different diagnoses were delivered to the Mission Advisory Group (MAG) and were discussed during a MAG meeting in June 2019. Three orbits were proposed by ESA, including one from CNES (G2). Below is a summary of the work performed so far, and first conclusions regarding oceanic needs:

Worst choice:
Orbit case 3: Sub-cycles of 4 / 31 / 66 / 365 days

- Drawback: No 15 days sub-cycle for mid-latitude mesoscale
- Drawback: No seasonal sub-cycles (90 days) for removing seasonal biases in polar MSS

Two remaining options:
1- *Orbit case 1: Sub-cycles of 2 / 7 / 30 / 67 / 365 days*

- Drawback: No 15 days sub-cycle for mid-latitude mesoscale
- Drawback: No seasonal sub-cycle of 90 days
- Advantage: **2 days subcycle for wave assimilation**

If the orbit would have a 16 & 90 days sub-cycle, as wanted by ESA, that would be the best candidate

2 – Orbit case G2: Sub-cycles of 5 / 14 / 33 / 113 / 372 days

- Drawback: No 2-3 days sub-cycles for wave assimilation
- Drawback: Seasonnal subcyle is tri-annual instead of 90 days
- Advantage: **14 days sub-cycles for mid-latitude mesoscale**

Conclusion

Regarding the considerable amount of work necessary to perform a serious orbit study, a CCN is currently proposed by ESA. Therefore, additional analysis and additional orbits will be looked at. This will allow the MAG to have all necessary inputs to make the best selection with regard to this crucial choice.

5.4.4. Analysis of the need of a microwave radiometer

The CRISTAL mission will embark a microwave radiometer aside the altimeter. Three designs of microwave radiometer are under study, and the best one to fulfill the mission requirements is still to be chosen. We only discuss here the choice of frequency, not the internal measurement strategy. Traditional observation channel of microwave radiometer aboard altimetry missions are centered around the water vapor absorption line at 22GHz, with a lower frequency channel measuring 18.7GHz for surface emissivity information (temperature and roughness) and a higher frequency channel sensible to cloud liquid water content (for instance 31.4GHz,34GHz, 36.5GHz , 37GHz). The first option is a Sentinel-3 radiometer, using two channels (23.8GH, 36.5GHz), used on European altimetry missions since ERS-1 (ERS-2, Envisat, AltiKa, Sentinel-3). Microwave radiometers aboard US altimetry missions have three observation frequencies: (18.7, 21, 37) for Topex/Poseidon, (18.7, 23.8, 34) for the Jason-1/2/3 series. The second option is a three channels radiometer with the AMR configuration. Sentinel6/Jason-CS will embark an AMR-C (three low frequencies) coupled to a high frequency MWR (89, 130, 165). Those higher frequencies are added to the original one, to improve the restitution of the wet tropospheric correction over ocean and in coastal areas. The third option is the so-called CoastRad set of frequencies based on the conclusions of the ACCRA and ACCRA-2 studies dedicated to the definition of a Coastal Altimetry Radiometer.

There are three main objectives of the CRISTAL mission that the microwave radiometer shall support. The microwave radiometer will of course provide valuable information over ocean and coastal areas by correcting the altimeter range of the excess path delay due to water vapor in the atmosphere. But it will also provide information over ice and snow surfaces.

Ocean

The first two configurations have in common that they have only low frequency measurements. The main difference resides in the absence/presence of the 18.7GHz channel in the 2-channels (S3) /3-channels (Jason) configuration. The 3-channels configuration (Jason) benefits from the presence of the 18.7GHz which provides more information on the surface (roughness and temperature) than the Sigma0 (only roughness). Two papers compared the information brought by brightness temperature at 18.7 GHz and Sigma0 in Ku or Ka band. Thao et al (2015) underlined the better performances using the 18.7GHz with respect to Sigma0 (Ku or Ka band), in neural network algorithms, based on simulations. But, as stated by Obligis et al (2009), sea surface temperature and atmospheric temperature lapse rate can be used to compensate the lack of sensitivity of the Sigma0 to the surface temperature. Indeed, Picard et al (2015) showed the good performances of a 5 inputs retrieval algorithm (2 BTs, Sigma0, SST, temperature lapse rate). The Ka Sigma0 seems to bring more information than the Ku band Sigma0.

Regarding the third configuration, the ACCRA study has shown the improvement when using high frequencies. This study was dedicated to the design of a microwave radiometer for coastal areas. But the selection of the frequencies was carried out in a more general case, covering ocean. In this study, the reference is a 3 frequencies configuration (18.7GHz, 23.8GHz,36.5GHz). To this configuration is added an additional frequency in an incremental way. Results, based on the rms of the difference between the reference and the retrieved WTC, are presented in Figure 29. We can see that the error with respect to the 3E configuration is reduced when adding high frequencies. This study was performed on geophysical simulations only, ie without consideration of the instrument and its resolution.

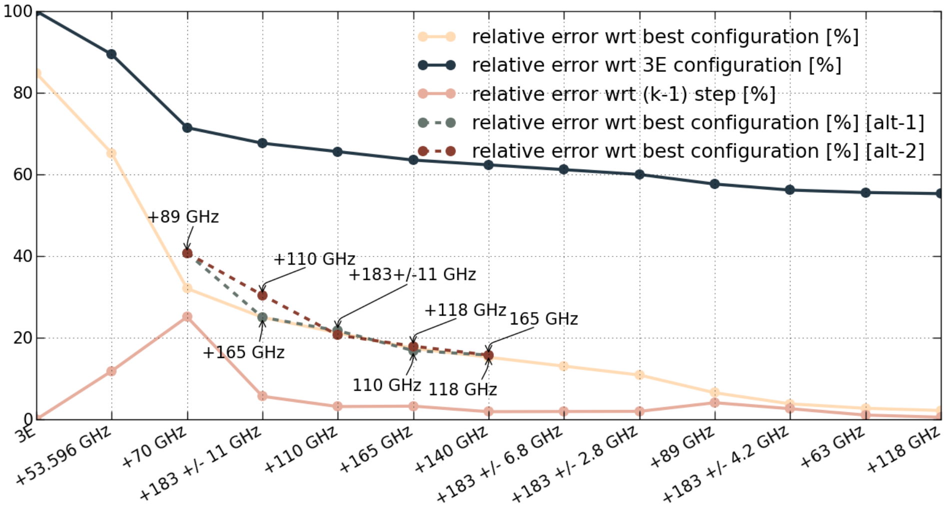

Figure 29 : Reduction of the retrieval error wrt to references, the "3E" and the "best" configuration (Result from ACCRA study).

Regarding the requirement MRD 480 (The standard deviation of the 1-second along-track averaged corrected measurements of sea surface height shall be less than 0.0294 m. **Note 4: The contribution of the wet tropospheric correction to the standard deviation of the 1-second along-track averaged corrected altimeter range shall be less than 1.4 cm for NTC**), we cannot provide at this day an along-track value of the uncertainty on the WTC. Performances of retrieval algorithms are usually evaluated by comparison to a model WTC. The standard deviation of the difference MWR-ECMWF WTC (D_WTC) is evaluated and monitored. This value is the combination of the error of the NWP model and of the error of the MWR (instrument + retrieval algorithm). Classical numbers are the following:

- for a Jason configuration (3 BTs and a log-linear algorithm), the standard deviation of D_WTC is around 1.2cm.
- for a S3 configuration (3BTs+sigma0 and a classical neural network), std of D_WTC is around 1.4cm, 1.5cm. These numbers can be reduced by using a 2BTs+sigma0+SST+Atmospheric temp. lapse rate (so-called enhanced algorithm).
- for a high frequency MWR configuration, std of D_WTC is not known yet, but we can expect that it will be smaller than 1.4cm.

The comparison between an enhanced retrieval NN (2BTs+sigma0+SST+Atmospheric temp. lapse rate), a high frequency MWR (pure MWR algorithm) has not been assessed. A dedicated study shall be carried out on that point.

Coastal areas

With the current generation of microwave radiometers, the coastal areas can be difficult to process because of the contamination of the main lobe by land. The retrieval algorithms developed for open ocean do not handle the land contamination. Different approaches have been considered to process these specific areas. For the radiometers aboard Jason missions, a dedicated processing has been developed to correct the brightness temperature for the land contamination before application of the ocean retrieval algorithms. Another approach is the development of retrieval algorithm specific to coastal areas based on empirical neural network. The drawback of these kind of algorithms is the loss of performances over ocean and their discontinuity with a pure-ocean algorithm.

For the new generation (Sentinel6/Jason-CS), high frequencies will be added to improve the retrieval in these areas. Indeed, the high frequencies have smaller resolution than the classical frequencies. A dedicated retrieval algorithm has been developed by JPL to use these frequencies for the retrieval of the wet tropospheric correction.

During the ACCRA and ACCRA-2 studies carried out at CLS, the impact of high frequencies was assessed over ocean but also over coastal areas. The integration over the instrument field of view has been simulated for low and high frequencies and dedicated retrieval algorithm has been developed. Additional results are shown on Figure 30. These results must be considered within the following context. The simulation context and the convolution required a high-resolution NWP model, thus the AROME model, covering Europe, has been selected. Consequently, these results are not global, but were generated in a regional context. Moreover, this study was a pure MWR study so no sigma0 was simulated. Thus, a 2TB+sigma0 or a 5TB+sigma0 is not assessed with respect to the pure MWR configurations. In Figure 30, we can see that a 2 channels MWR has lower performances than the other configurations in term of std even far from coast and retrieval near the coast. The 5-,7- and 8-channels configurations shows better results than the 3-channels in term of std. The 7-channels configuration seems the best one for all aspects.

The best compromise is the 5-channels configuration (23.8GHz, 36.5GHz, 89GHz, 165GHz, 172GHz) with a retrieval very close to the reference up to 10km from coast.

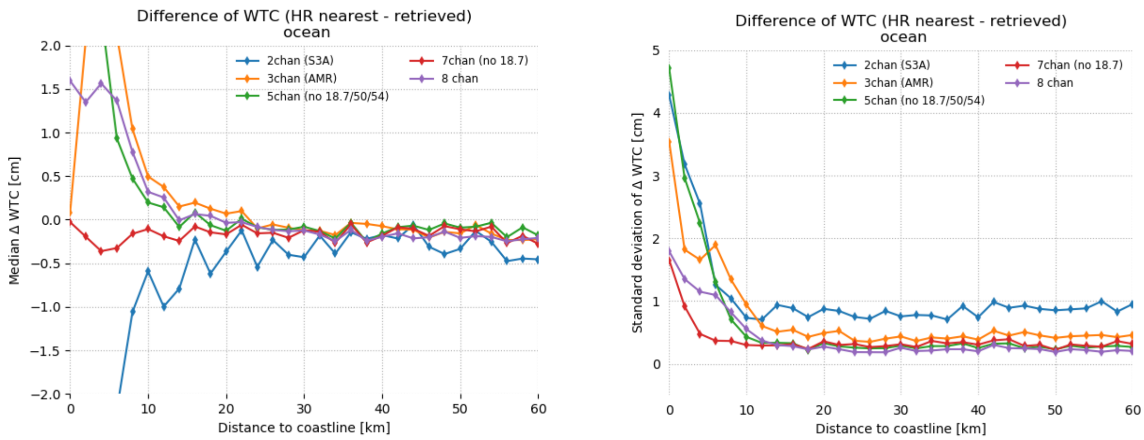

	18.7GHz	23.8GHz	36.5GHz	50GHz	54GHz	89GHz	165GHz	183GHz
3dB footprint (km)	30	25	25	15	15	10	10	10
2.5*t3dB/2 fooprint (km)	37.5	31.2	31.2	18.8	18.8	12.5	12.5	12.5

	18.7GHz	23.8GHz	36.5GHz	50GHz	54GHz	89GHz	165GHz	183GHz
3dB footprint (km)	30	25	25	15	15	10	10	10
2.5*t3dB/2 fooprint (km)	37.5	31.2	31.2	18.8	18.8	12.5	12.5	12.5

Figure 30 : Addition to ACCRA-2 study results : Difference of WTC (Ref – retrieved) wrt to Shoreline distance for different configuration of frequencies with realistic footprint size: mean difference (left), standard deviation (right)

Ice surfaces

Passive microwave radiometer is widely used in retrieval of Sea Ice Concentration, sea ice extent, ice classification. There is a high contrast between open water and sea ice brightness temperature, allowing the separation between the two surfaces. This contrast depends of the frequency (higher for lower frequencies). Observation in specific frequencies allows the sea-ice monitoring in cloudy atmospheres. Often, imaging radiometers (constant incidence around 55°) (SSM/I, AMSRE, …) are used for ice and sea-ice algorithms as they provide polarization information and provides measurements within a large range of frequencies. The separation between open water and sea ice can be determined by polarization ratio (difference of TB at different polarization, at lower frequencies). The separation of FY and MY ice can be determined by gradient ratio (difference of two frequencies at the same polarisation).

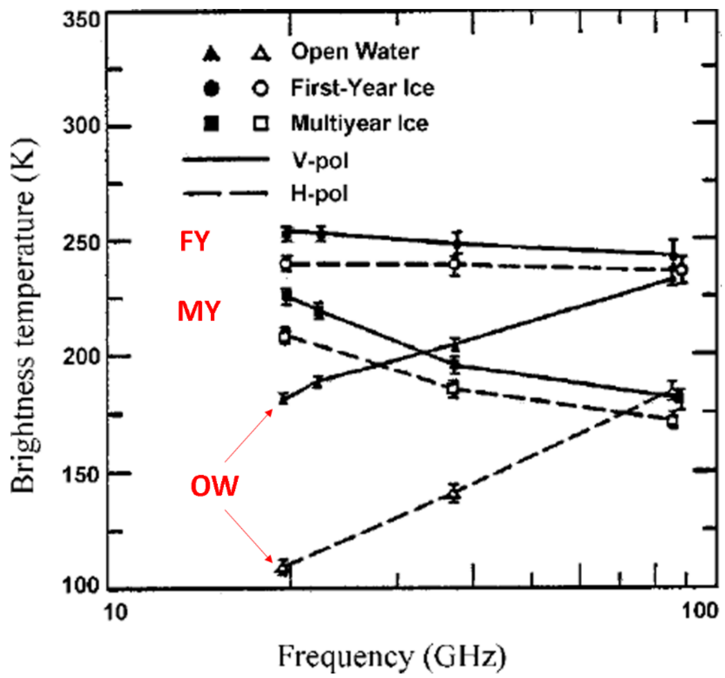

Figure 31 : polarisation and brightness temperatures of open water, first-year ice and multi-year ice (Eppler, D. T. and 14 others. 1992. Passive microwave signatures of sea ice. In Carsey, ED. and 7 others, eds. Microwave remote sensing of sea ice. Washington, DC, American Geophysical Union, 47–71. (Geophysical Monograph Series 68.)

Unfortunately, radiometers onboard altimetry missions are not imaging radiometers but near-nadir looking instruments, using only two to three observation frequencies. Indeed, their primary goal is to provide the correction of the altimeter range for the wet path delay. They thus measure using frequencies close to the 22GHz water vapor absorption band with an additional frequency for cloud liquid water content (34GHz, 36.5GHz). Some classification algorithms have been developed for this kind of radiometers, first for Envisat (Tran et al, 2009), later for Sentinel-3 (reviewed Envisat algorithm). These algorithms use the sigma0 from the altimeter in addition to the measurements from the MWR.

Looking for algorithm using higher frequencies, we have to analyse other instruments, such as AMSU-A. Indeed, all past and present radiometers aboard altimetry missions have only low frequencies instruments. AMSU-A is a sounding radiometer measuring with a scanning geometry with varying incidence angles. Some pixels in the middle of each scan are close to nadir. Moreover, AMSU provides measurements at 23.8GHz and 31.4GHz (ie close to the altimetry mission radiometer) but also higher frequencies channels. Of course, AMSU lacks the polarization information but has other advantages. For instance, nadir measurements are more sensitive to the emissivity assumption (Lambertian or specular) than incidence measurements. This kind of assumption has been used in Hermozo et al to provide an algorithm for sea-ice classification. Kongoli et al (2011) developed a sea-ice concentration algorithm using AMSU measurements (23, 31,50) and coincident MHS measurements (89 and 150).

To conclude, ice classification is feasible with a two or three channels radiometer. But the high frequencies will allow more possibilities.

5.4.5. Potential synergy with contemporaneous missions

In 2025, as already detailed in the Polar Monitoring TN1 (RD4), the following altimetry satellite constellation is predicted:

- **4 to 6 altimeters** are expected to be in operation during the 2025-2030 period
- 2 missions in SAR mode (**Sentinel-3C + Sentinel-3D**) + 2 missions in LRM (**HY2C+ HY2D**) + 2 missions in simultaneous SAR & LRM (**Sentinel-6A + Sentinel-6B**). All missions in Ku band.
- 2 Sentinel-6 missions on the reference Jason orbit 10-days orbit cycle; 2 Sentinel-3 missions on the 35-days orbit cycle of ERS/Envisat/AltiKa; 2 HY missions on a 14-days orbit cycle.
- The maximum geographical coverage will be up to +/- 82° only, leaving a big gap of observation up to the pole.

Open ocean

In this sub-section we discuss the added value of CRISTAL with respect to the predicted 2025-2030 constellation over open-ocean. Note that some elements were already raised in the TN1 gap analysis. Different studies can be found in the literature, assessing the **mesoscale mapping capabilities** of single or multiple altimeter missions. They showed that **at least two altimeters are required to accurately reconstruct the global ocean surface topography at a mesoscale resolution** (i.e., scales larger than 100–150 km and 10–15 days) [Pujol et al. 2012]. Specific studies, however, highlight the impact of near-real-time (NRT) versus delayed-time conditions. **In NRT up to four altimeters need to be merged for an accurate reconstruction of mesoscale signals** [Pascual et al. 2006, 2009]. In addition, there is an important sensitivity of NRT mesoscale sampling to the synchronization and phasing of the considered constellation [Dibarboure et al. 2011].

Nevertheless OSEs (Observing System Evaluations) and OSSEs (Observing System Simulation Experiments) are needed to optimize the future constellation 2020/2030 and assess the potential of future altimetry missions [Le Traon et al.,2019]. For now, without dedicated studies assessing the capabilities of a 5+ altimetry constellation to the global observation system, it is not straightforward to foresee the clear benefit of adding another mission.

We can anticipate that CRISTAL will provide highly valuable data, and will help improving the quality of the future L4 gridded products at mesoscales. In fact, recent analyses show that nearly 60% of the energy observed in altimetry along-track measurements at wavelengths ranging from 200 to 65 km are missing in the current CMEMS SLA gridded products (0.25°spatial resolution/daily temporal resolution for global products), generated with a three satellites constellation (AltiKa, Jason-2 and HY-2A). This is linked to the mapping methodology combined with the sampling capability of the altimeter constellation [Pujol et al.,2016]. With a 5 to 7 satellites constellation, the L4 gridded products could be generated at a finer spatial/temporal resolution, that would help to recover the small-mesoscale variability. To conclude on this aspect, recent works [Ballarotta et al. 2019] confirms that at least two altimeters are required to accurately map the SSH mesoscale and up to four altimeters are required for Near-Real-Time products. They also show that the level-4 products resolution capability increases ~10-20% at regional scale from two to three altimeters merging. And they expect > 5% finer resolution over period where more than 4 altimeters are available.

Finally, the orbit definition will be critical and will condition the added value of CRISTAL to the 2025-2030 observation system over open ocean. A full theorical study is required to address this problematic, and conclusions will have to be weighted with cryosphere needs as the open ocean remains a secondary objective for the mission.

Polar ocean

Over polar ocean, the synergy will depend on the orbit coverage of the future constellation:

- **At latitudes above +81°,** over the Arctic ocean, CRISTAL should be the only altimeter in operation, considering a CryoSat-2 ending before 2025. Similarly, ICESat-2 has a three-years lifespan and should not be in operation after 2025. Therefore, and as already stated, CRISTAL is essential to provide a high latitude coverage of the Arctic ocean and ensure a continuity with CryoSat-2. Furthermore, the lessons that will be gained with dual Ku/Ka measurements over the ice-covered ocean might allow to provide new methods to process the SAR Ku measurements, that could be beneficial for CryoSat-2 or Sentinel-3 data reprocessing.

- **At latitudes between 66° & 81°,** CRISTAL should be concomitant with two Sentinel-3 satellites + two HY2 satellites, providing a potential constellation of 5 altimeters. Again, the added value will completely be conditioned by the chosen orbit and its complementarity with the other missions. This potential future constellation is extremely promising to solve the polar mesoscales signals in this range of latitudes. Moreover, this constellation will consist of 3 satellites operating in SAR altimetry mode, which will be highly relevant over the ice-covered ocean. Improving the Mean Sea Surface (MSS) and the oceanic tides correction over this range of latitudes should be a major result allowed by the future constellation, and that could be retroactively beneficial for historical missions.

6. Specific MRD analyses required by MAG

Below is the list of requirements for which MAG needs feedbacks from the PolarMonitoring team. Most of these requirements come directly from the user requirements in the PEG reports, and MAG believe that they are unachievable in their current form with the CRISTAL observation concept:

MRD Requirement	Comment from industry	Proposal next MAG
MRD-280: The system shall be capable of retrieving sea ice freeboard to an accuracy of 0.03 m along orbit segments ≤ 25 km.	Could be possible as is but with gridded 25km x 25 km then could work.	TBD
MRD-330: The system shall be capable of delivering sea ice thickness measurements with a vertical uncertainty less than 0.1 m.	FYI ~40 cm MYI ~60 cm based on Ku-band. With Ka band and higher resolution the performance likely much better.	Relax TBC.
MRD-360: The system shall be capable of delivering surface elevation with a horizontal resolution of at least 100 m.	Gridded ok, but system resolution in closed burst is ~300m horizontal (azimuth impulse response)	TBD
MRD-410: The uncertainty of snow depth measurements over sea ice shall be less than 0.05 m.	Could be compliant for 25km x 25 km grid or possibly 6.5 cm TBC	Relax to ~6.5 TBC
MRD-460: The vertical uncertainty in sea level anomaly retrieval from Ku band (including sea-ice leads) shall be 0.02 m.	TBC. Vertical resolution of radar is ~ 31 cm. Not clear if this can be met	TBD
MRD-480: The standard deviation of the 1-second along-track averaged corrected measurements of sea surface height shall be less than 0.0294 m.	Based on S6 which is Ku + C band.	3.62 cm TBC

Table 12: List of specific requirements to be analysed upon MAG request

Below are the discussions/analyses made for each of these requirements by the PolarMonitoring team:

MRD-280: The system shall be capable of retrieving sea ice freeboard to an accuracy of 0.03 m along orbit segments ≤ 25 km. [FMI & LEGOS]

Tilling et al. (2018) found standard deviation of 0.09 m for individual monthly Arctic freeboard measurements from CryoSat-2, which is mainly related to speckle noise and accuracy of the actual sea-surface height. For gridded monthly products she concluded 0.02 m freeboard uncertainty. However, a monthly gridded product is different from a 25 km orbit segment. Overall a 0.03 m sea ice freeboard accuracy requirement is a strict one, but necessary for reasonable sea ice thickness accuracy.

The uncertainty of freeboard retrieval will also depend on the presence of leads along the orbit segment. Less leads to determine the local sea level results in more uncertainty in the freeboard product.

The definition of sea ice freeboard is also non-trivial. Sea ice freeboard is the distance from local water level to the sea ice - snow interface. However, especially with the presence of snow ice, the transition from ice to snow happens over several centimeters, in which cases exact sea ice freeboard will be hard to define. In every case, **validation of the freeboard requirement will require large scale airborne campaign(s) with ground truth teams to provide an uncertainty estimate for the sea ice freeboard derived from airborne snow radar and laser altimeter**.

Radar penetration will complicate the sea ice freeboard retrieval. It is known that for Ku-band the signal penetrates systematically all the way to the snow ice interface in only cold Arctic conditions - and not always even then (Willatt et al., 2011; Ricker et al., 2014). Thus **limiting this MRD (280) to the cold winter months in the Arctic might be considered**.

We would suggest the following options for MRD-280:

1. **Keep as it is, but reserve resources for dedicated studies about the orbit segment accuracy and possible improvements with SARIn and Ku/Ka combination.**
2. **Add another, relaxed accuracy requirement for summer months.**

MRD-330: The system shall be capable of delivering sea ice thickness measurements with a vertical uncertainty less than 0.1 m. [FMI & LEGOS]

The uncertainty requirement for sea ice thickness comes with a caveat, as the thickness uncertainty depends on the uncertainty of auxiliary products. In the case of CRISTAL, snow thickness will be measured by the system, but snow and ice densities will still have to be estimated by other means. Thus, **the sea ice freeboard (MRD-280) requirement should be considered the primary requirement**.

[Tilling et al., 2018] stated a 0.2 m thickness uncertainty for the monthly gridded product, where the uncertainty is scaled from the 0.02 m freeboard uncertainty. However, they calculated as little as 0.002 m average thickness difference between their CryoSat-2 and independent estimates.

Knowledge of radar propagation through the snow, as well as a better estimate of snow depth over sea ice, with related knowledge of uncertainties, that the addition of Ka-band will bring, is sure to bring down the vertical uncertainties in sea ice thickness. In freeboard to thickness conversion, snow depth is currently a main impactor in the sea ice thickness uncertainty budget [Ricker et al., 2014; Tilling et al., 2018], as much as up to 70 % of the total uncertainty [Zygmuntowska et al., 2014]. In the light of the current 0.2 m thickness uncertainty assessed by [Tilling et al., 2018] and the anticipated improvement from the dual-altimetry technology, especially in the snow depth and propagation estimates, **reaching vertical uncertainty below 0.1 m would seem reachable for winter monthly gridded product.** However, once again the uncertainty for summer months, and orbit product (level-2), will likely remain greater.

We would propose the following option for MRD-330:

1. **Relax the vertical uncertainty requirement to be “less than 0.5 m”.**
2. **Include different requirements for winter and summer, FYI and MYI.**

Additional note: “The sea ice freeboard (MRD-280) requirement should be considered the primary requirement.” could be added as a note under MRD-330 as sea ice thickness relies straight on freeboard.

MRD-360: The system shall be capable of delivering surface elevation with a horizontal resolution of at least 100 m. [Lancaster University]

Considering the along-track component, a horizontal resolution of 100 m is unachievable with a conventional Ku unfocused SAR in the CryoSat-2 orbit. To address this in the MRD, the following options could be considered:

1. This Mission Requirement is relaxed to specify a horizontal resolution ~300 m, thus reflecting current unfocussed SAR capability, e.g. as achieved by CryoSat-2 and Sentinel-3 ground segments.

2. Fully-focused SAR processing within the ground segment would allow the existing 100 m resolution requirement to be met; for instance the theoretical limit of a CryoSat-2-like fully-focused SAR would be sub-metre resolution.

3. At Ka-band the unfocused SAR azimuth resolution would be ~ 100 m; thereby meeting the requirements of the existing MRD, should this be framed in terms of either the Ku or Ka-band acquisition.

4. Flying the satellite at lower altitude would improve the azimuth resolution, albeit not to a point where the 100 m requirement could be met; for example at a 500 km ICESat-2-like orbit altitude, the Ku-band azimuth resolution would be ~ 185 m.

Considering the across-track component, the conventional pulse-limited footprint at the point of closest approach will exceed 1.3 km for a 500 Hz measurement bandwidth instrument, under the assumption that the satellite flies at 700 km altitude. As such, it is an order of magnitude lower resolution than currently stipulated in the MRD. It should be noted that, with swath processing, the across track resolution can be improved, depending upon the local incidence angle or the radar wave at each resolution cell.

Concerning this requirement in relation to gridded Level-3 and Level-4 products, it is of course possible to grid (e.g. average) the data from multiple orbits at 100 m posting as part of the ground segment processing. Nonetheless, the requirement itself is related to **"the system"**, therefore the comment from industry "gridded ok" is a bit ambiguous and confusing because gridded products don't really make sense for altimetry mono-mission (or at resolution much coarser than 100m). **Requirements from CRISTAL (level-2) & multi-missions products (level-4) must be separated.**

MRD-410: The uncertainty of snow depth measurements over sea ice shall be less than 0.05m. [CLS & FMI]

For the monthly gridded product of [Lawrence et al., 2018], a conservative average uncertainty estimate of snow depth of 0.08 m was given. This snow depth product was built from CryoSat-2 and AltiKa freeboard estimates, where the time lag between the measurements causes a great deal of uncertainty, which will not be the case for CRISTAL. Thus, **less than 0.05 m uncertainty seems reasonable for monthly gridded snow depth**. Furthermore, MRD-410 is extremely relevant for MRD-330 and MRD-280 since the snow depth will be required for the signal propagation speed correction as well as the freeboard to thickness conversion.

We would propose the following for MRD-410:

1. **Keep as it is, but add a note that the snow depth requirement is for monthly 25 km gridded snow depth estimate.**
2. **Keep as it is and have a dedicated study for the orbit segment accuracy for combined Ku/Ka band performance with e.g. a flight campaign. Possibly relax if the 0.05 m requirement is not met after this.**

MRD-460: The vertical uncertainty in sea level anomaly retrieval from Ku band (including sea-ice leads) shall be 0.02m. [CLS & FMI]

Open-ocean [CLS]

Here, we make the assumption that the "vertical uncertainty" refers to the accuracy of the measurement (≠ precision). The comment in the table above states that the vertical resolution of radar is ~31cm. This number means that the altitude/elevation of a single target can be detected with a +/- 0.15m uncertainty. Over open-ocean multiple small targets (ie: oceanic facets) contribute to the measured signal. Hence, the Sea Surface Height estimated reflects a mean elevation of these facets over the pulse-limited footprint (~2km disk diameter, ideally centred at nadir). The radar echo measured is a continuous signal, and the altimeter range can be interpolated between two radar samples of 31cm vertical resolution.

The retracking algorithms employed are based on physical models. As the interaction between radar wave and the oceanic surface is well understood, the physical models are faithful and the altimeter range estimated is accurate. In fact, **a 0.02m accuracy looks reachable** regarding the Sentinel-3A calibration results. [Bonnefond et al., 2018] shows a mean SSH accuracy of +0.022m & +0.007m, respectively in SAR mode & PLRM. Moreover, recent updated results presented at OSTST by Bonnefond showed a mean bias of +0.008m for Sentinel-3A & -0.0014m for Sentinel-3B (both in SAR mode). By providing an even better vertical resolution than Sentinel-3A (~31cm vs ~47cm), CRISTAL should therefore meet the requirement over open-ocean.

Leads over sea-ice [FMI/CLS]

Sea level anomaly in the ice field is interpolated from the sea surface measurements in leads. Several methods are currently under investigation to improve the accuracy and precision of the SLA. Considering that CRISTAL will be in SAR mode over sea-ice, physical retrackers must be considered (CNES/CLS Adaptive solution or SAMOSA ++ retracker [Dinardo et al., 2019]). Being based on physical modelling of the backscattered signal, as it is the case for deep ocean measurements, an accuracy of 0.02 m seems achievable. However, more studies will be necessary to fully demonstrate that this requirement is achievable.

Regarding Low Resolution mode, several studies have already been conducted. In particular, CNES/CLS have developed an "Adaptive solution" [Poisson et al., 2018] showing very promising results and especially showing that the continuity of SLA estimates is guaranteed when using a retracker based on a physical modelling. ALES+ solution [Passaro et al., 2018] has also shown that it brings over 0.02 m improvement (for Envisat) when compared with the widely used retracker by Laxon (1994), which was designed for specular waveforms. In fact, Passaro et al. note a mean error of 0.021 m for ALES+ in the sea ice covered comparison domain around Svalbard Islands, which is promising for reaching the 0.02 m requirement. Furthermore, sea level anomaly in leads should benefit from using InSAR mode retrievals [see Di Bella, 2019] which **makes MRD-460 reachable**.

MRD-480: The standard deviation of the 1-second along-track averaged corrected measurements of sea surface height shall be less than 0.0294 m [CLS]

Here there are two different options that can be taken for this requirement:

<u>1 – The requirement is kept as it is, with a single value describing the altimetry noise</u>

In that case, the 0.0294m is taken from Sentinel-6 requirement [Scharroo et al., 2016]. It corresponds to the residual sum of squares of several sea surface height errors component. These components are the **altimeter range noise**, **ionosphere correction, sea-state bias correction, dry tropospheric correction, wet tropospheric correction** & **radial component of the orbit** (as described in the requirement notes).

We suggest keeping the same range noise as for Sentinel-3A, as both altimeters configurations are similar over ocean (even if we can expect some improvements with respect to the Sentinel-3A bandwidth). And we also keep the same requirements taken Sentinel-3A for the other components. The absence of C-band could be problematic for ionospheric correction, but it was stated in RD-4 that the filtered ionospheric correction (over 300km) should be less than 0.5cm, using Ka band to correct Ku band.

At the end, the noise value should change from 0.0294m to 0.095m. Moreover, the requirement should be reformulated to make the definition more precise: **"The residual sum of squares (RSS) of the sea surface height error shall be less than 0.035m".**

As it is, the requirement, with all the error components, is reachable based on Sentinel-3A CalVal studies presented at the Sentinel-3 Validation Team meeting (March 2018), by M.Raynal. The presentation is available here:

https://www.eumetsat.int/website/home/News/ConferencesandEvents/DAT_3645214.html

<u>2 – The requirement is changed, based on the argument that all the noise/errors affecting the altimeter SSH cannot be mixed together</u>

The different contributors that are integrated to derive a single noise value for the SSH have not the same magnitude depending on the spatial/time scales. As an example, orbit errors and range high frequency errors cannot be accounted for at the same level (which is the case in the first solution described just before), one being a very large scale error, the other being a very short scales HF noise.

At OSTST 2019, [Thibaut. P et al, 2019] presented a new way to compute the uncertainties of an altimetric system, using a spectral approach to account for each contributor to the final noise level, depending on spatial and temporal scales. An error being defined by a variance and correlations (along track and temporal). This presentation is the result of a dedicated study made in the frame of the Polar-Ice project [RD-5] aiming at investigating this problematic. Different errors were characterized according to a mission scenario (orbit, altimeter…). A Mission Performance Simulator (MPS) has been developed to compute the general level of SLA uncertainty at all spatial and temporal scales.

<u>Results in Ku band</u>

The table below presents the error sources characteristics used in the simulation of CRISTAL

Error Source	STD (cm)	Spatial correlation length	Temporal correlation length	References
Altimeter Random error	0,8	0 km	0 day	S3 performance doc (CLS) + extrap. to Cristal
SSB Noise	0,3	300 km	Inf.	S3 performance doc (CLS) +extrap. To Cristal
SSB correlated	0,1	100 km	1 day	Tran & al, 2019
Ionosphere	0,3	600 km	0 day	S3 performance doc (CLS) + extrap. To Cristal
Wet Troposphere	1	50 km	1 hour	Brown & al, 2015; Stum & al, 2011
Dry Troposphere	0,2	600 km	2 days	S3 performance doc (CLS)
Mean Sea Surface	0,5	1 km	Inf.	Pujol & al, 2018
Ocean Tides	1	1000 km	< 1 day	Lyard & al, 2018
Orbit solution	1,5	> 10 000 km	< 1 day	Ollivier & al, 2018; Couhert & al, 2015

Table 13: CRISTAL Ku-band SLA error characterization (anticipated)

Based on this table defining the scenario for the MPS, the simulation of the CRISTAL performances over ocean in Ku band has been performed. The result is a 2D STD map presented in Figure 32:

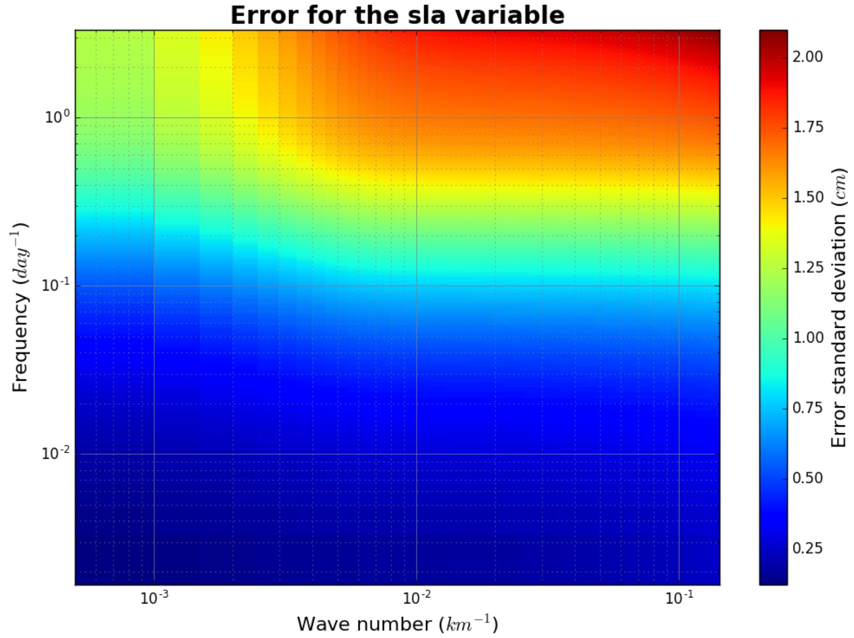

Figure 32: Simulated 2D STD computed using the MPS from anticipated uncertainty characteristics of the CRISTAL mission over ocean in Ku band

Thanks to the MPS simulation, we can see that the anticipated error budget for the CRISTAL mission over the ocean in Ku band is:

- ~2 cm at very short scales (upper right corner of the map)
- between 0.3 and 0.7 cm at mesoscales (center of the map)
- <0.3 cm at climatic scales (lower left corner of the map)

=> *In the end, the requirement could be reformulated and could include three values quantifying the error budget at three different spatial scales.*

=> *This study has also be performed for the ice covered ocean to quantify errors on ice freeboard or ice thickness. The results that have been obtained could be integrated as well. Similar requirements could be derived for characterizing the SLA in the leads.*

References

Abdalla, S. Ku-band radar altimeter surface wind speed algorithm. Marine Geodesy 35, 276–298 (2012).

Saleh Abdalla (2015) SARAL/AltiKa Wind and Wave Products: Monitoring, Validation and Assimilation, Marine Geodesy, 38:sup1, 365-380, DOI: 10.1080/01490419.2014.1001049

Amarouche, L., Thibaut, P., Zanife, O. Z., Dumont, J. P., Vincent, P., and Steunou, N. (2004). Improving the Jason-1 ground retracking to better account for attitude effects. *Marine Geodesy*, 27(1-2):171–197.

Arbic B. K, R. B. Scott, D. B. Chelton, J. G. Richman and J. F. Shriver, 2012, Effects on stencil width on surface ocean geostrophic velocity and vorticity estimationfrom gridded satellite altimeter data, J. Geophys. Res., vol117, C03029, doi:10.1029/2011JC007367

Bonnefond, P.; Verron, J.; Aublanc, J.; Babu, K.; Bergé-Nguyen, M.; Cancet, M.; Chaudhary, A.; Crétaux, J.F.;Frappart, F.; Haines, B.; et al. The Benefits of the Ka-Band as Evidenced from the SARAL/AltiKa Altimetric Mission: Quality Assessment and Unique Characteristics of AltiKa Data. Remote Sens. 2018, 10, 83.

Buchhaupt, Christopher, Luciana Fenoglio-Marc, Salvatore Dinardo, Remko Scharroo and Matthias Becker. “A fast convolution based waveform model for conventional and unfocused SAR altimetry.” (2017).

Di Bella, A.: Measurement of Arctic sea ice from satellite altimetry: the potential and limitations of CryoSat-2 SARIn mode. PhD Thesis. Technical University of Denmark, 2019.

Gaspar, P., F. Ogor, P.-Y. Le Traon, and O.-Z. Zanife, Estimating the sea state bias of the TOPEX and POSEIDON altimeters from cross-conditions are more frequent. It is also in such conditions that over differences, J. Geophys. Res., 99, 24,981-24,994, 1994

Gaspar, P., and J.-P. Florens, Estimation of the sea state bias in radar altimeter measurements of sea level: Results from a new nonparametric method, J. Geophys. Res.,103, 15,803-15,814, 1998.

Hermozo, L., Eymard, L., Karbou, F., 2017. Modeling sea ice surface emissivity at microwave frequencies: Impact of the surface assumptions and potential use for sea ice extent and type classification. IEEE Transactions on Geoscience and Remote Sensing 55, 943–961. doi:10.1109/TGRS.2016.2616920

Kongoli, C., Boukabara, S.A., ... Ferraro, R., 2011. A new sea-ice concentration algorithm based on microwave surface emissivitiesapplication to AMSU measurements, in: IEEE Transactions on Geoscience and Remote Sensing. pp. 175–189. doi:10.1109/TGRS.2010.2052812

Kumar U.M, Swain D., Sasamal S.K., Reddy N.N, Ramanjappa T., Validation of SARAL/Altika significant wave height and wind speed observations over North Indian Ocean, Journal of Atmospheric and Solar-Terrestrial Physics,135, pp. 174-180., 2015

Lawrence, I. R., Tsamados, M. C., Stroeve, J. C., Armitage, T. W. K., and Ridout, A. L.: Estimating snow depth over Arctic sea ice from calibrated dual-frequency radar freeboards, The Cryosphere, 12, 3551–3564, https://doi.org/10.5194/tc-12-3551-2018, 2018.

Laxon, S.: Sea ice extent mapping using the ERS-1 radar altimeter EARSeL Adv. Remote Sens., 3, pp. 112-116, 1994.

Obligis, E., Rahmani, A., Eymard, L., Labroue, S., & Bronner, E. (2009). An improved retrieval algorithm for water vapor retrieval: Application to the envisat microwave radiometer. IEEE Transactions on Geoscience and Remote Sensing, 47(9), 3057–3064. https://doi.org/10.1109/TGRS.2009.2020433

Passaro, M., Rose, S.K., Andersen, O.B., Boergens, E., Calafat, F.M., Dettmering, D., Benveniste, J. ALES+: Adapting a homogenous ocean retracker for satellite altimetry to sea ice leads, coastal and inland waters. Remote Sens. Environ., 211, 456–471, 2018.

Picard, B., Frery, M.-L., Obligis, E., Eymard, L., Steunou, N., & Picot, N. (2015). SARAL/AltiKa Wet Tropospheric Correction: In-Flight Calibration, Retrieval Strategies and Performances. Marine Geodesy, 38(sup1), 277–296. https://doi.org/10.1080/01490419.2015.1040903

Poisson, J. C., Quartly, G. D., Kurekin, A. A., Thibaut, P., Hoang, D., and Nencioli, F.: Development of an ENVISAT altimetry processorproviding sea level continuity between open ocean and Arctic leads, IEEE Transactions on Geoscience and Remote Sensing, pp. 1–21,https://doi.org/10.1109/TGRS.2018.2813061, 2018

Pujol, M.-I., Faugère, Y., Taburet, G., Dupuy, S., Pelloquin, C., Ablain, M., and Picot, N.: DUACS DT2014: the new multi-missionaltimeter data set reprocessed over 20 years, Ocean Sci., 12, 1067-1090, doi:10.5194/os-12-1067-2016, 2016

Ray C, Martin-Puig C, Clarizia MP, Ruffini G, Dinardo S, Gommenginger C, Benveniste J (2014) SARaltimeter backscattered waveform model. IEEE Trans Geosci Remote Sens 53(2):911–919. doi:10.1109/TGRS.2014.2330423

Ricker, R., Hendricks, S., Helm, V., Skourup, H., and Davidson, M.: Sensitivity of CryoSat-2 Arctic sea-ice freeboard and thickness on radar-waveform interpretation, The Cryosphere, 8, 1607–1622, https://doi.org/10.5194/tc-8-1607-2014, 2014.

Scharroo, Remko & Hans, Bonekamp & Ponsard, Christelle & Parisot, François & von Engeln, Axel & Tahtadjiev, Milen & de Vriendt, Kristiaan & Montagner, Francois. (2015). Jason continuity of services: continuing the Jason altimeter data records as Copernicus Sentinel-6. Ocean Science Discussions. 12. 2931-2953. 10.5194/osd-12-2931-2015.

Thao, S., Eymard, L., Obligis, E., & Picard, B. (2015). Comparison of Regression Algorithms for the Retrieval of the Wet Tropospheric Path. IEEE Journal of Selected Topics in Applied Earth Observations and Remote Sensing, 8(9). https://doi.org/10.1109/JSTARS.2015.2442416**Erreur ! Référence de lien hypertexte non valide.**

Thibaut, P., J.C.Poisson, M.Lievin, L.Amarouche, M.Ablain, M.Tsamados and R.Cullen, “A new way to assess and represent the error budget for any altimeter mission”, OSTST 2019, Chicago. 2019.

Tran N., D. Vandemark, B. Chapron, S. Labroue, H. Feng, B. Beckley, and P. Vincent, New models for satellite altimeter sea state bias correction developed using global wave model data, J. Geophys. Res., 111, C09009, doi:10.1029/2005JC003406, 2006

Tran, N., Girard-Ardhuin, F., ... Féménias, P., 2009. Defining a sea ice flag for envisat altimetry mission. IEEE Geoscience and Remote Sensing Letters 6, 77–81. doi:10.1109/LGRS.2008.2005275

Tran, Ngan, Doug Vandemark, Sylvie Labroue, Hui Feng, Bertrand Chapron, Hendrik L. Tolman, Juliette Lambin and Nicolas Picot. “Sea state bias in altimeter sea level estimates determined by combining wave model and satellite data.” (2010).

Tran N., D. Vandemark, E. Zaron, P. Thibaut, G. Dibarboure and N. Picot (2019): “Assessing the effects of sea-state related errors in high-rate Jason-3 altimeter sea level data precision”, submitted to *Advances in Space Research* journal, special issue on “25 years of progress in radar altimetry” (guest editors: J. Benveniste and P. Bonnefond)

Willat, R., Laxon, S., Giles, K., Cullen, R., Haas, C., and Helm, V.: Ku-band radar penetration into snow cover on Arctic sea ice using airborne data, Ann. Glaciol., 52, 197–205, doi:10.3189/172756411795931589, 2011.

Witter, Donna L. and Dudley B. Chelton. “A Geosat Altimeter Wind Speed Algorithm and a Method for Altimeter Wind Speed Algorithm Development.” (1991).

E. D. Zaron and R. deCarvalho, “Identification and reductionof retracker-related noise in altimeter-derived sea surface heightmeasurements,”Journal of Atmospheric and Oceanic Technology,vol. 33, no. 1, pp. 201–210, 2016. [Online]. Available:https://doi.org/10.1175/JTECH-D-15-0164.1

Zygmuntowska, M., Rampal, P., Ivanova, N., Smedsrud, L.H.: Uncertainties in Arctic sea ice thickness and volume: New estimates and implications for trends. Cryosphere 8, 705–720. http://dx.doi.org/10.5194/tc-8-705-2014, 2014.